4-18-2013

# Transient Stability Enhancement of Electric Power Grid by Novel Braking Resistor Models

Riya Saluja

# TRANSIENT STABILITY ENHANCEMENT OF ELECTRIC POWER GRID BY NOVEL BRAKING RESISTOR MODELS

by

Riya Saluja

A Thesis

Submitted in Partial Fulfillment of the

Requirements for the Degree of

Master of Science

Major: Electrical and Computer Engineering

The University of Memphis

May 2013

*This thesis is dedicated to my parents Rakesh Dhand and Palka Dhand for all their love and efforts they put together to make me a better person.*

ACKNOWLEDGEMENTS

I would first like to thank my advisor Dr. Mohd. Hasan Ali, for his constant support, patience, motivation, enthusiasm and continuous guidance for my research. I am extremely grateful to have him as my mentor, and much more.

I am grateful to my ex-advisor Dr. Eddie Jacobs, for his enthusiasm, support and trust on me that help me to reach this far.

I am grateful to my thesis committee members Drs. Eddie Jacobs, Dr. Russel Jerry Deaton and Dr. Dipankar Dasgupta who devoted their precious time for my research and thesis and for the valuable suggestions.

I would also like to thank my lab mates at the Electric Power and Energy Systems for their constant suggestions and discussions during my research.

Lastly I will be thankful to my family and friends for their constant support and encouragement.

# ABSTRACT

Saluja, Riya. M.S. The University of Memphis. May 2013. Transient Stability Enhancement of Electric Power Grid by Novel Braking Resistor Models. Major Professor: Dr. Mohd. Hasan Ali.

The dynamic braking resistor is one of the effective methods to enhance the transient stability of power grid system. In this work, two new braking resistor models, namely, rectifier controlled braking resistor and chopper rectifier controlled braking resistor models, using a single unit of braking resistor are proposed, and their performance is compared with the existing thyristor controlled braking resistor model. Comparison is made in terms of the speed indices, number of components used, heat loss, harmonics, and cost. The effectiveness of the proposed methodology is tested through Matlab/ Simulink simulations considering both temporary and permanent faults in power system. Simulation results for all braking resistor models are compared and analyzed. The performance of the proposed models is comparable to the existing braking resistor model. Therefore, the proposed braking resistor models can be considered as an alternative to the existing BR model for improving the transient stability of power systems.

TABLE OF CONTENTS

LIST OF TABLES

LIST OF FIGURES

# LIST OF ABBREVIATIONS

3LG: Three-line-to-ground fault or Three-phase-to-ground fault

3LS: Three-line- to-line fault or Three-phase-to-phase fault

2LG: Two-line-to-ground fault or Two-phase-to-ground fault

2LS: Two-line- to-line fault or Two-phase-to-phase fault

1LG: One-line-to-ground fault or One-phase-to-ground fault

BR: Braking Resistor

CRCBR: Chopper Rectifier Controlled Braking Resistor

IGBT: Insulated Gate Bipolar Transistor

RCBR: Rectifier Controlled Braking Resistor

TCBR: Thyristor Controlled Braking Resistor

# I. INTRODUCTION

Due to the continuous increase in the power demand and the limited non-renewable resources for generating the power, many renewable energy power plants such as wind, solar, etc., are merged into the existing power grid system to meet the increasing demand without overburdening the existing system. Also, the flexible alternating current transmission systems (FACTS) devices are designed to help in transmitting the bulk power from one location to other. Simultaneously, research is also going on to make the existing system a smart gird one, which is self-sufficient, reliable and more efficient to help maintain a continuous and reliable power supply and decrease any failures occurring in the system due to human error.

The development of the modern power system has led to an increasing complexity in the study of the power systems, and also presents new challenges to power system stability, in particular, to the aspects of transient stability and small signal stability [1]. Transient stability plays a vital role in the bulk transmission of power by ensuring the stable operation during the events of large disturbances and faults. The various control strategies to maintain the power system stability with non-linear control theories are available in literature.

Insertion of braking resistors in the power grid system to improve the transient stability and to maintain the continuity of power supply during any fault conditions is a well-known power system stability method [2], [3]. The various implementation of braking resistors for the improvement of bulk power transmission is available in literature. The earlier work mentions the use of braking resistors in Russia for the improvement of the dynamic stability of the hydro synchronous generators [4], [5] as well as in United States

to improve the transient stability of Arizona Public Service Company for bulk transmission of the power [2]. With the advancement in technology, braking resistors implementation is playing a vital in improving the low-voltage ride-through of a wind turbine [6], in damping the sub-synchronous resonance of the power grid system [7], etc.

### *A. PROBLEM SATEMENT*

Due to the technology developments, integration of non-renewable power plants, and interconnection of complete grid system has increased the necessity of having a stable and synchronized power grid system. The cascading effects of failures, caused due to any three-phase-to-ground faults, lead to [2] the power outages and instability of the turbine-generator system. So, it has become a priority for power engineers to add some external means to avoid the complete power outages and to supply a reliable power to the consumers.

The live braking resistor model consists of three banks of resistors connected in parallel at the output terminal of the synchronous generators [2-4], [8-10]. The braking resistor is inserted in the power grid system following the transient conditions such as sudden insertion of a large load, falling of a tree branch on long transmission line causing three-phase-to-ground faults, etc. The braking resistors are switched in and out of the power circuit either manually by a plant engineer or automatically by the close-loop control switch.

The stability of the synchronous generator can be defined by equations (1) and (2). The operation of a synchronous generator can be modeled by the swing equation given by (2). During steady state, the mechanical power, $P_m$, send by the prime mover to the synchronous generator counter balances the electrical power, $P_e$, generated by the generator.

Thus, at steady state, $P_m = P_e$, and accelerating power, $P_a = 0$, as in (1). During a fault condition, all the current flows through the transmission line to the fault point, since the transmission network is of low impedance. The transmission network is basically inductive that makes the generator current 90˚ out of phase with the generator voltage. Thus, the real power delivered by the generators decreases, while the input mechanical power through the turbine to the generator remains approximately the same. The net torque on the generator shaft then causes the generator to accelerate resulting in accelerating power, $P_a$.

$$P_a = P_m - P_e \tag{1}$$

$$\boldsymbol{M\frac{d^2\delta}{dt^2} + D\frac{d\delta}{dt} = P_m + P_e} \tag{2}$$

where $\delta$ is the angle of machine relative to the synchronous angle of the system, $M$ is the inertia constant, $D$ is damping coefficient, $P_m$ is mechanical power, and $P_e$ is electrical power. Due to the accelerating power, $P_a$, the synchronous generator may lose its synchronism. The most effective method to restrict the increasing speed is to provide a brake by applying an artificial load for short duration. It is achieved by inserting a braking resistor into the system.

The control laws based on different inputs such as change in active power, rotor angle and/or voltage of synchronous generators, etc., of machines have been reported in literature for switching operation of braking resistors in the power network. By using nonlinear control analysis methods, the control parameters for braking resistors are suggested in the literature [1].

The power electronic devices played a vital role for the development of the control switches for the switching operation of the braking resistors in the power grid system. These switches are triggered by the triggering pulses generated by the controller. These switches also helps in the design of economical braking resistor models with use of minimum number of braking units to provide a better control on the three phase system. The work of C.S. Rao and et al. in seventies [11-16] on braking resistor models mention the use of thyristor switches for controlling the insertion of the braking resistor unit in the give power grid system. The full wave thyristor controlled [11-13], and the half-wave thyristor controlled [14-16] switches have been designed to provide economical braking resistor models. The control strategies designed for braking switches take change in speed of the synchronous generator as an input and is fed to the controller. Later, fuzzy controlled half wave braking resistor was also reported [16].

The reported braking resistor models with close-loop control switch are designed using three units of braking resistors giving an independent control on each phase of the power grid system. The fuzzy logic controlled braking resistors [17-26] the optimal control dynamic braking resistor [27], microprocessor controlled dynamic braking resistor [28], heuristic controlled dynamic braking resistor [29] are few other examples for the design of the thyristor controlled three phase model design.

An effective braking resistor model which is economical, smaller in size, has better switching operation & control and minimum heating loss and harmonics, is still to be explored. With the availability of the power electronics devices, new switches can be designed that can give better ON/OFF control of the braking resistor unit. So, along with

the modeling of the braking resistor models, a discrete controller is also needed that can trigger the respective switch at the right instant.

### *B. LITERATURE REVIEW:*

The barking resistor is a dummy load that is added in the power grid system during any transients occurring in the system. It not only improves the transient stability of the electric power grid, but also helps in the bulk power transmission without going out of synchronism. It is switched-in at the terminal of the electrical machine such as synchronous generator, to decrease the accelerating speed of the generator as required by the system, and is switched-out after getting the desired speed. It can be connected in series or in parallel with the system depending on its purpose such as improving the dynamic stability, low-voltage ride through of induction machines, etc.

The braking resistors are used to improve the dynamic stability of hydro generators [4], [5]. The interval for which braking resistors are inserted in the power grid system is very important to know beforehand, because longer duration of insertion of braking resistor will cause instability of the complete power grid system. The studies have been done to analyze this duration as well as the repeated use of braking resistor for achieving better transient stability. The work [4] suggests that electrical multi-cycle braking employing optimum control based on the measurement of slip and excess power is more efficient method of damping swings and improving the stability of a hydro-electric generator as compared to either single-cycle braking or high-response automatic reclouser. The bang-bang control was employed at the 1330-MW Zeya hydroelectric power plant for dynamic braking resistors [30].

In Arizona Public Service Company 292-mile transmission system from the Four Corners Plant to Phoenix [2], decelerating braking resistors are implemented for improving the transient stability as well as to increase the bulk power transmission in the existing system. It was suggested that adding 300 MW braking resistor in the existing plant would be more feasible and cost effective as compared to adding other line capacity on long transmission system for improving the transient stability of the system.

In Canada, the implementation of braking resistor was done in the Peace River 500-kV transmission system for improving the transient and dynamic stability of grid system [8]. In 1960's, a 138 kV 600 MW braking resistor, consisting of three banks at 200 MW each, was installed on the BC Hydro system located on Peace River in order to meet design stability. One of those three resistor banks was replaced in 1987 with a new type of resistor. A load test was run onsite to verify the capability of the resistor [31] . It was shown that the stability was maintained following faults by employing a braking resistor and additional stabilizing signal to the generator excitation system.

In Japan, the transient stability limit power, of the Owase 275-kv, 141 km long trunk line, was 500-600 MW. In addition to that, two-phase to ground or three-phase faults occurring in the system will completely shut down the transmission line. So, a study was made to avoid the limitations by adding the electric braking resistors with the transmission lines. The transient stability of the system was improved effectively by means of electric braking, by connecting a damping resistor in parallel with the generator bus line at the fault occurrence [9].

Similarly, by installing 1400-MW dynamic braking resistor at the Bonneville Power Administration's Chief Joseph Substation, system stability in the Pacific Northwest [10]

has been enhanced. The capacity of the Pacific Northwest-Southwest Intertie was also increased by the use of resistor braking for faults in the Pacific Northwest-Southwest.

The control strategies are needed to determine the insertion interval of the braking resistor, so that over-loading of the power grid system as well as the over-heating of the braking resistors can be avoided. So, a lot of research studies have been done which were more concentrated on the control strategies of switching operation of braking resistor. A simple strategy based on speed deviation signal [32] was developed and successfully utilized for automatic single or multiple insertion of braking resistor, whenever required. The study showed that a fair degree of agreement between the analytical and experimental results enhances confidence in their reliability. Another control algorithm based on discrete-level generalized predictive control was examined as a possible approach for optimal control of the brake. Prony analysis was used to identify system transfer functions, which were then related to control design considerations and robustness properties [33]. Another control strategy of a variable structure control for dynamic braking resistors reported in literature [34] was tested in a multi-machine power system to improve the transient performance as well as to increase the transfer capability.

A generic methodology reported in the literature used physical control means to alleviate transient stability crisis. The minimum-angle and minimum-norm aiming strategies were used to provide explicit feedback solutions to the control problem. Several choices of the aim state were proposed in [35] and [36] . Simulation results show that both these methods result in an improvement of the critical clearing time, and that they result in a more desirable state trajectory than simple on/off control based on angular-velocity measurements.

For enhancing the transient stability of hydro generators, a dynamic braking resistor is proposed together with a tuned-existing governor to improve the stability margin of a hydro generator [37]. Root locus and Routh's stability criterion are used to obtain proportional-integral-derivative (PID) controller parameters of the governor. The dynamic braking resistor was designed to operate with reduced harmonic injection during its operation. The proposed technique prevents the speed going beyond its limit, when load rejection takes place due to fault in the power system. Hence, the total or partial power system failures can be avoided.

Besides the control strategies, studies have been done for the integrated use of braking resistors with any other stability improving devices such as the study of integrated and coordinated control of generator exciter, steam turbine and shunt braking resistor [38] to provide the maximum benefits of transient and steady state stability for a wide range of operating conditions, the study of dynamic braking strategy and excitation control for arresting the first swing instability [27], the study of the braking resistors and static var compensator (SVC) for enhancing transient stability [39], the study of coordinated fast valving and braking resistor control for balancing the mismatch between mechanical input power and electrical output power [40], etc. In [27], a comparison is made among braking resistor, resistor-reactor and resistor-capacitor strategies with and without excitation control. The control strategies are obtained in terms of system states and other measurable quantities.

The combined effect of FACTS devices and braking resistors such as the fault current limiter and the thyristor controlled braking resistor (TCBR) [41], [42], thyristor controlled resistive brake and SVC [43], system damping resistor and series - shunt capaci-

tors [44], are also reported in the literature. It is suggested in [41], [42] that by using both the fault current limiter and the TCBR, the transient stability can be enhanced. Following a major disturbance in power system, the fault current limiter operates for limiting of the fault current, enhancement of the transient stability and suppression of the turbine shaft torsional oscillation, and then the TCBR operates with the objective of fast control of generator disturbances. The study indicates a significant power system stability enhancement and damping turbine shaft torsional oscillations. The combination of thyristor controlled resistive brake and SVC [43] are modeled and coordinated for the small signal stability investigation. The performance of the systems studied is based on the minimum integral squared error.

The transmission capability limit of a system can be enhanced by using system damping resistor and series - shunt capacitors [44]. The system damping resistor is very effective for short distance transmission lines such as 50 km or so. For long distance transmission lines, experimental results indicate that the transmission lines compensated by series capacitor are effective. By using the FACTS technology, the new system stabilizing technique was proposed [45].

During any large load interruption, maintaining transient stability is more important. Hence it is required that the proper switching operation of switchable supplementary controls such as dynamic brakes, shunt reactor, series capacitor, thyristor switched resistor, etc. should occur. Many switching controls based on different input from generators are reported in literature. For dynamic brakes, shunt reactor or series capacitor, a dynamic programing based switching strategy in the form of close-loop is analyzed [46]. For dynamic braking resistor and shunt reactor, a control strategy based on the time optimal

control is proposed [47]. The time optimal control is derived as a function of synchronous machine power, its rotor angular position, and speed deviation. It is found that the strategy is very effective in controlling the first swing instability. Similarly, for series capacitor control and braking resistor control, a control strategy based on nonlinear, variable-structure control theory is proposed [48]. For the idealized control, only two switching applications are required, which suggests that the controller will be easily realized and reliable.

For thyristor controlled braking resistor (TCBR), a closed-loop control strategy derived using direct Lyapunov method and non-linear multi-machine system model is noted in literature [49]. The control law has been derived using direct Lyapunov method and non-linear multi-machine system model. It is optimal in the sense that it causes the quickest dissipation of the power system energy released by a disturbance. Another close-loop control strategy, for TCBR based on equal area criterion (EAC) is designed for generating triggering pulses for the thyristor switch [50]. A conventional and a fuzzy logic controller have been developed and compared. It has been shown that the mentioned approach provides a simple and effective method for the transient stability improvement.

Another control method for the thyristor controlled dynamic braking resistor and the nonlinear optimal control theory noted in literature is based on a hierarchical framework for coordinating multiple dynamic-braking units during the transients ensuing major disturbances [51-55]. The control strategy considered is designed for two different hierarchy frameworks, a two-level hierarchy and multi-level hierarchy. This creates a multiple local feedback controllers that can be realistically implemented using only local measurements and whose performance is consistent with respect to changes in network configuration,

loading and power transfer conditions. For the control strategy mentioned, following a major disturbance, the rotor angle and rotor speed of each generator unit are determined and the firing angle of the thyristor switch associated with the braking resistor is calculated by the local controllers.

The closed-loop control laws, capable to realize multiple switching operations of a resistive brake aiming at enhancement of power system stability, is formulated as a multi-stage decision problem. By using a model-based reinforcement learning method, known as prioritized sweeping, the control law is computed [56], [57].

The implementation of braking resistor in a network not only supports the bulk power transmission, but also helps improve the transient stability. There are impacts on the turbine-generator shaft sections when subjected to various power system disturbances and switching operations [58].

The dynamically controlled, three phase resistor bank, can be used to damp shaft torsional oscillations in large steam turbo-generators [59]. The torsional damping can be achieved by using a control strategy based on generator speed. The substantial damping can be achieved with a relatively small resistor bank, thus reducing the risk of significant shaft damage due to electrical disturbances. Another mentioned control strategy for thyristor-controlled dynamic resistance braking for damping torsional oscillations in a power system is based on modal control theory. A PID controller is designed for thyristor-controlled dynamic resistance braking in order to stabilize all sub-synchronous resonance modes in the power system [60].

Similarly, for damping the torsional oscillations in large turbo generators, the control system of TCBR is designed by using the pole placement technique [61] and [62]. A dy-

namic fundamental frequency model for TCBR is developed. The study indicates that substantial damping is achieved not only for the torsional oscillatory modes but also for the inertial mode by using the proposed control system. It presents a new concept for damping electro-mechanical oscillations in a large turbo generator. The proposed concept is based on coordination between power system stabilizer and TCBR. This coordination will enhance the stability of the inertial and torsional oscillatory modes.

Series compensation has been proven to increase stability in transmission of electric power, whereas series capacitor results in severe sub-synchronous torques leading to generator-turbine shaft damage. The mitigation of sub-synchronous transient torques is achieved through resistor bank controlled by fuzzy logic controller [63].

During unsuccessful reclosing of circuit breakers, the damping of turbine-generator shaft torsional oscillations can also be achieved by the coordinated implementation of fuzzy logic-controlled braking resistor and optimal reclosing [19]. The effect of the coordination of optimal reclosing and fuzzy logic-controlled braking resistor on the transient stability of a multi-machine power system in case of an unsuccessful reclosing of circuit breakers is studied. The studies show that the transient stability performance of the coordinated operation of optimal reclosing and fuzzy controlled braking resistor is better than that of the coordinated operation of conventional auto-reclosing and fuzzy controlled braking resistor [18].

More control strategies for damping the slowly growing sub synchronous resonant frequency oscillations are noted in literature, such as a control strategy for dynamic braking resistors employing generator speed variation, rotor angle and power variation signals to switch in braking resistors at the generator terminal [64], control strategy for dynamic

braking designed through fuzzy logic control theory through classical minimum-time strategy [65]. The dynamically switched braking resistors are proved to control the unstable modes very effectively.

The use of dynamic braking as a cost-effective measure for damping inter-area oscillations is also noted in literature. The control scheme for this purpose is based on commanded electrical power calculated by the respective model transformation. The model is formed based on the measurements provided by phasor measurement units and data collected from energy management system [66]. Fuzzy controlled braking resistors are designed for providing better control of BR unit for switching in and out from the grid system to improve the transient stability of the system [17-26].

With all the existing models and design available, it is necessary to implement a cost effective, low maintenance generator brake. Many topologies have been proposed but a standard topology is not yet formed. A full wave thyristor controlled and a half wave TCBR models have been proposed to provide a more cost effective and economic braking resistor models [11-16]. A fuzzy logic based control law is designed for both the braking resistor models. Similarly, other two types of braking resistor configuration, a 3-phase, bi-directional, full wave, Y-connected phase-controlled ac/ac converter, and a 3-phase, full wave, thyristor-controlled rectifier bridge, have also been noted in literature [67] [29]. A simple rule-based ‘ON-OFF’ control law for braking resistor based on the local measurements of generator output real power and its derivative is designed.

It is established that the application of a braking resistor at the generator terminal enhances significantly the power transfer limit over a transmission line. A cost effective brake resistor is also proposed using developments in thick film, metal oxide resistors.

The brake has very low resistance and virtually no inductance, allowing its use during a fault to slow a generator's acceleration [68].

The application of the dynamic braking resistor for improving the transient stability of synchronous generators used for hydro-power plants and thermal power plants is well established. Now, its implementation with induction generators is also explored. An induction generator draws a large amount of reactive power from the system if it accelerates to a high speed, which could result in voltage collapse. The voltage collapse occurring can be mitigated by using braking resistor based method [69] and the stability performance of distribution systems with induction generators can be enhanced. Also, the coordinated operation of static synchronous compensator (STATCOM) and dynamic braking resistor improves the stability of a large wind farm [70]. The STATCOM supplies the reactive power demand of the wind farm dynamically in order to maintain the network voltage. The dynamic braking resistor is controlled by Liapunov's stability criterion to absorb the active power of the wind farm during the network fault.

A control scheme for the low-voltage ride-through capability of a 2 MW full converter wind turbine with permanent magnet synchronous generator is designed emphasizing the regulation of the dc-link voltage and minimization of the drive train torque surplus [6].

The fault-ride through is a necessary grid requirement for all the large wind farms interconnected to the power network. A novel alternative technology is proposed that inserts series resistance into the generation circuit. The series dynamic braking resistor dissipates active power and boosts generator voltage, potentially displacing the need for pitch control and dynamic reactive power compensation [71].

The renewable energy power plants are being integrated with the existing power grid system. Many of these generators are synchronous machines with low values of inertia, and thus possess short critical clearance times to avoid the onset of transient instability. With fault clearance times of up to 1s occurring in distribution networks, there is the potential for a growing problem, as distributed generation makes up a larger proportion of installed capacity. The series braking resistors, switched into circuit at the generator terminals, improve the transient stability [72]. Similar close-loop braking resistor control strategy for wind generator synchronous is introduced to enhance the transient stability of the grid system [25].

### *C. NOVELTY IN THIS WORK*

Based on all the available literature for the dynamic braking resistor and power electronic switches, the highly efficient braking resistor models are designed and tested on the simulated power grid system. The initial purpose is to design a braking resistor model using a single unit of braking resistor that will not only reduce the size of the braking resistor model, but also reduce the overall cost of the braking resistor.

Two new braking resistor models, namely rectifier controlled braking resistor (RCBR) model and chopper rectifier controlled braking resistor (CRCBR) model are designed in this work. The switches of these models are designed by using highly efficient power electronics devices. Novelty of these models is that both models use one unit of braking resistor as compared to three units of braking in the existing thyristor controlled braking resistor (TCBR) model [17] for the three phase system.

The other important part is to design a closed-loop controller that will sense the change in the characteristics of the synchronous generators connected to a grid system

and generate required triggering pulse. As mentioned earlier, the deviation in the active power, rated voltage, rotor angle or speed can be used to design the controller input. For this work, the change in speed is taken as the input to the controller and respective triggering pulse is generated.

Models are implemented by using MATLAB/Simulink software, and are tested considering both balanced and unbalanced temporary and permanent faults in a single generator and multi-machine power grid models.

# II. POWER SYSTEM STABILITY AND ITS CLASSIFICATION

With the integration of non-renewable power plants and the expansion of existing power grid system, the necessity to maintain the power system stability increases especially in terms of transient stability. The stabilization of transient stability helps in maintaining the continuous power supply, as well as transmission of bulk power through the long transmission lines without adding new transmission line.

## *A. BASIC CONCEPTS OF POWER SYSTEM STABILITY*

Power system stability is broadly defined as the property of the power system that enables the system to remain in a state of operating equilibrium after being subjected to a disturbance [73]. Instability in a power system is manifested in many different ways depending on the system configuration and operating mode. Traditionally, the stability problem has been one of maintaining synchronous operation. Since power systems rely on synchronous machines for generation of electrical power, a necessary condition for satisfactory system operation is that all synchronous machines remain in synchronism or, colloquially, “in-step”. This aspect of stability is influenced the dynamics of generator rotor angles and power-angle relationships. Instability may also be encountered without loss of synchronism such as the collapse of load voltage due to induction motor load fed by a synchronous generator. This chapter describes the basic concepts and problems of power system stability [74].

The stability is a condition of equilibrium between two opposing forces namely the mechanical input power and the electrical output power as in (1). The electrically connected synchronous machines try to maintain the synchronism by the restoring forces acting between them. When there is any fault in the system, due to opening of circuit break-

ers, power supply to some of the loads is interrupted. This results in the decrease in the electrical power but the mechanical power input to the system remains the same. This mismatch results in the increase in the speed of the synchronous generators in terms of accelerating power. This leads to the instability of the system.

The transient disturbances occurring in the system could be continuous change in load, the transmission line faults, the sudden drop in large load from the system, or switching of the large induction machines, etc. Depending upon the disturbances occurring, the measures are taken to maintain the stability and the synchronism of the power grid system. The understanding of stability problems is greatly facilitated by the classification of stability into various categories.

### *B. CLASSIFICATION OF POWER SYSTEM STABILITY*

The classification of power system stability is needed to analyze and study the stability problems properly. The classification of power system proposed in [73] is based on the following considerations:

a) The physical nature of the resulting mode of instability as indicated by the main system variable in which instability can be observed.

b) The size of the disturbance considered which influences the method of calculation and prediction.

c) The devices, processes and the time span that must be taken into consideration in order to assess stability.

The power system stability is broadly classified as rotor angle stability, frequency stability and voltage stability. The complete classification of power system stability, suggested in [73], is shown in Figure 1.

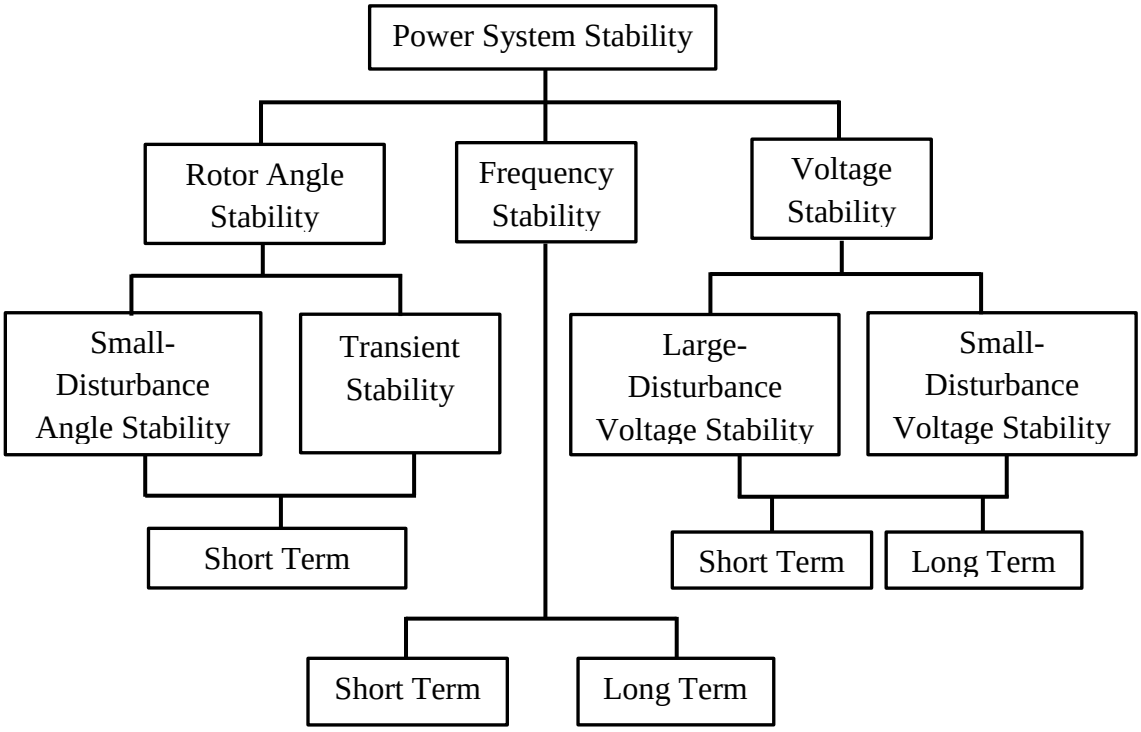


Figure 1: Classification of power system stability.

The disturbances occurring in the system may cause the instability of the system and may cause the interruption of power supply to the consumers as well as affect the plant economy. The instability depends on the system configurations and operating modes.

### *C. TRANSIENT STABILITY*

Transient stability is related to the ability of the power system to maintain synchronism when subjected to severe disturbance, such as short circuit on transmission line, sudden loss of a large load, etc. It depends on both the initial operating state of the system and the severity of the disturbance [74]. Various control strategies to improve the transient stability are discussed in literature review section of this thesis. The literature review indicates that the measures to improve the transient stability depend on transient stability limit and critical clearing time of the power grid system.

The transient stability limit refers to the maximum flow of power possible through a point in the system without the loss of stability when a sudden disturbance occurs.

The critical clearing time is the maximum time between the fault initiation and it's clearing such that the power system is transiently stable. This includes relay and breaker operating times and possibly the time elapsed for the trip signal to reach the other end breaker. Clearing times are in the range of a few power frequency cycles in modern power systems employing high-speed circuit breakers (1-cycle breakers are in service) and solid-state relays.

The methods to improve transient stability can be classified under four categories as mentioned below:

i) Minimization of disturbance severity and duration

ii) Increase in forces restoring synchronism

iii) Reduction of accelerating torque by reducing input mechanical power

iv) Reduction of accelerating torque by applying artificial load

The recovery of a power system subjected to a severe large disturbance is of interest to system planners and operators. Typically the system must be designed and operated in such a way that a specified number of credible contingencies do not result in failure of quality and continuity of power supply to the loads. These calls for accurate calculation of the system dynamic behavior, which includes the electro-mechanical dynamic characteristics of the rotating machines, generator controls, SVC, loads, protective systems and other controls. The commonly known methods to enhance the transient stability of a system are as follows:

a) High-speed fault clearing,

b) Reduction of transmission system impedance

c) Shunt compensation

d) Dynamic braking

e) Reactor switching

f) Independent and single-pole switching

g) Fast-valving of steam systems

h) Generator tripping

i) Controlled separation

j) High-speed excitation systems

k) Discontinuous excitation control

l) Control of high voltage direct current (HVDC) links

Transient stability analysis can be used for dynamic analysis over time periods from few seconds to few minutes depending on the time constants of the dynamic phenomenon modeled. The insertion of braking resistor is an effective measure to improve the transient stability of the system.

# III. MODELING OF BRAKING RESISTOR MODELS

Braking resistor is one of the most efficient and widely used external control methods to improve the transient stability of the power grid system. It is a dummy load connected in series or in parallel with the synchronous generators to maintain power system stability of the power system whenever any large disturbances occur in the system. The proposed two new braking resistor models are designed and the performance of the newly designed models is compared with the existing TCBR model. The design of new models and existing models are described in details in following section. The controller designed for all three models to generate their respective triggering pulses is also described in the following sections.

## *A. CONNECTING POINT OF BRAKING RESISTOR:*

The braking resistor models can be connected in two ways with the synchronous generators. They can be connected directly to the terminals of the synchronous generators, as shown in Figure 2 [13] but it will increase the cost of implementing the braking resistor, and also if a number of generators are connected in parallel in a network, then braking resistor is needed to be added at each generator terminal. The other position of adding braking resistor model without exceeding the basic cost is at the high voltage side of the synchronous generator step-up transformer as shown in Figure 3 [22]. For a multi-machine system, an optimal insertion point for braking resistors can be determined so that minimum braking resistor models can be used without increasing the cost [75].

For this work, the braking resistor model is connected at the high voltage terminal of the synchronous generator (Tr.-SG) through a step-down transformer (Tr.-BR) as shown in Figure 3. A step-down transformer is needed for the insertion of braking resistor, be-

cause the rated voltage ratings for the power electronics devices assumed for this work is 6.6 kV.

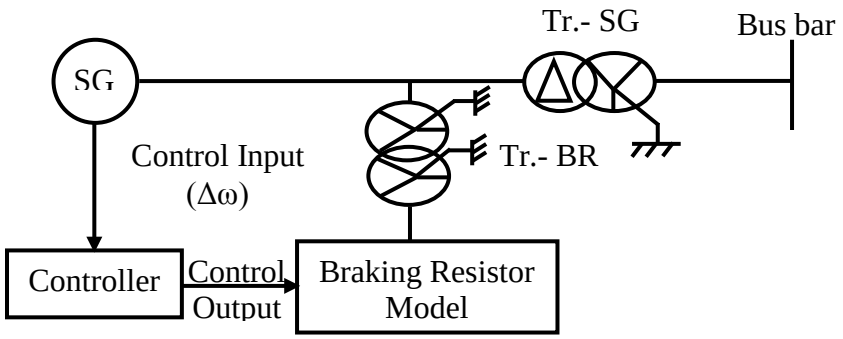


Figure 2: Line diagram of braking resistor model connected directly at the terminal of the synchronous generator.

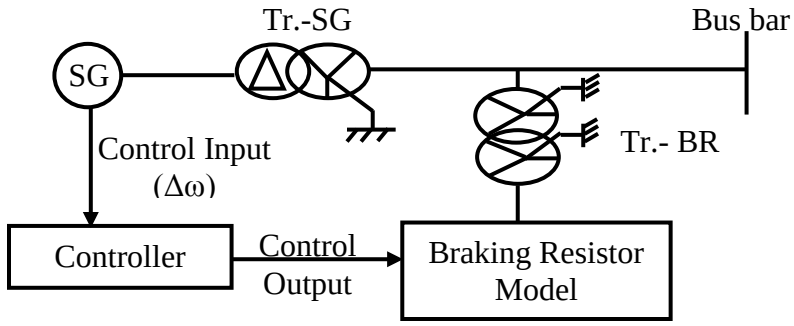


Figure 3: Line diagram of braking resistor model connected on high voltage side of synchronous generator.

### *B. Switch Elements Of Braking Resistor Models*

Due to the development of power electronic devices, different switching mechanisms have been developed for improving the power system stability. In this work, thyristors,

diodes and insulated gate bipolar transistor (IGBT) power electronic devices have been used for designing three different switches for the braking resistor models.

A thyristor is a solid-state three-terminal power electronic device with larger power handling capability [76]. It is actually a latching device that can be turned on by the control terminal (gate) but cannot be turned-off by the gate. It acts as a directional switch because of its property to conduct only once in one cycle of input voltage signals. If the thyristors are forward biased, then they conduct for the positive half-cycle of the input voltage signal; and if reverse biased, then they conduct for the negative half-cycle of the input voltage signal. This property of thyristor is exploited in designing the existing TCBR model switch as well as rectifier controlled braking resistor model switch. The switching of thyristor is done by the firing angle or delay angle, $\alpha$, which is defined as the electrical angle at which the thyristor is turned on, after it is forward-biased or reverse-biased.

An IGBT is a three-terminal power semiconductor device primarily used as an electronic switch. It requires less base current for turning on of the transistor, thereby reducing the size and complexity of the gate drive circuit [77]. It is a highly efficient and fast switching device. This property is used to design a DC to DC converter also called as chopper circuit in the chopper rectifier controlled braking resistor model switch.

Another power electronic device used to design the braking resistor models is diode. It is a two-terminal solid state unidirectional device with asymmetric transfer characteristic. It offers low resistance path to current for a forward biased diode. Hence, current can flow only in one direction. It is an uncontrolled power electronic device used to design an uncontrolled rectifier circuit in chopper rectifier controlled braking resistor model switch. The basic design of all three models is described in detail in next sections.

*C. BRAKING RESISTOR MODEL DESIGNS*

The designs of the existing braking resistor model and the proposed braking resistor models are discussed in next sections.

*1. Thyristor Controlled Braking Resistor (TCBR) Model*

The TCBR model taken from [17] is used as a reference model to provide a comparative study with the proposed models. The TCBR model, as shown in Figure 4, consists of two controlled thyristors connected back-to-back in series with the single braking resistor unit, BR, which is grounded, for a per phase system. The Figure 4 shows three phase configuration for the power system network which is connected to the main system through step-down transformer (Tr.-BR). The back-to-back connected thyristors are acting as a controlling switch for the braking resistor model, hence the firing angle, $\alpha$, for this circuit varies between 0˚ and 180˚.

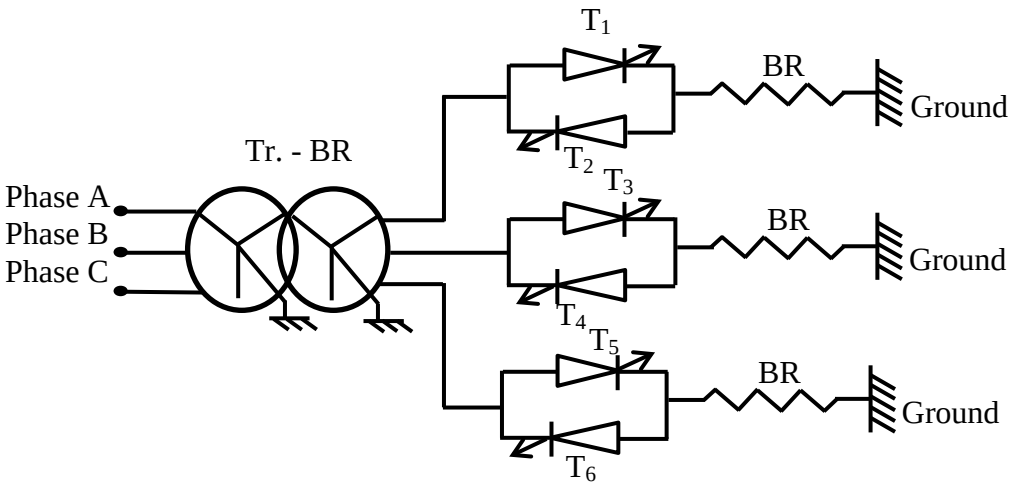


Figure 4. Line diagram of Thyristor Controlled Braking Resistor (TCBR) model.

Thyristors $T_1$, $T_3$ and $T_5$, shown in Figure 4, are forward-biased, so they operate for the positive half cycle of voltage waveform, and thyristors $T_2$, $T_4$ and $T_6$ are reverse-biased, so they operate for negative half cycle of voltage waveform. Following a fault, the current will flow through the BR unit, if the thyristors $T_1$, $T_3$ and $T_5$ or thyristors $T_2$, $T_4$ and $T_6$ are in ON state. The thyristors are triggered by the firing angle, α, generated by the designed controller. The braking resistor unit BR consumes the excessive transient energy and decreases the accelerated power by consuming excessive transient energy. The average power consumed by the braking resistor unit is given by

$$P_{BR} = \frac{1}{\pi}\int_0^{\pi} v.i_R.d(\omega t) = \frac{{V_g}^2.}{\pi R_{BR}}(\pi - \alpha + 0.5\,Sin(2\alpha)) \quad (W) \qquad (3)$$

where, $v$ is the instantaneous value of generator terminal bus voltage, $i_R$ is the instantaneous value of current through BR unit, $V_G$ is the rms value of generator terminal bus voltage, $\alpha$ is the firing angle needed to trigger the thyristor switch, $P_{BR}$ is the average power absorbed by the braking resistor and $R_{BR}$ is the resistance value of BR unit for the TCBR model.

*2. Rectifier Controlled Braking Resistor (RCBR)Model*

The proposed RCBR model, shown in Figure 5, consists of a rectifier circuit in series with single BR unit [78]. The three phase rectifier circuit consisting of six controlled thyristors, coverts AC voltage into DC voltage, which is fed to the single BR unit. All the thyristors are connected in forward biased condition and form control switch for the BR unit. Once the thyristors are triggered by the firing angle, $\alpha$, they act as unidirectional diode device.

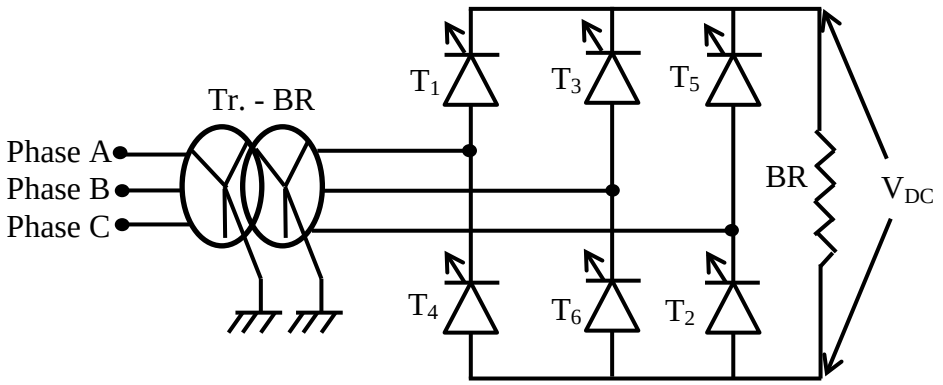


Figure 5: Line diagram of Rectifier Controlled Braking Resistor (RCBR) Model.

For rectifier operation, the firing angle, $\alpha$, should vary between 0˚ and 90˚. The DC voltage, $V_{DC}$, that appears across the BR is calculated by using (4), and the power consumed by the braking resistor unit BR is calculated by (5)

$$V_{DC} = \frac{3\,V_m}{\pi}\cos\alpha \;\; (V) \tag{4}$$

$$P_{BR} = \frac{(V_{BR})^2}{R_{BR}} \;\; (W) \tag{5}$$

where, $V_{DC}$ is voltage across BR, $V_m$ is the peak of the line voltage across the thyristor rectifier circuit, $\alpha$ is firing angle for thyristors, $P_{BR}$ is total power absorbed by the BR unit, and $R_{BR}$ is the resistance value of the BR unit of RCBR model.

*3. Chopper Rectifier Controlled Braking Resistor (CRCBR) Model*

The proposed CRCBR model consists of uncontrolled diode rectifier and chopper circuit. The CRCBR model has better benefits over RCBR model in terms of high efficiency and fast switching circuit [77] with reduced harmonic contents. The uncontrolled diode

rectifier converts the AC voltage into DC voltage, and the chopper switch converts the DC voltage into DC voltage that acts as DC/DC converter.

The CRCBR model, as shown in Figure 6, consists of three phase uncontrolled diode rectifier circuit, DC link capacitor, controlled chopper switch (CS) and single BR unit. The uncontrolled diodes are unidirectional devices, connected in forward biased condition. The diode rectifier unit transforms AC voltage and current into DC voltage and current. A capacitor (C) is needed to maintain minimum DC voltage across the diode rectifier and given by (6). When the voltage across the capacitor increases beyond its rated capacity, extra voltage is dissipated as heat energy through the BR unit. The chopper circuit consists of IGBT power electronic device. The function of chopper switch is to turn-on when the duty cycle, *d*, is 1 for full conduction of BR unit and turn-off when duty cycle, *d*, is 0 for no conduction of BR unit.

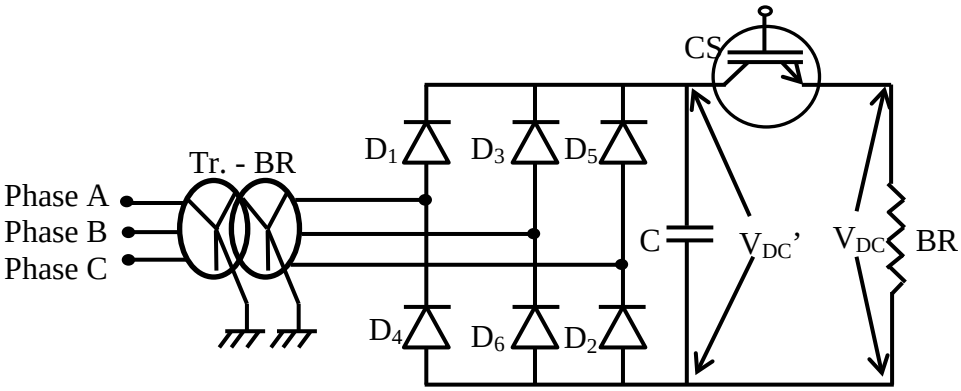


Figure 6: Line diagram of Chopper Rectifier Controlled Braking Resistor (CRCBR) Model**.**

Following a fault, the current will flow through the BR unit passing through the diode rectifier circuit and chopper switch only when the IGBT is in ON state. BR unit decreases

the accelerated power by consuming excessive transient energy. The DC voltage, $V_{DC}$, across the BR unit and the power absorbed is calculated by using (7) and (5) respectively.

$$V_{DC}' = \frac{3\,V_m}{\pi} \quad (V) \tag{6}$$

$$V_{DC} = d\,V_{DC}' \quad (V) \tag{7}$$

where, $V_m$ is the peak of the line voltage across the diode rectifier, $V_{DC}$' is the DC voltage across the capacitor and also the input voltage to the chopper, $d$ is the duty cycle of chopper, and $V_{DC}$ is the voltage across the BR.

*D. Braking Resistor Values For All Models:*

The braking resistor resistance value desired for the braking operation should be such that it should not affect the synchronism of the system, provide an instant brake to the increasing speed of the synchronous generators, and can easily be coupled to the circuit network. The braking resistors were initially connected through circuit breakers, so it was necessary to know the maximum current rating of the circuit breaker that it will allow to pass through it. Secondly, the voltage rating of the braking resistors should be higher than the terminal voltage of the synchronous generators; otherwise it will affect the coupling of breakers with the network. But an exact value of braking resistors to be employed in the network is still under research.

For this work, the effectiveness of the braking resistor models were analyzed for different per unit values of braking resistors. It was found that the speed responses of all models improved with increasing per unit value of braking resistors. Hence, for this work, resistance value of the braking resistor unit for different models is calculated based

on 1.0 per unit rated power. In other words, the power absorbed by the braking resistors is equivalent to the rated power of the complete network. The resistance value of BR unit for all models is calculated considering full conduction mode.

For the TCBR model switch, the firing angle, $\alpha$, is 0˚ for full conduction of BR unit. By solving the power equation (3) for $\alpha = 0$, the resistance of BR unit, $R_{BR}$ (8) can be derived. For the RCBR model switch, the firing angle, $\alpha$, is 0˚ for full conduction of BR unit. So, by solving the voltage equation (4) for $\alpha = 0$, and substituting $V_{DC}$ in (5), the resistance of BR unit, $R_{BR}$ (9) is derived. Now for the CRCBR model switch, the chopper switch action is based on ON/OFF status. So, the duty cycle, $d$, for this switch should be 1 for full conduction. From (6), the voltage across capacitor, $V_{DC}'$, will completely be reflected across the BR unit, hence $V_{DC} = V_{DC}'$. The resistance of BR unit can be calculated by (9).

$$R_{BR} = \frac{{V_g}^2}{P_{BR}} \quad (\Omega) \tag{8}$$

$$R_{BR} = \frac{{V_{DC}}^2}{P_{BR}} \quad (\Omega) \tag{9}$$

Where, $V_g$ is the voltage across BR unit for TCBR model, $V_{DC}$ is the voltage across BR unit for RCBR and CRCBR models and $P_{BR}$ is the power absorbed by BR unit.

*E. CONTROLLER DESIGN FOR BRAKING RESISTOR MODELS*

As mentioned in literature, multiple inputs such as rotor angle, voltage, speed, power, and etc. from the synchronous generator can be sending as an input to the controller for designing a suitable braking resistor model. In this work, change in speed of the synchro-

nous generator (i.e., the speed at transient state - the speed at steady state), $\Delta\omega$, is considered as an input to the controller and the respective output is generated.

Three different BR models, discussed in this work, need different switching pulses for triggering respective switches. A control block diagram of the controller designed for this work is shown in Figure 7. It consists of a classical PID controller and a limiter. The controller takes the change in speed of synchronous generator, $\Delta\omega$, as an input, and provides its output to the limiter block. A limiter is used to limit the output of PID controller within the range $L_{Min}$ and $L_{Max}$ as required by each model. The final control output from the controller block is fed to the respective switch of each model as shown in Figure 4-6.

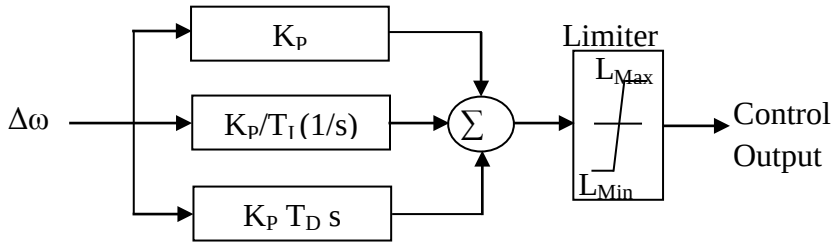


Figure 7: A control block of controller designed for all braking resistor models.

The change in speed of the generators, $\Delta\omega$, connected in the network, can be measured by using phasor measurement unit (PMU) or the remote terminal units (RTUs). Then it can send to the controller to generate the triggering pulses.

The TCBR model, shown in Figure 4, needs firing angle, α for triggering the two thyristors connected back-to-back. For the positive half cycle, the thyristor, $T_1$, operates, and for the negative half cycle, the other thyristor, $T_2$, operates. For full conduction of the BR, the firing angle, α, should be $0^o$ and for no conduction of BR unit, it should be $180^o$.

Therefore, the controller block generates control output as firing angle, α, which varies between $0^o$ and $180^o$.

The RCBR model, shown in Figure 5, needs firing angle, α, for triggering the thyristor full wave rectifier circuit. For full conduction of BR unit, the firing angle, α, for thyristors, should be $0^o$ and for zero conduction of BR unit, it should be maintained at $90^o$. Therefore, the controller block generates control output firing angle, α, that varies between $0^o$ and $90^o$.

The CRCBR model, shown in Figure 6, needs duty cycle, *d*, for triggering the uncontrolled diode rectifier and controlled IGBT chopper switch, CS. The controller switch needs 1 and 0 for ON and OFF states of IGBT device. Therefore, the controller block generates control output duty cycle, *d*, which varies between 0 and 1.

The insertion of braking resistor model is needed in the circuit only when the $\Delta\omega$ exceeds a preset value. For avoiding excessive heating of braking resistor units and chattering effect in the TCBR model BR unit, a preset limit for $\Delta\omega$ is set at 0.001 p.u. of rated speed. This limit for controller is also chosen such that the power grid system gets stabilized as quickly as possible, and the BR is not inserted into power grid system for a long time so as to avoid overheating of BR units.

When $\Delta\omega$ increases beyond this preset value, the control output is generated and fed to the respective switches of braking resistor models. The triggering of the respective switches of the braking resistor model inserts the braking resistor model in the network, resulting in decrease in speed of the generator.

# IV. TRANSIENT STABILITY ANALYSIS OF SMIB SYSTEM

The effectiveness of the proposed models is needed to be tested and compared with the effectiveness of the existing braking resistor models before its implementation with the real power grid system. Matlab/Simulink software is used to simulate and test all braking models with two power grid systems, namely a single machine system and a multi-machine system. The performances of all three braking resistors are analyzed and compared in case of both balanced and unbalanced temporary and permanent fault conditions for a simulation time of 15 sec.

## *A. SINGLE MACHINE INFINITE BUS SYSTEM (SMIB) MODEL DETAILS*

The SMIB power grid system [23] is shown by a single line diagram in Figure 8. The system model consists of a single synchronous generator (SG, rated as 1000MVA, 20KV, 50 HZ) feeding an infinite bus through a step up transformer rated as (20KV/500KV) and a double circuit transmission line system. The parameters for the synchronous generator used in this work are taken from [23] and shown in Table 1, and also the transmission line parameters are shown in Figure 8. The governor system (GOV) and the automatic voltage regulator (AVR) system are also used for the analysis purpose to provide transient stability to the power grid system. The circuit breakers (CB), are connected in the power grid system as a primary protection device during the fault condition. The steady state values obtained for the synchronous generator are shown in Table 2.

### *1. Elements of Power Grid System*

The governor system also known as speed governor system controls the steam input to the turbine connected to the synchronous generators. It senses a speed deviation or a power change command and converts it into appropriate valve action [79]. It controls the

mechanical input to the system. The control system block of the governor system used for this work is taken from [21], and is shown in Figure 9. The $\omega_m$ and $\omega_{mo}$ are actual speed and reference speed, respectively, of the synchronous generator. The $P_{fdo}$ is the reference power input set for the GOV system and P is the actual power input to the synchronous generator.

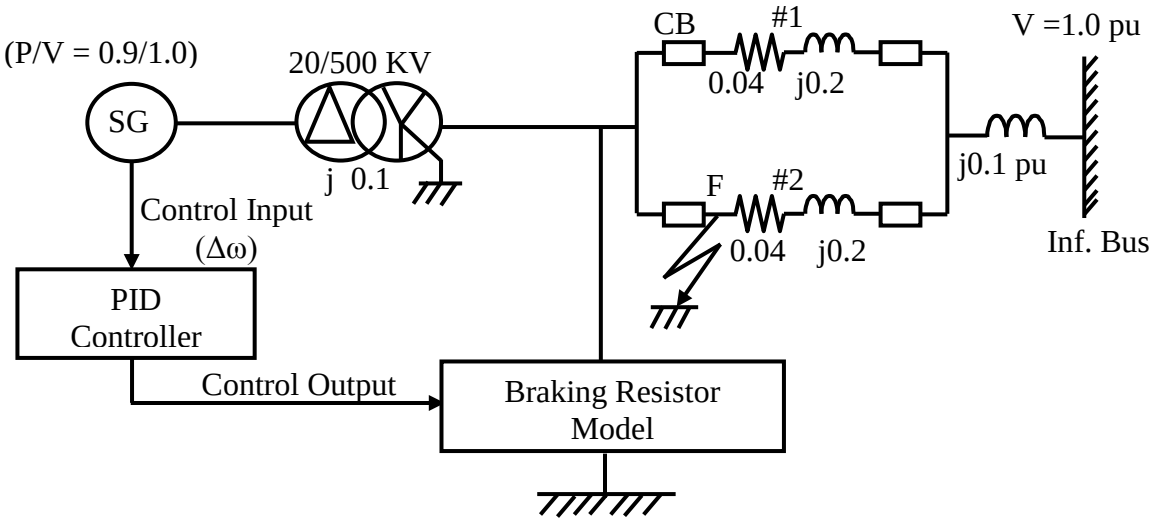


Figure 8: Single line diagram of single generator infinite bus system (SMIB).

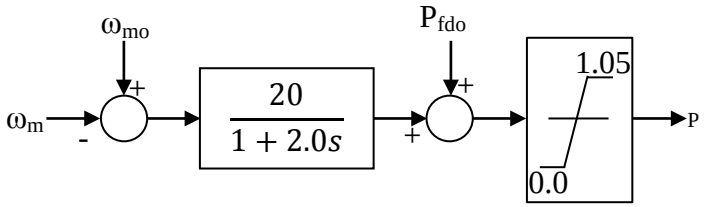


Figure 9 : The control block of governor (GOV) model.

Table 1: Synchronous generator simulation parameters for SMIB system

| | |
|---|---|
| Frequency [Hz] | 50 |
| Generator power ratings [MVA] | 1000 |
| Armature Resistance, $r_a$ [pu] | 0.003 |
| Armature leakage reactance, $x_a$, [pu] | 0.139 |
| d-axis synchronous reactance, $X_d$, [pu] | 1.79 |
| q-axis synchronous reactance, $X_q$ [pu] | 1.71 |
| d-axis transient reactance, $X'_d$ [pu] | 0.169 |
| q-axis transient reactance, $X'_q$ [pu] | 0.228 |
| d-axis sub-transient reactance, $X''_d$ [pu] | 0.135 |
| q-axis sub-transient reactance, $X''_q$ [pu] | 0.20 |
| Zero sequence reactance, $X_0$ [pu] | 0.13 |
| d-axis open circuit transient time constant, $T'_{do}$ [s] | 4.30 |
| q-axis open circuit transient time constant, $T'_{qo}$ [s] | 0.85 |
| d-axis open circuit sub-transient time constant, $T''_{do}$ [s] | 0.032 |
| q-axis open circuit sub-transient time constant, $T''_{qo}$ [s] | 0.05 |
| Inertia constant, H [s] | 2.894 |

Table 2: Generator initial values for SMIB system

| | |
|---|---|
| Generator output | 0.9 p.u. |
| Generator terminal voltage | 1 p.u. |
| Generator load angle | 60˚ |

The automatic voltage regulator also known as excitation system regulates the field voltage of the synchronous generator. For a large synchronous generator, the exciter may be required to supply field currents [79]. It is also combined with the power system stabilizer to stabilize the voltage of the power grid system. The generator output voltage is compared with a reference voltage and an error is amplified and fed to the field of a special high gain dc generator. The control system block of the automatic voltage regulator is taken from [21] and is shown in Figure 10.The $V_t$ and $V_{to}$ are actual voltage and reference voltage, respectively, of the synchronous generator. The $E_{fdo}$ is the reference excitation voltage and $E_{fd}$ is the actual excitation voltage for the synchronous generator.

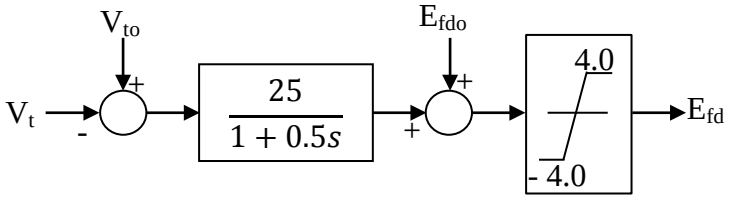


Figure 10 : The control block of Automatic Voltage Regulator.

The circuit breaker is a primary element connected in the power system to operate when a severe condition such as a fault occurs in the network. The relays connected with the circuit breaker senses the abnormality in the transmission lines such as high flow of line current and send signal to the circuit breaker to operate and cut down the faulted line from the healthy line [79].

*B. CONTROLLER PARAMETERS FOR SMIB*

The SMIB system consists of one synchronous generator. Therefore, the input to the controller, $\Delta\omega$, shown in Figure 7, is fed from the generator SG as shown in Figure 8.

Following a fault condition, when $\Delta\omega$ increases beyond the set limit of 0.001 p.u. or 3 rpm, the triggering pulses will be generated and fed to the respective braking resistor models.

The controller parameter values, $K_P$, $T_I$, and $T_D$, calculated by the trial and error method, for all different braking resistor models are shown in Table 3. The $L_{Min}$, and $L_{Max}$, is the limiter value required to limit the triggering pulses within the range. The value of braking resistor unit is calculated based on the 1 p.u. of power.

As mentioned earlier, each BR model is implemented with the same type of controller, but as triggering is different for each model, different controller parameters are required to generate required control output.

Table 3: Controller parameters and braking resistor values

| Model Type | Controller Parameter | | | Limiter parameters | | $R_{BR}$ (Ω) |
|---|---|---|---|---|---|---|
| | $K_P$ | $T_I$ | $T_D$ | $L_{Max}$ | $L_{Min}$ | |
| TCBR | 10 | 0.0001 | 0.01 | 180 | 0 | 0.04356 |
| RCBR | 7 | 0.01 | 0.0001 | 90 | 0 | 0.07952 |
| CRCBR | 1.0 | 0.0001 | 0.0001 | 1 | 0 | 0.07952 |

### *C. SIMULATION RESULTS*

For analyzing the effectiveness of the braking resistor models to enhance the transient stability of the power system network, a speed index performance, $\Delta\omega_c$, is calculated by (7). The smaller the $\Delta\omega_c$ is, the better the performance of model is.

$$\Delta\omega_c = \int_0^T |\Delta\omega|\, dt \quad p.u.\ sec \tag{10}$$

where, $T$ is the simulation time of 15.0 sec, $\Delta\omega$ is change in speed of synchronous generator. Both balanced (3LG: three phase-to-ground and 3LS: three-phase short circuit) and unbalanced (2LG: double line-to-ground, 2LS: line-to-line, and 1LG: single line-to-ground) temporary and permanent faults are considered at the fault point F of the SMIB system as shown in Figure 8.

For temporary fault, it is considered that the fault occurs at 0.1 sec and is cleared at 0.6 sec, the CB opens at 0.2 sec and recloses at 1.2 sec. For permanent fault conditions, the CB reopens at 1.3 sec, while the other simulation conditions are the same as the temporary faults. The time step and simulation time are chosen as 0.00005 sec and 15 seconds, respectively.

The speed index values, calculated by using (10) for both balanced (3LG and 3LS) and unbalanced (2LG, 2LS and 1LG) temporary and permanent faults with and without BR models are shown in Tables 4 and 5. The speed index values indicate that the proposed models performance is comparable to the existing model performance for all fault conditions. It also indicates that the proposed CRCBR model's performance is better than the proposed RCBR and existing TCBR model performances for temporary faults, but for permanent fault condition, the RCBR model performance is better than the existing TCBR and the proposed CRCBR model performances.

The speed curves for a duration of 5 seconds in case of balanced (3LG) and unbalanced (2LG and 1LG) temporary and permanent faults are shown in Figures 11 to 13 and Figures 14 to18.

The speed curves with respect to speed index, is varying accordingly for all models. The speed responses of proposed CRCBR model show better performance as compared to other proposed and existing models. The proposed RCBR model speed curves show slow decay as compared to TCBR model speed deviation curves for all faults. They also indicate that both proposed models and the existing model is stabilizing synchronous generator within small period of time without exceeding the speed limit set for 0.001 p.u. or 3 rpm by the controller.

The total power absorbed in mega-watt (MW) by braking resistor units of all three braking resistor model is shown in Tables 6 and 7. The values imply that the power absorbed by CRCBR model is more as compared to the RCBR and TCBR models. The better the speed index values, the higher the power absorbed by the braking resistor units is.

The more power absorbed by the braking resistors may result in increase in temperature of the braking resistor and affects its performance for braking. But, it is concluded that increase in temperature does not affect the performance of the braking resistor and consequently the transient stability [22].

The firing angle and power absorbed by braking resistor unit responses for TCBR, RCBR and CRCBR braking models for 3LG temporary fault are shown in Figures 17-22 and for permanent fault in Figures 23-28. The power absorbed by braking resistor follows the corresponding firing angle generated by the controller. The firing angle curves for all models indicate that the steady state stability is achieved within 2 seconds for temporary fault conditions and within 3 seconds for permanent fault condition with multiple insertion of braking resistor units. The power absorbed by braking resistor units for proposed RCBR model and existing TCBR model does not exceed the 1000 MW, but for the pro-

posed CRCBR model, the power absorbed for the first peak is 1700 MW. The CRCBR model's braking resistor unit absorbs accelerating power as well as the power generated by the synchronous generator resulting in instant decrease in speed of the generator.

Table 4 : Speed index values (in $10^{-3}$ p.u. sec) for temporary fault conditions

| Types of Fault | Without BR | With TCBR | With RCBR | With CRCBR |
|---|---|---|---|---|
| 3LG | 8.109 | 3.792 | 4.02 | 3.970 |
| 3LS | 7.968 | 3.667 | 3.97 | 3.961 |
| 2LG | 5.753 | 2.270 | 2.956 | 2.142 |
| 2LS | 3.052 | 2.203 | 2.418 | 2.242 |
| 1LG | 2.483 | 1.924 | 2.029 | 1.952 |

Table 5 : Speed index values (in $10^{-3}$ p.u. sec) for permanent fault conditions

| Types of Fault | Without BR | With TCBR | With RCBR | With CRCBR |
|---|---|---|---|---|
| 3LG | 12.35 | 6.028 | 5.415 | 5.689 |
| 3LS | 12.19 | 5.93 | 5.341 | 5.638 |
| 2LG | 11.78 | 4.231 | 4.666 | 3.872 |
| 2LS | 6.216 | 3.227 | 3.418 | 3.341 |
| 1LG | 5.287 | 2.991 | 3.303 | 3.050 |

Table 6 : Total power consumed (in MW) by the braking resistor for temporary fault conditions

| Types of Fault | With TCBR | With RCBR | With CRCBR |
|---|---|---|---|
| 3LG | 139.3 | 119.7 | 175.5 |
| 3LS | 139.9 | 117.1 | 176.2 |
| 2LG | 101.8 | 93.40 | 122.9 |
| 2LS | 76.96 | 55.59 | 87.00 |
| 1LG | 41.02 | 27.91 | 55.98 |

Table 7 : Total power consumed (in MW) by the braking resistor for permanent fault conditions

| Types of Fault | With TCBR | With RCBR | With CRCBR |
|---|---|---|---|
| 3LG | 268.2 | 156.4 | 256.1 |
| 3LS | 265.9 | 154.8 | 248.7 |
| 2LG | 285.2 | 1.72.8 | 319.1 |
| 2LS | 125.5 | 74.60 | 161.8 |
| 1LG | 79.24 | 59.48 | 102.8 |

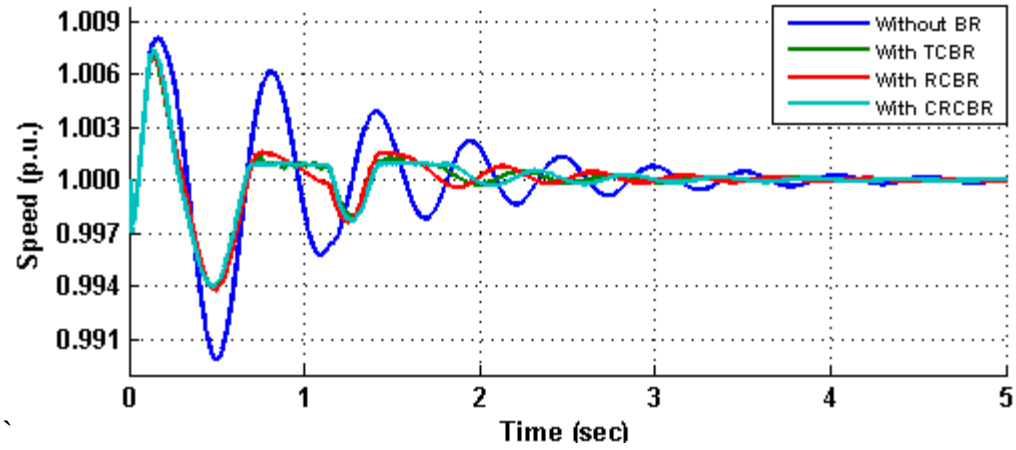


Figure 11 : Speed curves for 3LG temporary fault.

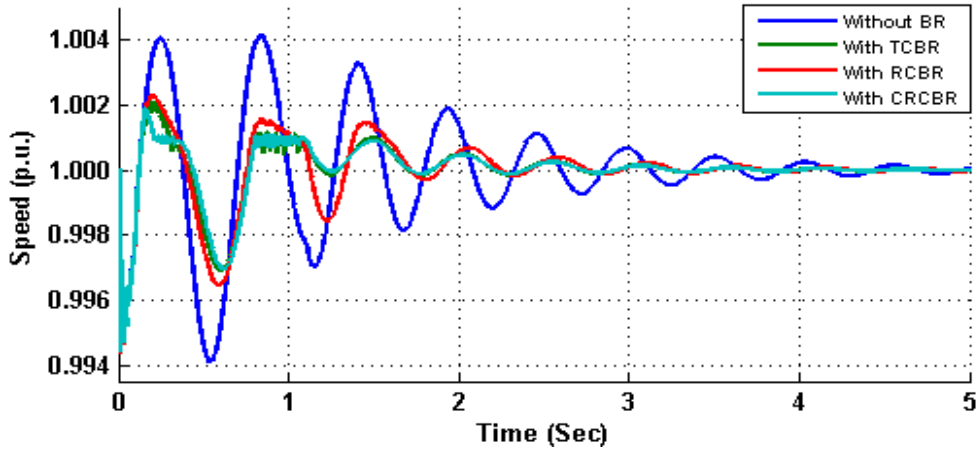


Figure 12 : Speed curves for 2LG temporary fault.

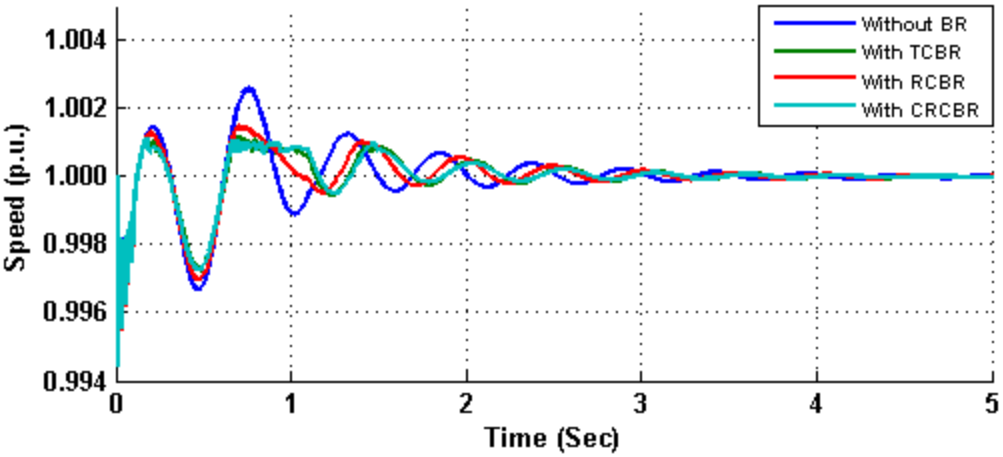


Figure 13 : Speed curves for 1LG temporary fault.

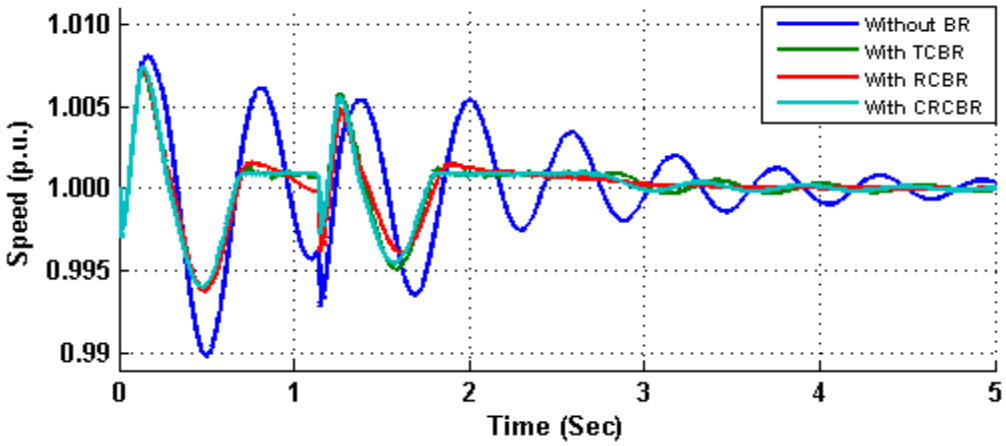


Figure 14 : Speed curves for 3LG permanent fault.

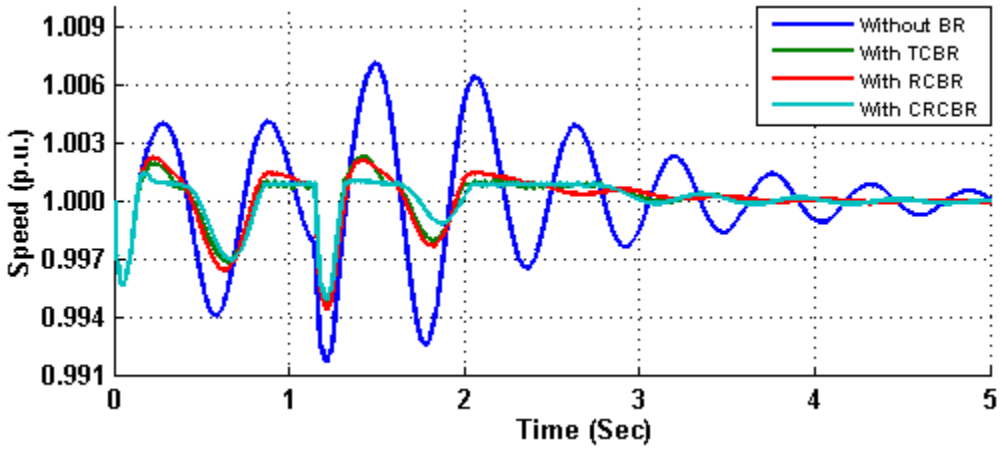


Figure 15 : Speed curves for 2LG permanent fault.

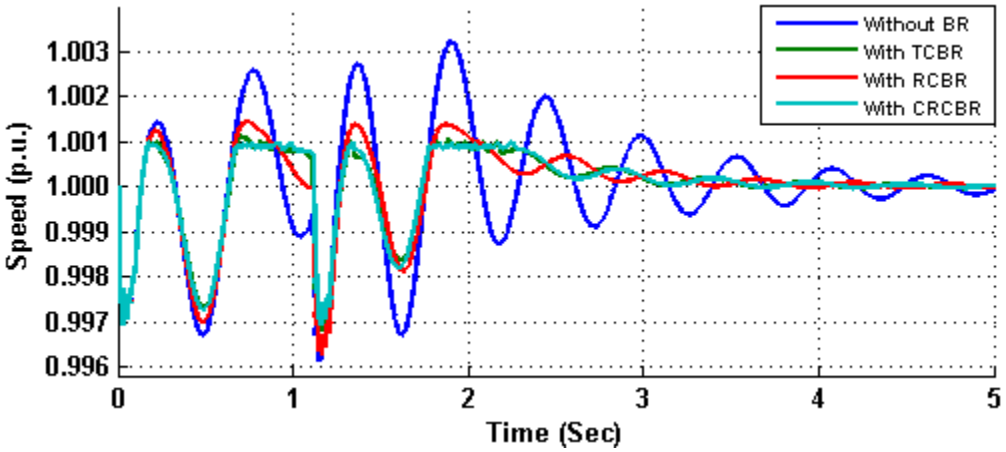


Figure 16 : Speed curves for 1LG permanent fault.

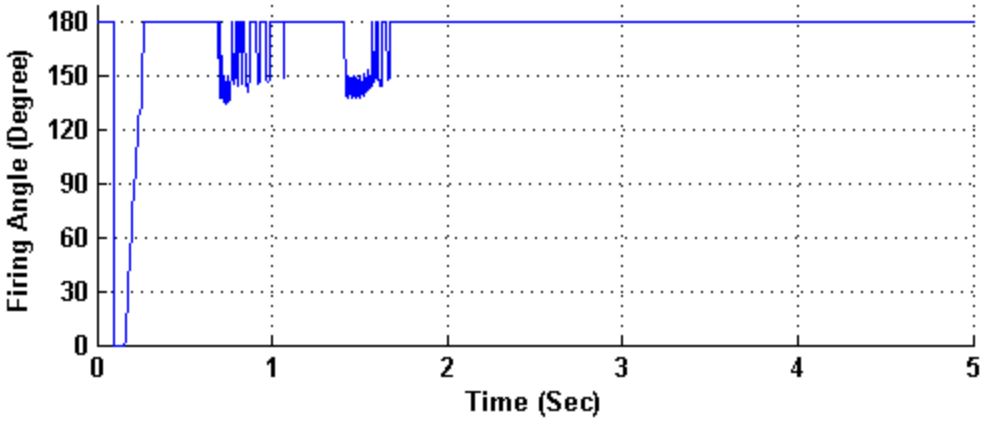


Figure 17: Firing angle generated through the controller for 3LG temporary fault for the TCBR model.

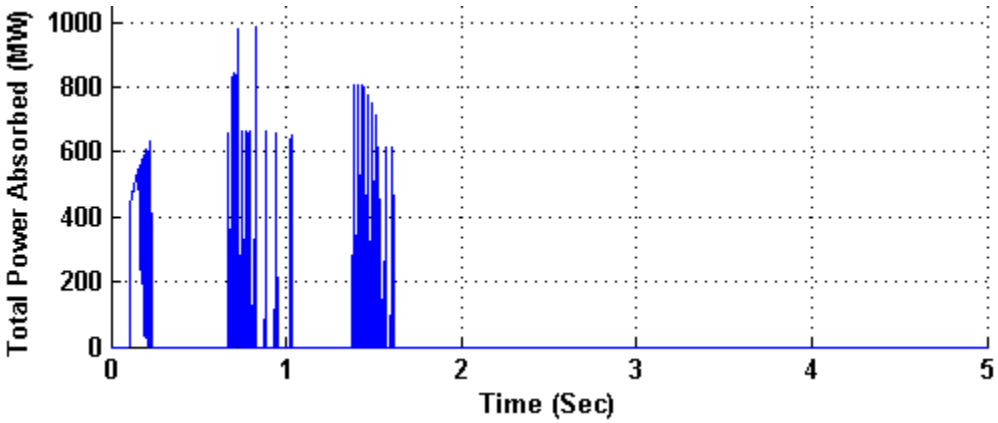


Figure 18: Total power absorbed by the braking resistor unit of TCBR model for 3LG temporary fault for the TCBR model.

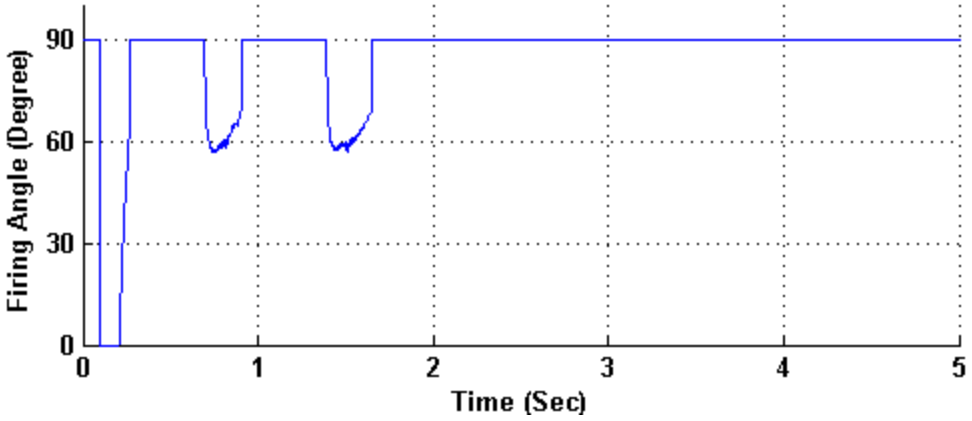


Figure 19: Firing angle generated through the controller for 3LG temporary fault for the RCBR model.

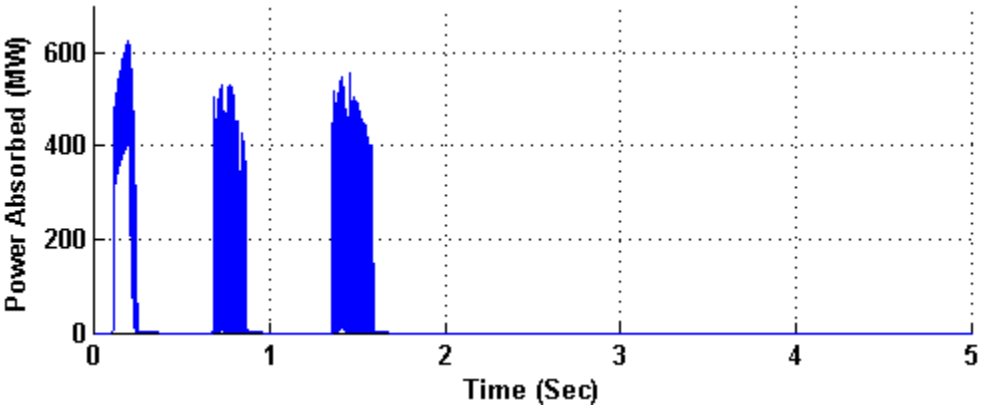


Figure 20: Power absorbed by the braking resistor unit of TCBR model for 3LG temporary fault for the RCBR model.

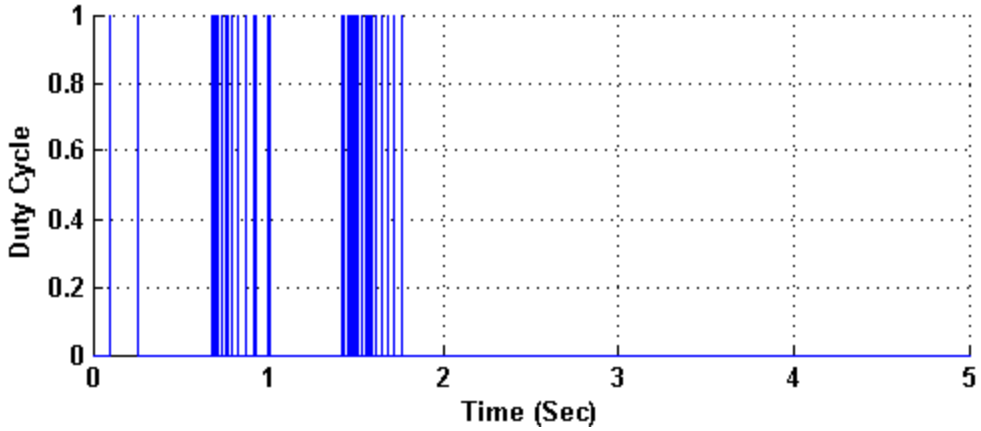


Figure 21: Duty cycle generated through the controller for 3LG temporary fault for the CRCBR model.

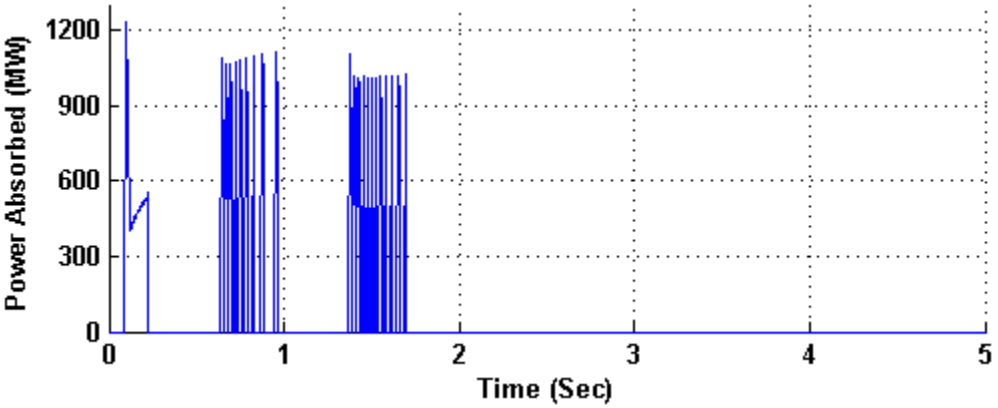


Figure 22: Power absorbed by the braking resistor unit of TCBR model for 3LG temporary fault for the CRCBR model.

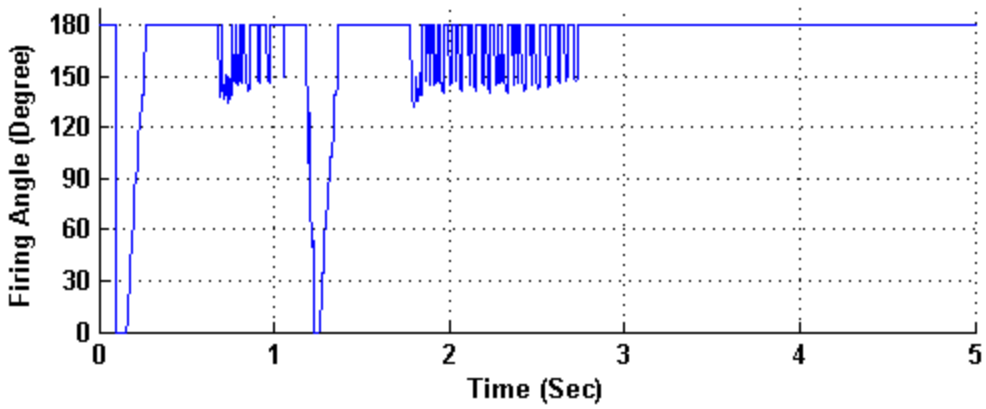


Figure 23: Firing angle generated through the controller for 3LG permanent fault for the TCBR model.

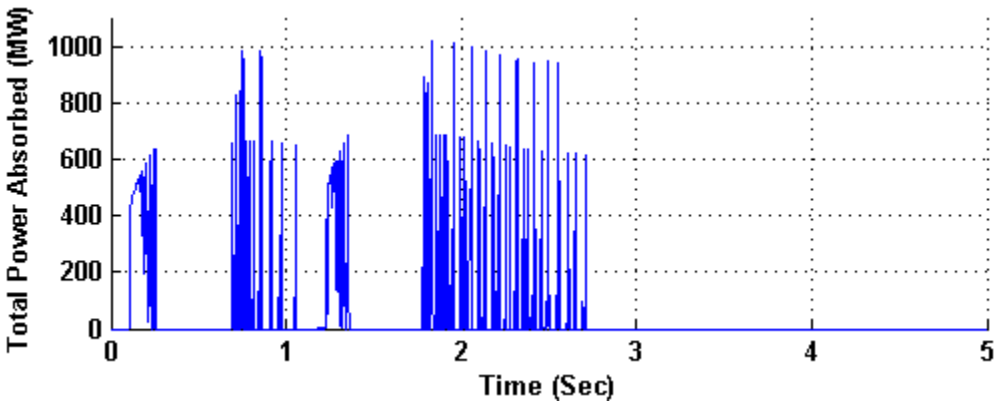


Figure 24: Total power absorbed by the braking resistor unit of TCBR model for 3LG permanent fault for the TCBR model.

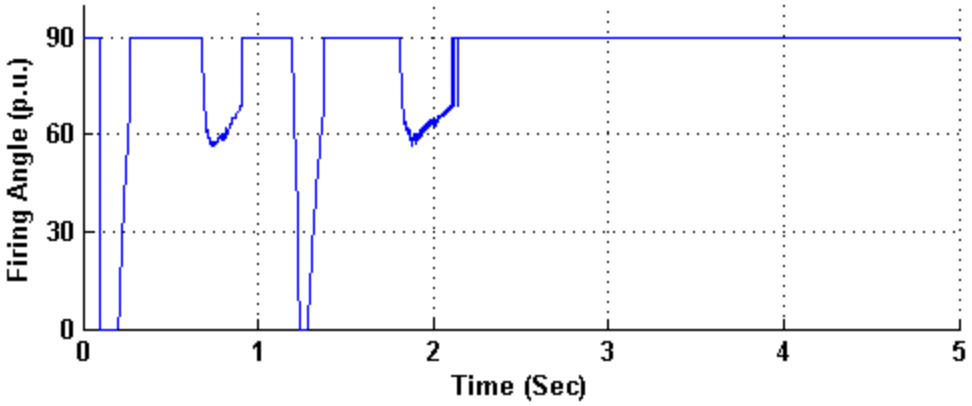


Figure 25: Firing angle generated through the controller for 3LG permanent fault for the RCBR model.

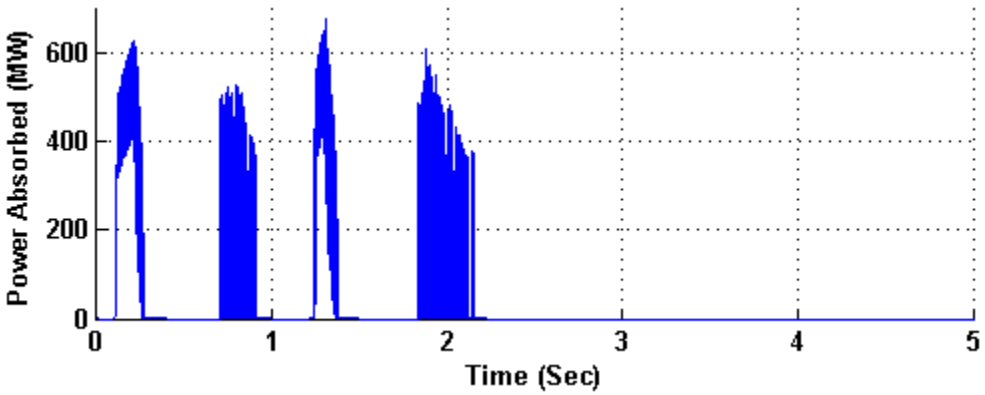


Figure 26: Power absorbed by the braking resistor unit of TCBR model for 3LG permanent fault for the RCBR model.

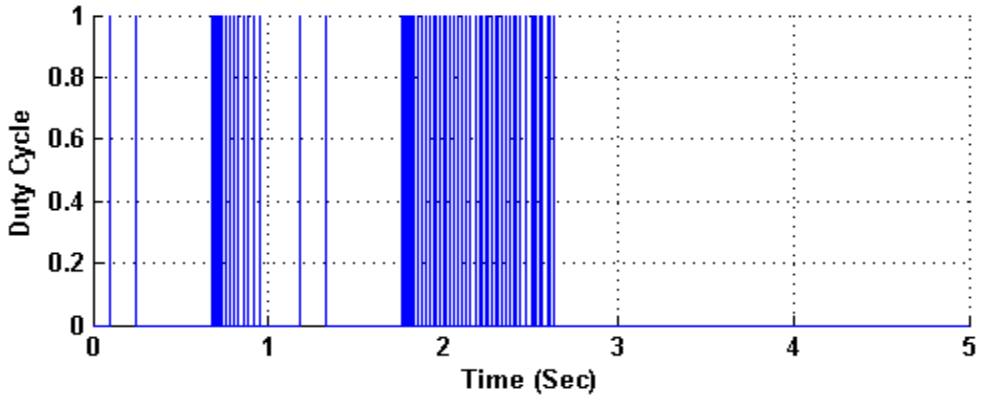


Figure 27: Duty cycle generated through the controller for 3LG permanent fault for the CRCBR model.

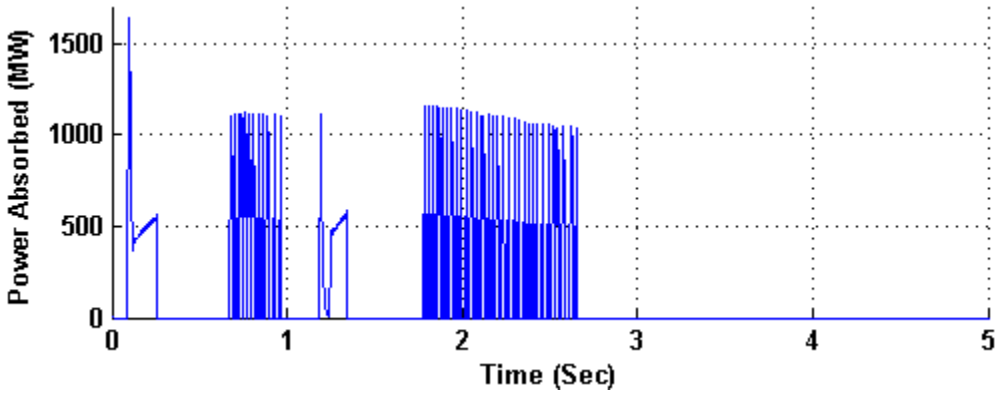


Figure 28: Power absorbed by the braking resistor unit of TCBR model for 3LG permanent fault for the CRCBR model.

# V. TRANSIENT STABILITY ANALYSIS OF IEEE 9-BUS POWER SYSTEM

The effectiveness of the proposed models and the existing braking resistor models are also tested on a two machines system i.e., the IEEE-9 bus power system. It is a standard power system model that is used to analyze the transient stability. The IEEE-9 bus power system model consists of two synchronous generators; hence the transient analysis is done for the single-speed input and multiple-speed input to the controller and also for single insertion point and multiple insertion point of braking resistor model into the power system model. The speed index performances of all three braking resistors are analyzed and compared for balanced and unbalanced temporary and permanent fault conditions by measuring the speed performance index for a simulation time of 15 seconds.

## *A. IEEE- 9 BUS POWER SYSTEM MODEL DETAILS*

The IEEE–9 bus power system model, shown by the line diagram Figure 29 [21], consists of two synchronous generators $G_1$ (200 MVA) and $G_2$ (130 MVA) feeding three loads and an infinite bus through transformers Tr-1 ((20.2/20 KV), Tr-2 (20.4/20 KV) and Tr-3 (20 kV/20.8 KV) and double circuit transmission lines. It is noteworthy here that the step-down voltage ratio for transformer Tr-1 and Tr-2 are assumed for this simulation work. However, in real field applications, these ratings of transformers do not exist.

The synchronous generators parameters used to simulate for this work is shown in Table 8 and the initial values obtained for both the generators are shown in Table 9. The double circuit transmission line parameters consisting of resistance (R), reactance (X) and susceptance (B) are shown in Figure 29. The circuit breakers (CB) are the primary protective device installed to cut-off faulted line.

The GOV and AVR control blocks used for IEEE-9 bus power system model are discussed in earlier section and shown by the block diagrams in Figures 9 and 10, respectively.

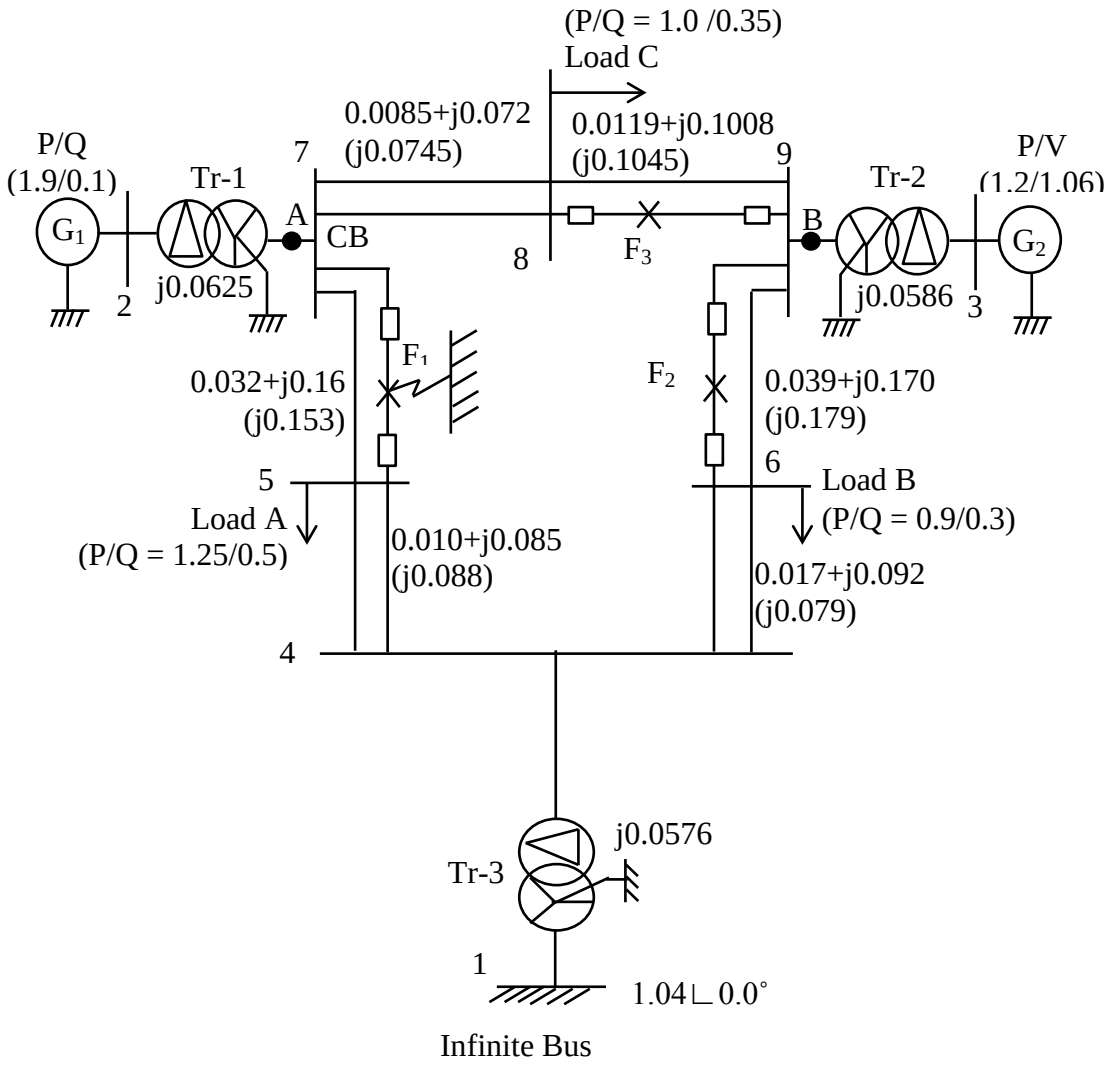


Figure 29: Single line diagram of standard IEEE-9 bus system model.

Table 8: Synchronous generator parameters for IEEE-9 bus model used for simulation

| Synchronous generator parameters | $SG_1$ | $SG_2$ |
|---|---|---|
| Generator power rating [MVA] | 200 | 130 |
| Armature resistance, $r_a$ [pu] | 0.003 | 0.004 |
| Armature reactance, $x_a$ [pu] | 0.102 | 0.078 |
| d-axis synchronous reactance, $X_d$ [pu] | 1.651 | 1.220 |
| q-axis synchronous reactance, $X_q$ [pu] | 1.590 | 1.160 |
| d-axis transient reactance, $X'_d$ [pu] | 0.232 | 0.174 |
| q-axis transient reactance, $X'_q$ [pu] | 0.380 | 0.25 |
| d-axis sub-transient reactance, $X''_d$ [pu] | 0.171 | 0.134 |
| q-axis sub-transient reactance, $X''_q$ [pu] | 0.171 | 0.134 |
| d-axis open circuit transient time constant, $T'_{do}$ [s] | 5.90 | 8.970 |
| q-axis open circuit transient time constant, $T'_{qo}$ [s] | 0.535 | 1.500 |
| d-axis open circuit sub-transient time constant, $T''_{do}$ [s] | 0.033 | 0.033 |
| q-axis open circuit transient time constant, $T''_{qo}$ [s] | 0.078 | 0.141 |
| Inertia constant, H [s] | 9.000 | 6.000 |

Table 9: Synchronous generator initial values for IEEE-9 bus system model

| | G1 | G2 |
|---|---|---|
| Generator output | 1.9 p.u. | 1.2 p.u. |
| Generator terminal voltage | 1.02 p.u. | 1.06 |
| Generator load angle | 59.9˚ | 64.9˚ |

*1. Braking Resistor Model Connected to Generators*

A braking resistor model can be connected directly to the terminals of the synchronous generator or at the terminal of the high voltage side of the generator transformer. For this work, the braking resistor model is connected on the high voltage side as shown in Figure 30. Therefore, the transient stability enhancement can be achieved by adding a single model's of braking resistor within the system, at locations A or B shown in Figure 29, or by adding two models of braking resistors in the system together, at both locations A and B as shown in Figure28.

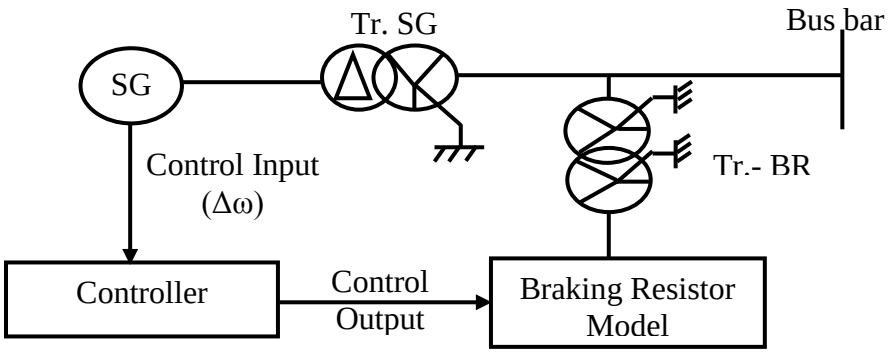


Figure 30: Line diagram of the braking resistor model connected to the high transmission side of the generator transformer.

*B. CONTROLLER PARAMETER FOR IEEE-9 BUS MODEL*

For a multi-machine system, possible location of inserting braking resistor model to enhance transient stability is equivalent to the number of synchronous generators in the system. Therefore, there are two possible locations for inserting braking resistor models in the system, location A, closer to synchronous generator $G_1$ and location B, closer to synchronous generator $G_2$, as shown in Figure 35. Hence, for this work, the transient analysis is done depending on the number of braking resistors inserted in the power sys-

tem models, as well as considering the number of input to the controller, $\Delta\omega$, shown in Figure 7. For this work, the input to the controller is the change in speed of the synchronous generator. The controller can be fed only with the change in speed of the synchronous generator which has braking resistor model connected to its step up transformer or fed with the sum of the deviation in speed of both the generators; even though only one braking resistor model is connected to the terminal of synchronous generator. The analysis is grouped as follows:

i) Single synchronous generator speed deviation input to the controller, $\Delta\omega = \Delta\omega_1$ or $\Delta\omega_2$:
   a. Braking resistor model connected at location A, the speed deviation input $\Delta\omega = \Delta\omega_1$, the speed deviation of the synchronous generator $G_1$
   b. Braking resistor model connected at location B, the speed deviation input $\Delta\omega = \Delta\omega_2$, the speed deviation of the synchronous generator

ii) Sum of the speed deviations of both synchronous generators as an input to the controller, $\Delta\omega = \Delta\omega_1 + \Delta\omega_2$
   a. Braking resistor model connected at location A
   b. Braking resistor model connected at location B
   c. Braking resistor model connected at locations A & B

The controller parameter values, $K_P$, $T_I$, and $T_D$, calculated by the trial and error method, for IEEE-9 bus power system model for all different braking resistor models are shown in Table 10. For two different input conditions for the controller, the values calculated are assumed to be the same. The $L_{Min}$ and $L_{Max}$ are the limiters required to limit the triggering pulses within the range, and are shown in the Table 10.

As mentioned earlier, each BR model is implemented with the same type of controller, but as triggering is different for each model, different controller parameters are required to generate required control output. Different parameter values, $K_P$, $T_I$, $T_D$, $L_{Min}$, and $L_{Max}$, as required by each controller for each model are shown in Table 10.

Table 10: Controller parameters and braking resistor values

| Model Type | Controller parameters for | | | | | | Limiter parameters | | $R_{BR}$ (Ω) |
|---|---|---|---|---|---|---|---|---|---|
| | $\Delta\omega = \Delta\omega_1$ or $\Delta\omega_1$ | | | $\Delta\omega = \Delta\omega_1 + \Delta\omega_2$ | | | | | |
| | $K_P$ | $T_I$ | $T_D$ | $K_P$ | $T_I$ | $T_D$ | $L_{Max}$ | $L_{Min}$ | |
| TCBR | 12 | 0. 1 | 0.001 | 12 | 0.1 | 0.001 | 180 | 0 | 0.4356 |
| RCBR | 7 | 0.01 | 0.0001 | 7 | 0.01 | 0.0001 | 90 | 0 | 0.7952 |
| CRCBR | 1 | 0.0001 | 0.0001 | 1.0 | 0.0001 | 0.0001 | 1 | 0 | 0.7952 |

### *C. Simulation Results*

For analyzing the effectiveness of the braking resistor models to enhance the transient stability of the power system network, the system performance is done based on two different input conditions to the controller as mentioned in earlier section. The speed index performance $\Delta\omega_c$, for single speed input and two speeds input, is calculated by using (11).

$$\Delta\omega_c = \int_0^T (|\Delta\omega_1| + |\Delta\omega_2|)\, dt \qquad \text{p.u. sec} \tag{11}$$

where, $T$ is the simulation time of 15.0 sec, $\Delta\omega_1$ and $\Delta\omega_2$ are change in speed of synchronous generators $G_1$ and $G_2$, respectively. The smaller the $\Delta\omega_c$, the better the performance is.

Both balanced (3LG: three phase-to-ground and 3LS: three-phase short circuit) and unbalanced (2LG: double line-to-ground, 2LS: line-to-line, and 1LG: single line-to-ground) temporary and permanent faults are considered at the fault points $F_1$, $F_2$, and $F_3$ of the IEEE-9 bus power system model as shown in Figure 29.

For temporary fault, it is considered that fault occurs at 0.1 sec and is cleared at 0.6 sec, the CB opens at 0.2 sec and closes at 1.2 sec. For permanent fault conditions, the CB reopens at 1.3 sec, while the other simulation conditions are the same as the temporary faults. The time step and simulation time are chosen as 0.00005 sec and 15 seconds, respectively.

The speed index values calculated for all three fault locations for both temporary and permanent fault conditions are shown in Table 11. It can be seen from the table that the speed index values for the fault location $F_3$ are higher as compared to the speed index values at fault locations $F_1$ and $F_2$. It implies that $F_3$ is a critical fault point and hence the controller parameters are designed for this critical point considering that if any fault occurs in this section, then the system should be stabilized soon without losing synchronism of the power network.

*1. Single speed deviation input to the controller*

For transient analysis, the speed deviation input to the controller, $\Delta\omega$, is the individual speed deviation of the synchronous generator $G_1$ or $G_2$, i.e. $\Delta\omega = \Delta\omega_1$ or $\Delta\omega_2$ corresponding to the terminal where braking resistor model is inserted. The possible locations of inserting the braking resistor models are as follows:

i) Braking resistor model connected at location A

ii) Braking resistor model connected at location B

Table 11: Speed index values (in $10^{-3}$ p.u. sec) for all fault condition without implementation of braking resistor models

| Types of Faults | Temporary fault | | | Permanent fault | | |
|---|---|---|---|---|---|---|
| | Fault at F1 | Fault at F2 | Fault at F3 | Fault at F1 | Fault at F2 | Fault at F3 |
| 3LG | 29.20 | 25.16 | 33.55 | 29.48 | 28.69 | 35.79 |
| 3LS | 28.89 | 24.89 | 33.25 | 29.18 | 28.39 | 35.57 |
| 2LG | 19.13 | 15.69 | 28.36 | 22.09 | 20.34 | 34.00 |
| 2LS | 13.29 | 11.17 | 19.71 | 15.62 | 14.44 | 26.03 |
| 1LG | 8.79 | 6.995 | 15.53 | 12.03 | 10.45 | 21.82 |

The speed index values calculated by using (11) for balanced and unbalanced temporary and permanent fault with and without braking resistor models, inserted at above mentioned locations, in case of fault locations $F_1$ are shown in Tables 12 and 13.

As can be seen from Table 11, the fault location $F_1$ is an intermediate critical point for both the temporary and permanent fault conditions. It is closer to the synchronous generator $G_1$, as shown in Figure 29. For this fault location, insertion of the braking resistor models at location A gives better speed index performance results as compared to the insertion of braking resistor models at location B. It also indicates that the proposed CRCBR model's performance is better than the proposed RCBR and existing TCBR model performances for permanent fault condition, and comparable for temporary fault condition. Tables 12-13 also indicate that the location A is a better braking resistor insertion point for the existing TCBR model and the proposed RCBR model for fault at $F_1$.

With the CRCBR model, both insertion location points give comparable speed index values.

The power absorbed by the braking resistor units of the corresponding braking resistor models for fault at location $F_1$, for temporary and permanent faults are shown in Tables 14 and 15, respectively. The power absorbed by the proposed CRCBR model is higher as compared to the proposed RCBR and existing TCBR models.

For single input to the controller, the single speed deviation is fed as an input for analysis. Speed responses for generator G1 and G2 with single speed deviation input to controller and braking resistor models inserted at location A and B for balanced 3LG temporary and permanent fault at location $F_1$ are shown in Figures 31-38. The speed curves follow the speed index values shown in Table 12and 13.

Table 12: Speed index values (in 10-3 p.u. sec) for temporary fault at $F_1$ for single speed deviation input to the controller

| Type of Fault | Without BR | TCBR location | | RCBR location | | CRCBR location | |
|---|---|---|---|---|---|---|---|
| | | At A | At B | At A | At B | At A | At B |
| 3LG | 29.20 | 9.988 | 17.05 | 11.91 | 17.16 | 10.11 | 10.64 |
| 3LS | 28.89 | 9.914 | 17.09 | 11.82 | 17.05 | 10.01 | 10.59 |
| 2LG | 19.13 | 8.623 | 13.08 | 9.733 | 12.93 | 6.189 | 9.466 |
| 2LS | 13.29 | 7.728 | 10.09 | 8.085 | 10.34 | 5.122 | 8.687 |
| 1LG | 8.79 | 7.57 | 7.36 | 6.875 | 7.373 | 5.029 | 6.236 |

Table 13: Speed index values (in $10^{-3}$ p.u. sec) for permanent fault at $F_1$ for single speed deviation input to the controller

| Type of Fault | Without BR | TCBR location | | RCBR location | | CRCBR location | |
|---|---|---|---|---|---|---|---|
| | | At A | At B | At A | At B | At A | At B |
| 3LG | 29.48 | 11.05 | 20.29 | 13.80 | 21.57 | 10.41 | 13.77 |
| 3LS | 29.18 | 11.01 | 20.35 | 13.71 | 21.44 | 10.17 | 13.75 |
| 2LG | 22.09 | 9.474 | 17.53 | 11.22 | 17.52 | 7.48 | 12.88 |
| 2LS | 15.62 | 8.264 | 13.73 | 9.476 | 13.62 | 6.733 | 11.0 |
| 1LG | 12.03 | 8.676 | 11.56 | 8.597 | 10.97 | 6.121 | 9.055 |

Table 14: Total power consumed (in MW) for temporary fault at $F_1$ for single speed deviation input to the controller.

| Types of Fault | TCBR location | | RCBR location | | CRCBR location | |
|---|---|---|---|---|---|---|
| | At A | At B | At A | At B | At A | At B |
| 3LG | 53.89 | 37.66 | 61.37 | 49.99 | 97.12 | 54.44 |
| 3LS | 53.16 | 36.78 | 61.77 | 48.96 | 94.78 | 53.4 |
| 2LG | 33.05 | 17.69 | 41.91 | 27.12 | 35.32 | 20.24 |
| 2LS | 20.42 | 8.58 | 28.71 | 10.9 | 16.35 | 8.194 |
| 1LG | 10.9 | 2.976 | 8.806 | 2.124 | 7.375 | 3.886 |

Table 15: Total power consumed (in MW) for permanent fault at $F_1$ for single speed deviation input to the controller

| Types of Fault | TCBR location | | RCBR location | | CRCBR location | |
|---|---|---|---|---|---|---|
| | At A | At B | At A | At B | At A | At B |
| 3LG | 57.41 | 41.13 | 59.93 | 56.63 | 54.57 | 48.74 |
| 3LS | 56.7 | 40.27 | 59.65 | 55.67 | 51.98 | 47.95 |
| 2LG | 42.8 | 27.68 | 50.93 | 37.35 | 38.4 | 28.51 |
| 2LS | 24.19 | 14.58 | 35.47 | 15.6 | 22.37 | 14.6 |
| 1LG | 18.72 | 7.631 | 23.35 | 6.495 | 14.56 | 9.25 |

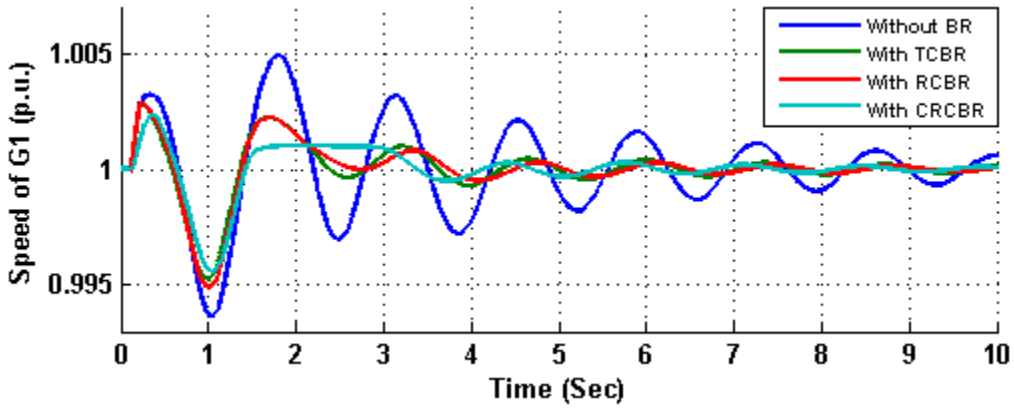


Figure 31: Speed response of G1generator for 3LG temporary fault at location $F_1$ [Single speed deviation input to the controller and braking resistor inserted at location A].

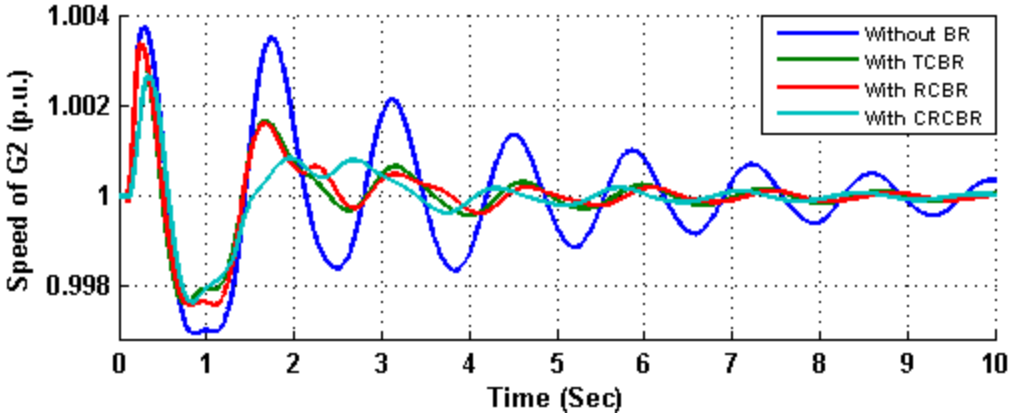


Figure 32: Speed response of G2generator for 3LG temporary fault at location $F_1$

[Single speed deviation input to the controller and braking resistor inserted at location A].

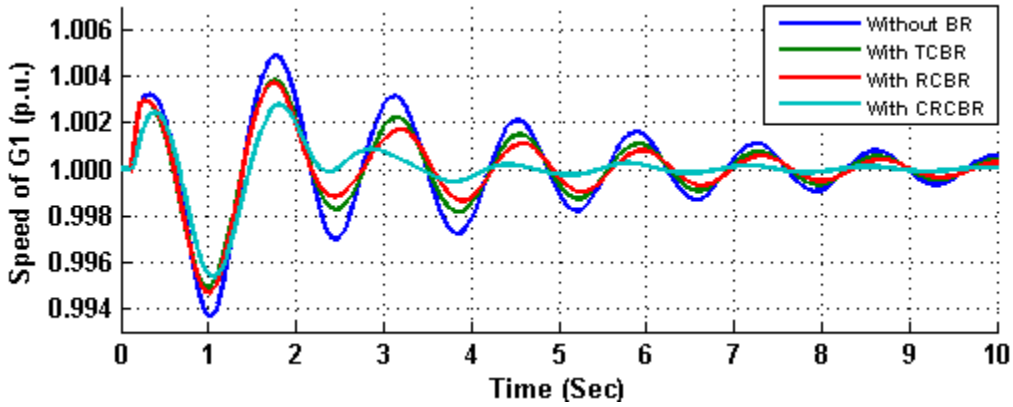


Figure 33: Speed response of G1generator for 3LG temporary fault at location $F_1$

[Single speed deviation input to the controller and braking resistor inserted at location B].

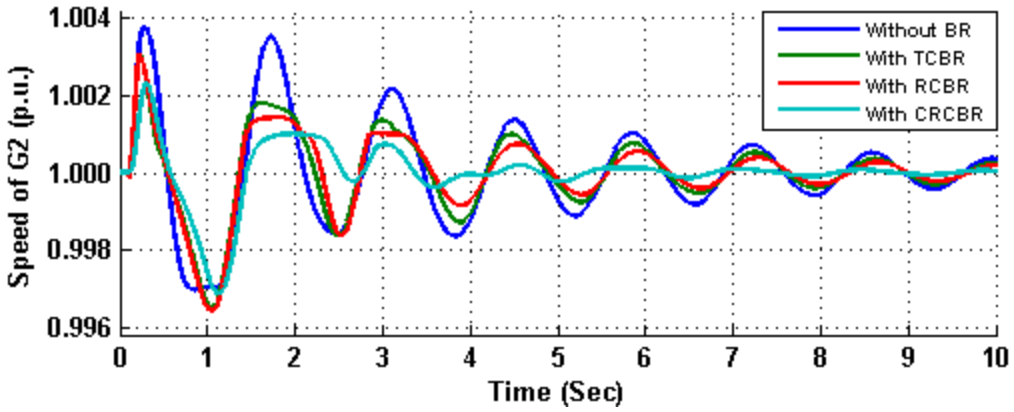


Figure 34: Speed response of G2 generator for 3LG temporary fault at location $F_1$

[Single speed deviation input to the controller and braking resistor inserted at location B].

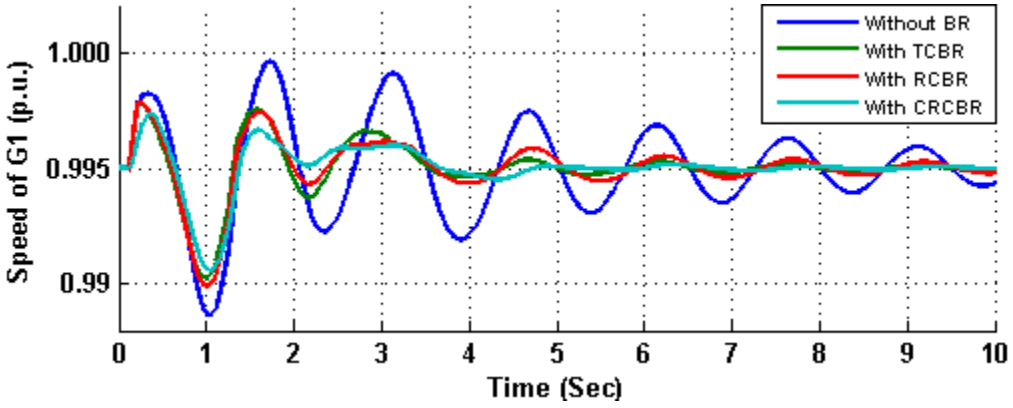


Figure 35: Speed response of G1generator for 3LG permanent fault at location $F_1$

[Single speed deviation input to the controller and braking resistor inserted at location A].

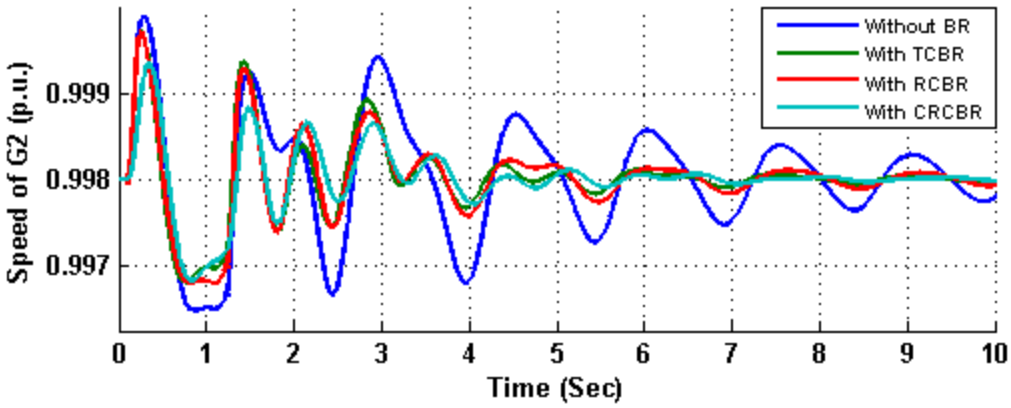


Figure 36: Speed response of G2generator for 3LG permanent fault at location $F_1$

[Single speed deviation input to the controller and braking resistor inserted at location A].

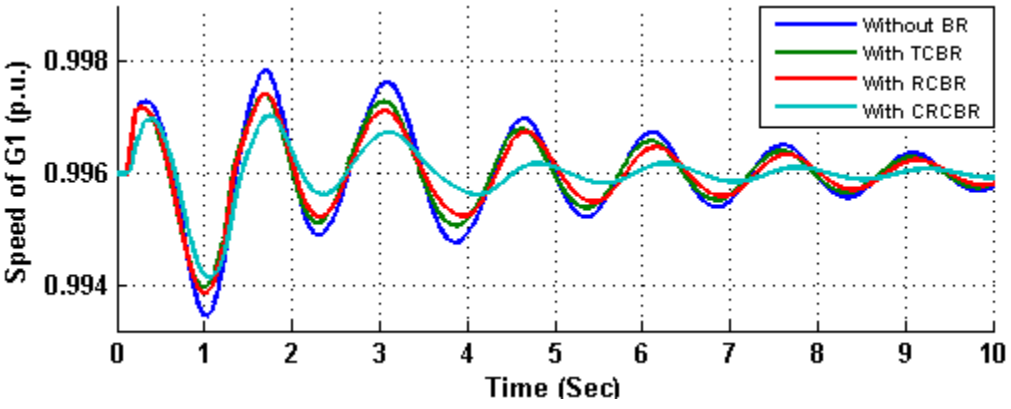


Figure 37: Speed response of G1generator for 3LG temporary fault at location $F_1$

[Single speed deviation input to the controller and braking resistor inserted at location B].

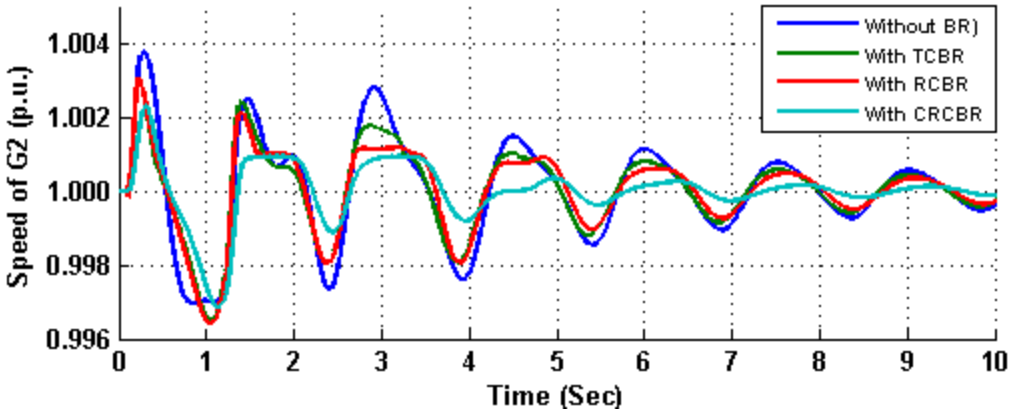


Figure 38: Speed response of G2 generator for 3LG temporary fault at location $F_1$ [Single speed deviation input to the controller and braking resistor inserted at location B].

From Table 11, it can be seen that fault location $F_2$ is a least critical point to disturb the network and is closer to the synchronous generator $G_2$. For this fault location and single speed deviation input to the controller, the speed index values calculated by using (11) for both balanced (3LG and 3LS) and unbalanced (2LG, 2LS and 1LG) temporary and permanent faults are shown in Tables 16-17. The insertion of the braking resistor models at location B gives better speed index performance results as compared to the insertion of braking resistor models at location A for the proposed CRCBR model and the existing TCBR model. But with the proposed RCBR model, the location A for braking resistor model gives better results. It also indicates that the proposed CRCBR model's performance is better than the proposed RCBR and existing TCBR model performances for temporary faults as well as for permanent fault conditions.

The power absorbed by the braking resistor units of the proposed CRCBR and RCBR models and existing TCBR models for temporary and permanent faults are shown in Tables 18-19. The CRCBR model absorbs more power as compared to the RCBR and

TCBR models for temporary faults at location A, but for permanent faults, the TCBR absorbs more power.

For single input to the controller, the single speed deviation of generator with the braking resistor model is fed as an input for analysis. Speed responses for generator $G_1$ and $G_2$ with single speed deviation input to controller and braking resistor models inserted at location A and B for balanced 3LG temporary and permanent fault at location $F_2$ are shown in Figures 39-46. The speed curves follow the speed index values shown in Table 16 and 17.

Table 16: Speed index values (in $10^{-3}$ p.u. sec) for temporary fault at for $F_2$ single speed deviation input to the controller

| Type of Fault | Without BR | TCBR location | | RCBR location | | CRCBR location | |
|---|---|---|---|---|---|---|---|
| | | At A | At B | At A | At B | At A | At B |
| 3LG | 25.16 | 10.29 | 8.267 | 12.31 | 14.06 | 10.10 | 9.615 |
| 3LS | 24.89 | 10.28 | 8.255 | 12.24 | 13.89 | 10.32 | 9.462 |
| 2LG | 15.69 | 9.389 | 5.269 | 10.03 | 10.45 | 6.544 | 6.698 |
| 2LS | 11.17 | 8.47 | 4.93 | 8.643 | 8.386 | 6.354 | 5.802 |
| 1LG | 6.995 | 6.838 | 4.263 | 6.688 | 6.024 | 6.106 | 4.792 |

Table 17: Speed index values (in $10^{-3}$ p.u. sec) for permanent fault at $F_2$ for single speed deviation input to the controller.

| Type of Fault | Without BR | TCBR location | | RCBR location | | CRCBR location | |
|---|---|---|---|---|---|---|---|
| | | At A | At B | At A | At B | At A | At B |
| 3LG | 28.69 | 10.91 | 15.69 | 14.35 | 19.00 | 10.90 | 11.51 |
| 3LS | 28.39 | 10.75 | 15.83 | 14.21 | 18.88 | 10.84 | 11.47 |
| 2LG | 20.34 | 9.33 | 14.24 | 10.98 | 15.49 | 7.511 | 10.92 |
| 2LS | 14.44 | 8.296 | 11.38 | 9.499 | 12.17 | 7.186 | 9.162 |
| 1LG | 10.45 | 7.778 | 9.681 | 8.013 | 9.485 | 6.427 | 7.347 |

Table 18: Total power consumed (in MW) for temporary fault at $F_2$ for single speed deviation input to the controller

| Types of Fault | TCBR location | | RCBR location | | CRCBR location | |
|---|---|---|---|---|---|---|
| | At A | At B | At A | At B | At A | At B |
| 3LG | 49.52 | 68.44 | 61.97 | 40.46 | 77.32 | 48.57 |
| 3LS | 49.06 | 67.2 | 61.55 | 40.2 | 74.39 | 47.92 |
| 2LG | 26.61 | 37.13 | 38.71 | 23.63 | 31.38 | 20.9 |
| 2LS | 14.05 | 26.18 | 22.74 | 15.74 | 13.38 | 12.20 |
| 1LG | 26.08 | 14.83 | 2.307 | 4.57 | 2.67 | 4.834 |

Table 19: Total power consumed (in MW) for permanent fault at $F_2$ for single speed deviation input to the controller

| Types of Fault | TCBR location | | RCBR location | | CRCBR location | |
|---|---|---|---|---|---|---|
| | At A | At B | At A | At B | At A | At B |
| 3LG | 49.06 | 37.74 | 57.17 | 46.13 | 49.62 | 47.18 |
| 3LS | 48.36 | 37.15 | 56.92 | 45.08 | 54.21 | 46.43 |
| 2LG | 35.77 | 23.05 | 45.79 | 29.41 | 31.04 | 27.7 |
| 2LS | 21.59 | 12.16 | 29.79 | 11.69 | 16.23 | 15.09 |
| 1LG | 13.87 | 46.76 | 16.89 | 4.406 | 7.8 | 9.24 |

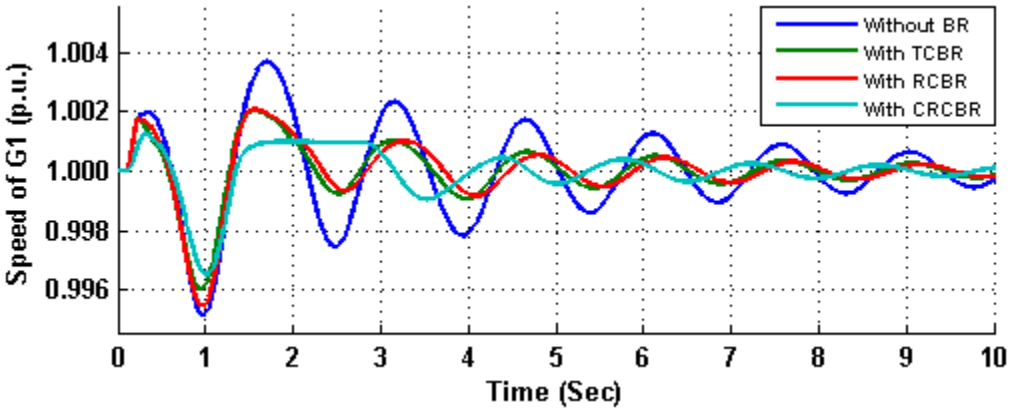


Figure 39: Speed response of G1generator for 3LG temporary fault at location $F_2$ [Single speed deviation input to the controller and braking resistor inserted at location A].

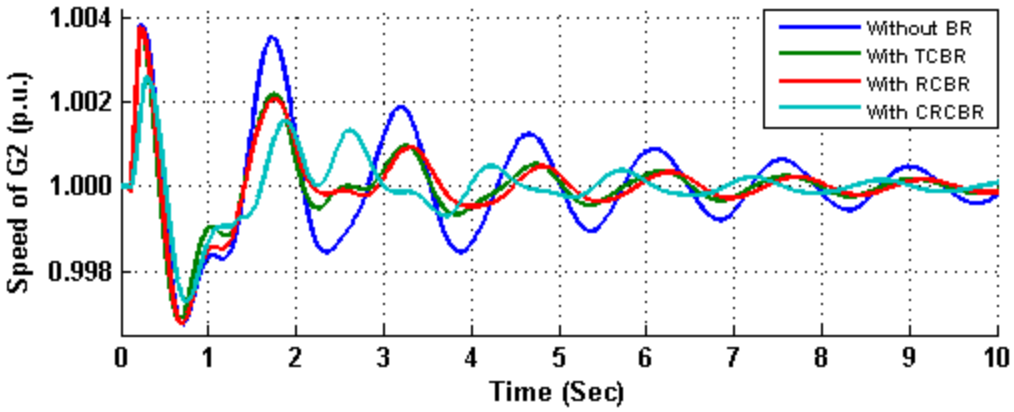


Figure 40: Speed response of G2generator for 3LG temporary fault at location $F_2$

[Single speed deviation input to the controller and braking resistor inserted at location A].

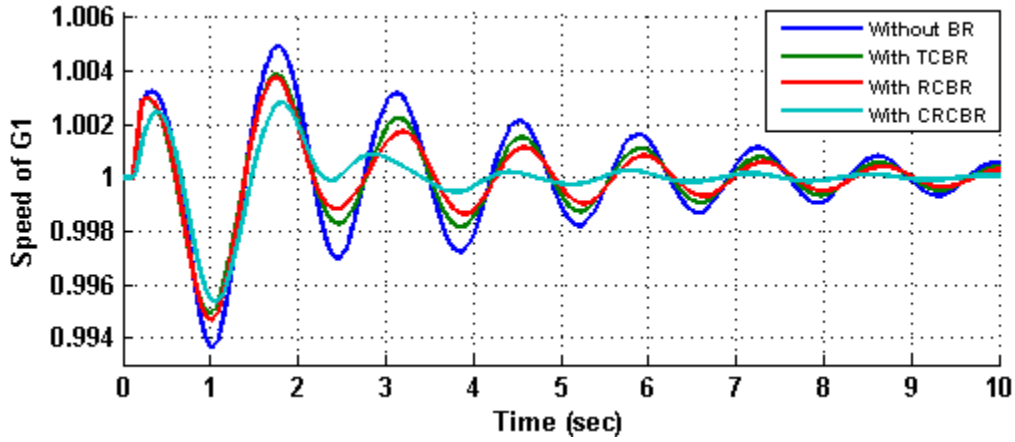


Figure 41: Speed response of G1generator for 3LG temporary fault at location $F_2$

[Single speed deviation input to the controller and braking resistor inserted at location B].

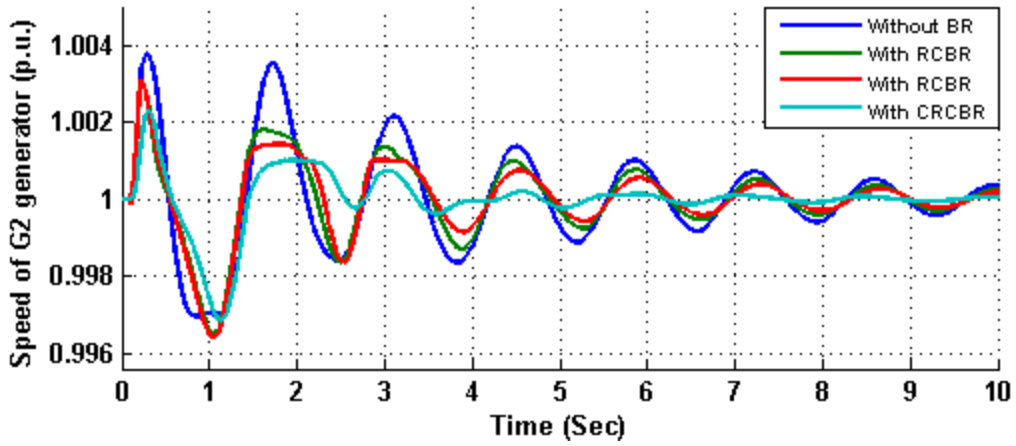


Figure 42: Speed response of G2 generator for 3LG temporary fault at location $F_2$

[Single speed deviation input to the controller and braking resistor inserted at location B].

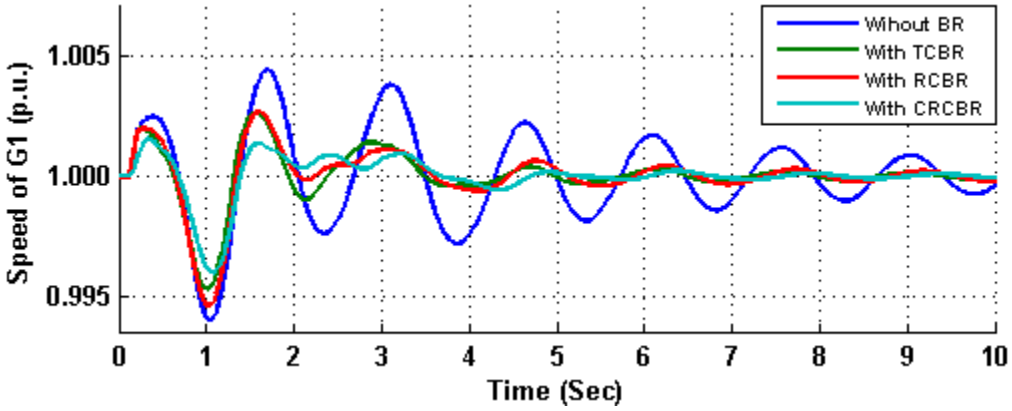


Figure 43: Speed response of G1generator for 3LG permanent fault at location $F_2$

[Single speed deviation input to the controller and braking resistor inserted at location A].

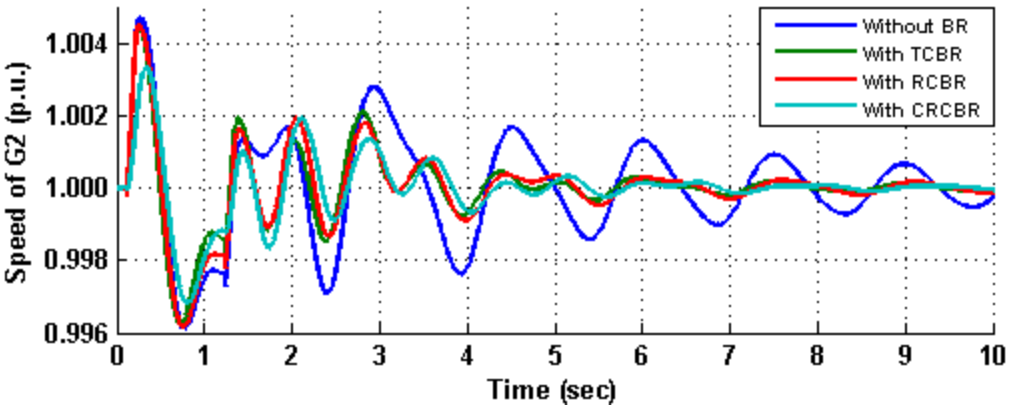


Figure 44: Speed response of G2generator for 3LG permanent fault at location $F_2$

[Single speed deviation input to the controller and braking resistor inserted at location A].

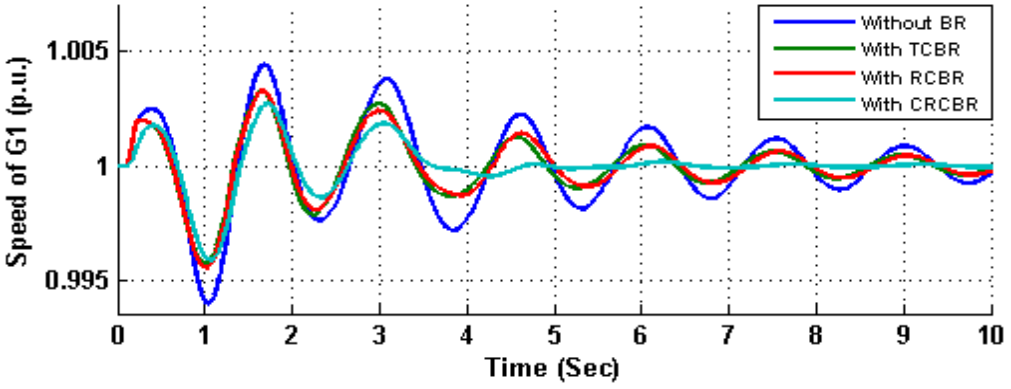


Figure 45: Speed response of G1generator for 3LG permanent fault at location $F_2$

[Single speed deviation input to the controller and braking resistor inserted at location B].

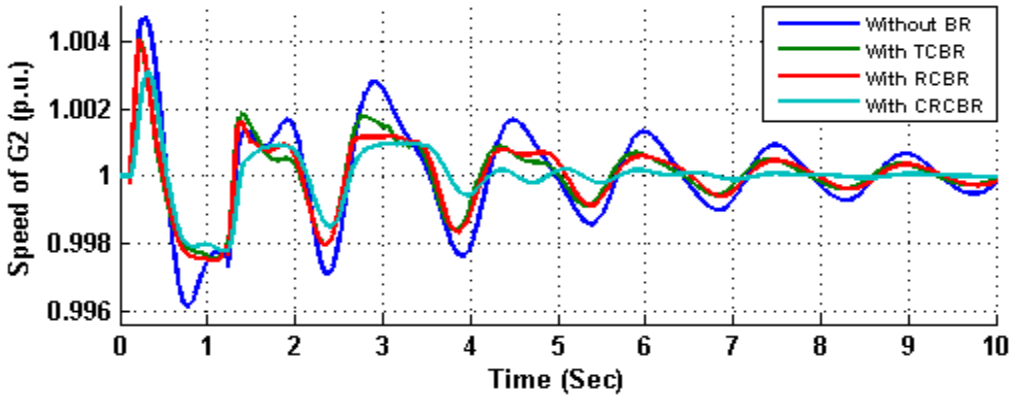


Figure 46: Speed response of G2 generator for 3LG permanent fault at location $F_2$ [Single speed deviation input to the controller and braking resistor inserted at location B].

As can be seen from Table 11, fault location $F_3$, is a critical point for both the temporary fault conditions and permanent fault conditions and it is located in between both the synchronous generators $G_1$ and $G_2$ as shown in Figure 29. The speed performance indices calculated by using (11) for single input to the controller, and two insertion points of braking resistors, in case of balanced and unbalanced temporary and permanent faults are shown in Tables 20-21.

It can be seen from Tables 20-21 that, for the fault location $F_3$, the insertion of the braking resistor models at location A gives better speed index performance results as compared to the insertion of braking resistor models at location B. The indices values also indicate that the proposed CRCBR model's performance is comparable to the proposed RCBR and existing TCBR model performances for temporary faults as well as for permanent fault condition. The speed index values for the existing TCBR model are better than the speed index values of the proposed RCBR model.

The power absorbed by the braking resistor units of the proposed CRCBR and RCBR models and existing TCBR models for balanced and unbalanced temporary and permanent faults are shown in Tables 22 and 23, respectively. The power absorbed by the braking resistor units is more which means that the speed index value is lower; hence the system is stabilized within short period of time. The more the power is dissipated through the braking resistors, the more the system is stabilized.

Speed responses for generator G1 and G2 with single speed deviation input to controller and braking resistor models inserted at location A and B for balanced 3LG temporary and permanent fault at location $F_3$ are shown in Figures 47-54. The speed curves follow the speed index values shown in Table 20 and 21.

Table 20: Speed index values (in $10^{-3}$ p.u. sec) for temporary fault at $F_3$ for single speed deviation input to the controller

| Type of Fault | Without BR | TCBR location | | RCBR location | | CRCBR location | |
|---|---|---|---|---|---|---|---|
| | | At A | At B | At A | At B | At A | At B |
| 3LG | 33.55 | 11.55 | 19.41 | 14.23 | 19.75 | 12.57 | 14.70 |
| 3LS | 33.25 | 11.46 | 19.32 | 14.15 | 19.63 | 12.53 | 14.75 |
| 2LG | 28.36 | 10.36 | 17.87 | 12.82 | 17.93 | 11.32 | 11.96 |
| 2LS | 19.71 | 9.539 | 14.91 | 10.91 | 14.22 | 8.939 | 9.825 |
| 1LG | 15.53 | 8.808 | 12.52 | 9.783 | 12.22 | 6.165 | 9.099 |

Table 21: Speed index values (in $10^{-3}$ p.u. sec) for permanent fault at $F_3$ for single speed deviation input to the controller

| Type of Fault | Without BR | TCBR location | | RCBR location | | CRCBR location | |
|---|---|---|---|---|---|---|---|
| | | At A | At B | At A | At B | At A | At B |
| 3LG | 35.79 | 16.39 | 22.5 | 17.74 | 23.17 | 19.46 | 18.54 |
| 3LS | 35.57 | 16.2 | 22.42 | 17.56 | 23.07 | 19.26 | 18.32 |
| 2LG | 34.00 | 14.25 | 21.38 | 15.63 | 21.89 | 16.59 | 15.48 |
| 2LS | 26.03 | 11.42 | 15.94 | 12.46 | 18.15 | 16.15 | 12.42 |
| 1LG | 21.82 | 10.07 | 16.48 | 10.87 | 16.09 | 7.439 | 11.78 |

Table 22: Total power consumed (in MW) for temporary fault at $F_3$ for single speed deviation input to the controller

| Types of Fault | TCBR location | | RCBR location | | CRCBR location | |
|---|---|---|---|---|---|---|
| | At A | At B | At A | At B | At A | At B |
| 3LG | 83.86 | 55.13 | 79.09 | 66.23 | 98.52 | 78.85 |
| 3LS | 83.41 | 54.44 | 78.53 | 65.68 | 98.14 | 78.76 |
| 2LG | 69.49 | 43.29 | 69.4 | 55.63 | 86.72 | 61.61 |
| 2LS | 42.24 | 22.72 | 52.88 | 32.52 | 66.02 | 31.02 |
| 1LG | 30.06 | 14.48 | 40.26 | 21.41 | 45.26 | 17.53 |

Table 23: Total power consumed (in MW) for permanent fault at $F_3$ for single speed deviation input to the controller

| Types of Fault | TCBR location | | RCBR location | | CRCBR location | |
|---|---|---|---|---|---|---|
| | At A | At B | At A | At B | At A | At B |
| 3LG | 89.15 | 58.87 | 88.05 | 62.28 | 153.3 | 90.82 |
| 3LS | 88.4 | 58.34 | 87.58 | 61.77 | 152.5 | 89.58 |
| 2LG | 75.61 | 54.52 | 76.85 | 60.61 | 123.6 | 79.44 |
| 2LS | 51.88 | 47.45 | 61.07 | 61.02 | 80.86 | 60.01 |
| 1LG | 42.28 | 27.51 | 51.38 | 36.93 | 39.13 | 34.01 |

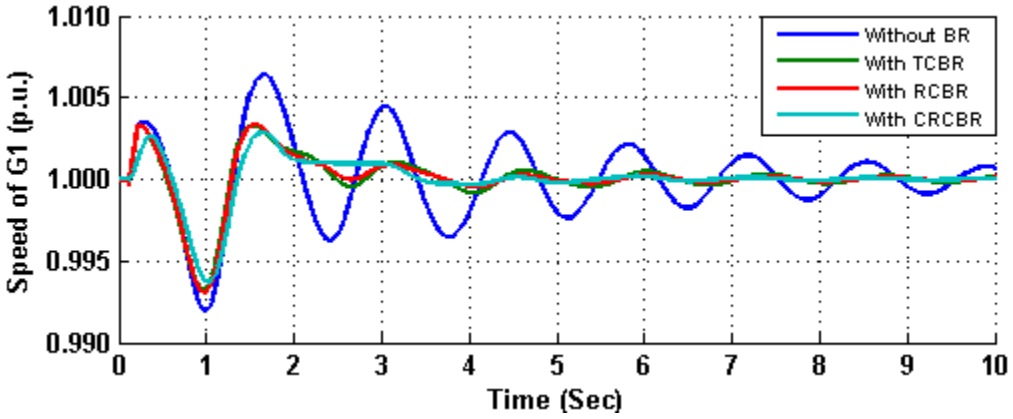


Figure 47: Speed response of G1 generator for 3LG temporary fault at location $F_3$ [Single speed deviation input to the controller and braking resistor inserted at location A].

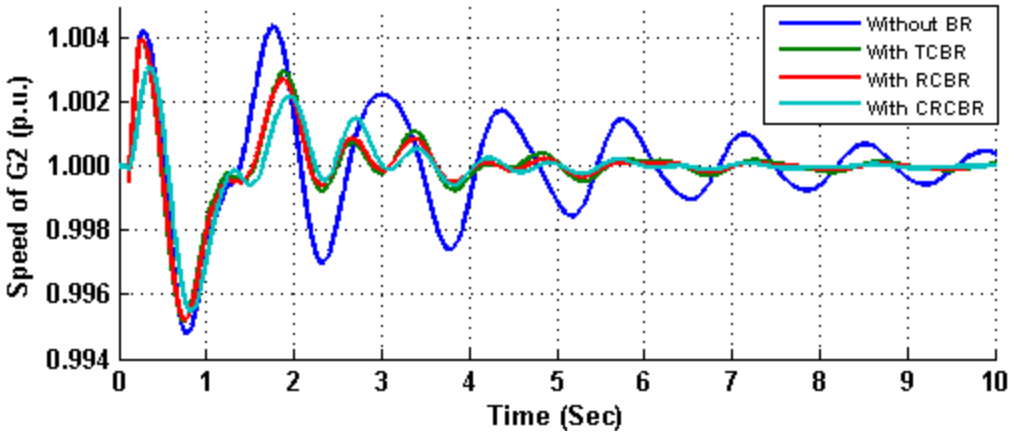


Figure 48: Speed response of G2 generator for 3LG temporary fault at location $F_3$

[Single speed deviation input to the controller and braking resistor inserted at location A].

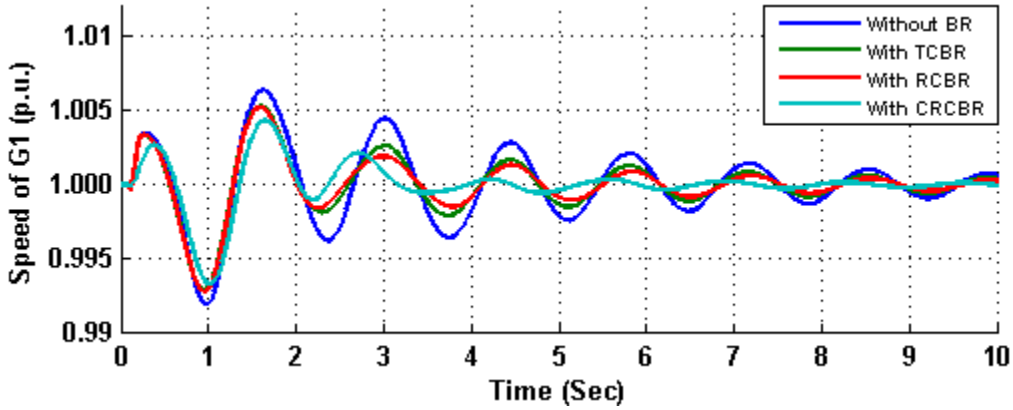


Figure 49: Speed response of G1generator for 3LG temporary fault at location $F_3$

[Single speed deviation input to the controller and braking resistor inserted at location B].

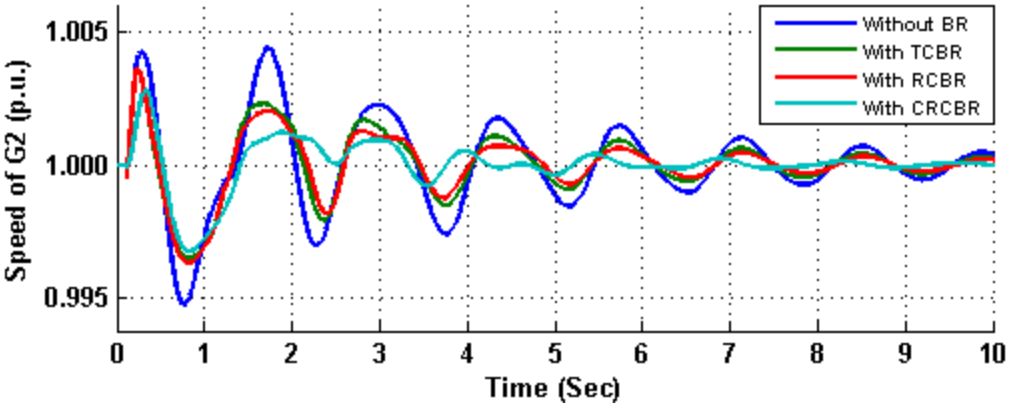


Figure 50: Speed response of G2 generator for 3LG temporary fault at location $F_3$

[Single speed deviation input to the controller and braking resistor inserted at location B].

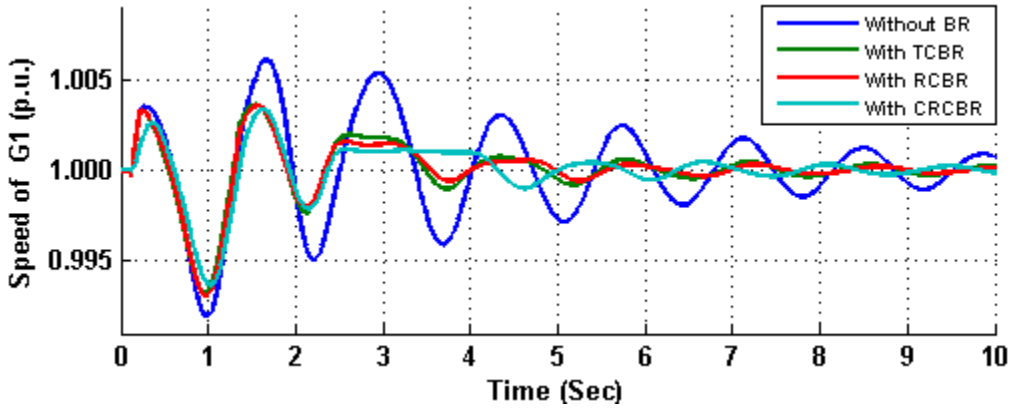


Figure 51: Speed response of G1generator for 3LG permanent fault at location $F_3$

[Single speed deviation input to the controller and braking resistor inserted at location A].

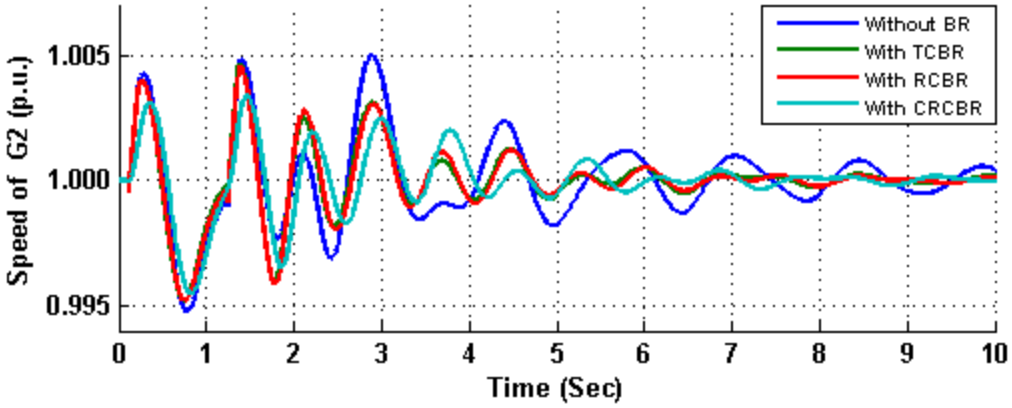


Figure 52: Speed response of G2generator for 3LG permanent fault at location $F_3$

[Single speed deviation input to the controller and braking resistor inserted at location A].

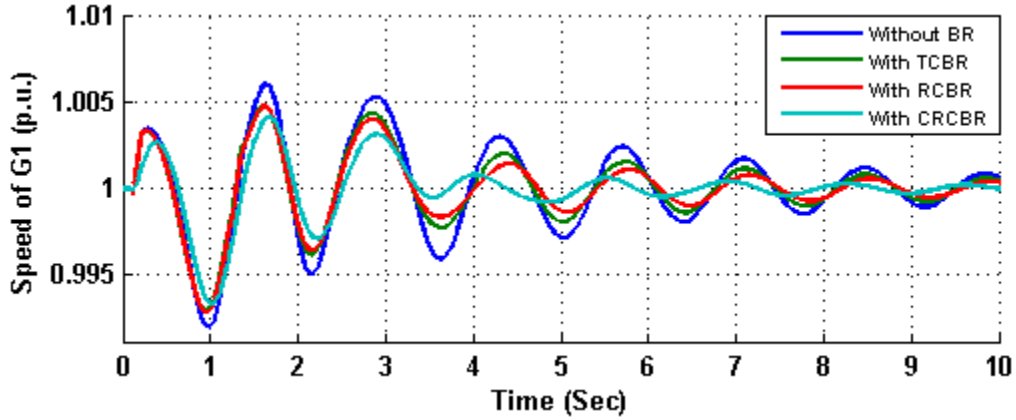


Figure 53: Speed response of G1generator for 3LG permanent fault at location $F_3$

[Single speed deviation input to the controller and braking resistor inserted at location B].

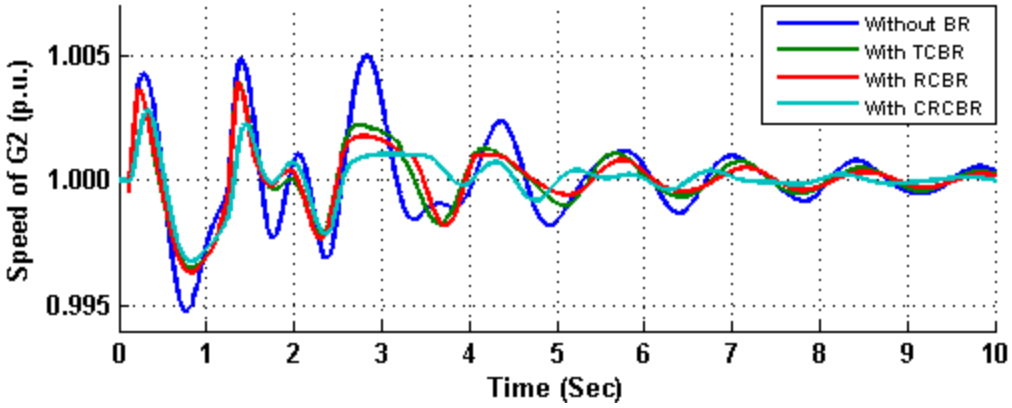


Figure 54: Speed response of G2 generator for 3LG permanent fault at location $F_3$ [Single speed deviation input to the controller and braking resistor inserted at location B].

The speed index values for the proposed models are comparable to the existing model performance for all fault locations. Although the insertion of braking resistor model at any terminal point of generator in the system will increase a substantial load on the complete power grid system, the effect of its insertion will be more on the corresponding terminal of the synchronous generator due to the corresponding speed input to controller. Therefore, the controller designed with single speed deviation input will control the increase in speed of the corresponding synchronous generator, but will not able to control the speed of the other synchronous generator connected in the power grid system as effectively, as can be seen in speed curves of PQ and PV generators. The fault locations and the synchronous generator capacity will play a vital role in enhancing the transient stability.

2. *Sum of speed deviation of both synchronous generators as an input to the controller*

For transient analysis purpose, the speed deviation input to the controller shown in Figure 7 and 30 is the sum of speed deviations of $G_1$ and $G_2$, i.e. $\Delta\omega = \Delta\omega_1 + \Delta\omega_2$. The

three configurations for inserting braking resistor models are possible with this input to controller and are discussed in earlier section and are as stated as follows:

i) Braking resistor model connected at location A

ii) Braking resistor model connected at location B

iii) Braking resistor model connected at location A & B

For the fault location $F_1$, the speed index values calculated by using (11) in case of balanced and unbalanced temporary and permanent faults for the proposed RCBR and CRCBR models and existing TCBR model, is shown in Tables 24 and 25. The speed index values for all three models are comparable. The proposed RCBR model provides better transient stability as compared to proposed CRCBR model and existing TCBR model for temporary faults. For permanent faults, the proposed CRCBR model provides better control compared to TCBR and RCBR model's performances.

The total power consumed by the braking resistor units of proposed CRCBR and RCBR models and existing TCBR models is shown in Table 26 and 27 for temporary and permanent fault conditions respectively. The power absorbed by braking resistor units is higher for the models which have better speed index values. The more the power absorbed, the lower the speed index value is.

The input to the controller is the sum of the speed deviation of both the synchronous generators, wherever the braking resistor model is inserted. The total speed deviation curves for the input to the controller for 3LG temporary and permanent fault at location $F_1$ for braking resistor models inserted only at location A, only at location B and both at locations A and B, are shown in Figures 55-60. The speed deviation curves indicate that the controller generates corresponding triggering pulses when the total speed deviation

exceeds the preset limit of 0.001 p.u., and hence the total speed deviation does not exceed the set limit. The generators G1 and G2 get stabilized without exceeding the speed limits.

Table 24: Speed index values (in $10^{-3}$ p.u. sec) for temporary fault at $F_1$ for sum of two speed deviation input to the controller

| Types of Fault | Without BR | TCBR location | | | RCBR location | | | CRCBR location | | |
|---|---|---|---|---|---|---|---|---|---|---|
| | | At A | At B | At A&B | At A | At B | At A&B | At A | At B | At A&B |
| 3LG | 29.20 | 9.44 | 8.52 | 8.51 | 8.58 | 8.9 | 8.25 | 9.99 | 10.2 | 8.83 |
| 3LS | 28.89 | 9.40 | 8.46 | 8.46 | 8.51 | 8.78 | 8.13 | 9.62 | 10.1 | 9.08 |
| 2LG | 19.13 | 7.86 | 7.24 | 8.06 | 6.46 | 6.2 | 6.62 | 6.74 | 6.64 | 6.04 |
| 2LS | 13.29 | 7.25 | 6.72 | 8.08 | 5.62 | 5.62 | 6.16 | 4.19 | 5.59 | 4.47 |
| 1LG | 8.79 | 6.57 | 5.84 | 7.43 | 4.92 | 4.92 | 5.04 | 2.54 | 2.88 | 2.40 |

Table 25: Speed index values (in $10^{-3}$p.u. sec) for permanent fault at $F_1$ for sum of two speed deviation input to the controller

| Types of Fault | Without BR | TCBR location | | | RCBR location | | | CRCBR location | | |
|---|---|---|---|---|---|---|---|---|---|---|
| | | At A | At B | At A&B | At A | At B | At A&B | At A | At B | At A&B |
| 3LG | 29.48 | 10.5 | 11.5 | 10.2 | 11.5 | 11.4 | 10.8 | 11.9 | 10.8 | 9.89 |
| 3LS | 29.18 | 10.4 | 11.5 | 10.1 | 11.4 | 11.3 | 10.7 | 11.8 | 10.9 | 9.37 |
| 2LG | 22.09 | 9.0 | 10.0 | 9.5 | 9.32 | 9.08 | 9.10 | 7.68 | 7.73 | 6.23 |
| 2LS | 15.62 | 7.8 | 9.1 | 9.8 | 7.95 | 8.04 | 8.43 | 5.42 | 5.14 | 4.05 |
| 1LG | 12.03 | 7.4 | 8.1 | 11.3 | 6.68 | 7.13 | 6.93 | 4.19 | 4.29 | 3.65 |

Table 26: Total power consumed (in MW) for temporary fault at $F_1$ for sum of two speed deviation input to the controller

| Types of Fault | TCBR location | | | RCBR location | | | CRCBR location | | |
|---|---|---|---|---|---|---|---|---|---|
| | At A | At B | At A&B | At A | At B | At A&B | At A | At B | At A&B |
| 3LG | 61.3 | 65.8 | 78.6 | 73.4 | 78.3 | 104 | 168 | 154 | 193 |
| 3LS | 60.6 | 65.0 | 77.6 | 72.9 | 77.5 | 103 | 167 | 155 | 188 |
| 2LG | 36.8 | 39.6 | 53.4 | 43.7 | 54.1 | 75.4 | 67.1 | 83.9 | 831 |
| 2LS | 27.3 | 27.9 | 43.9 | 35.8 | 41.0 | 57.9 | 26.8 | 32.5 | 29.8 |
| 1LG | 18.9 | 16.5 | 31.4 | 23.3 | 25.2 | 28.1 | 12.4 | 14.4 | 13.2 |

Table 27: Total power consumed (in MW) for permanent fault at $F_1$ for sum of two speed deviation input to the controller

| Types of Fault | TCBR location | | | RCBR location | | | CRCBR location | | |
|---|---|---|---|---|---|---|---|---|---|
| | At A | At B | At A&B | At A | At B | At A&B | At A | At B | At A&B |
| 3LG | 66.9 | 77.1 | 94.1 | 87.8 | 97.4 | 132 | 86.2 | 101 | 105 |
| 3LS | 66.5 | 76.5 | 93.5 | 87.1 | 96.4 | 131 | 83.7 | 98.3 | 103 |
| 2LG | 49.4 | 57.8 | 76.9 | 63.9 | 75.4 | 104 | 57.1 | 62.3 | 63.4 |
| 2LS | 33.2 | 40.2 | 60.9 | 48.9 | 56.8 | 76.5 | 34.7 | 33.6 | 37.63 |
| 1LG | 27.1 | 30.2 | 63.5 | 38.8 | 42.6 | 51.7 | 23.4 | 23.8 | 26.0 |

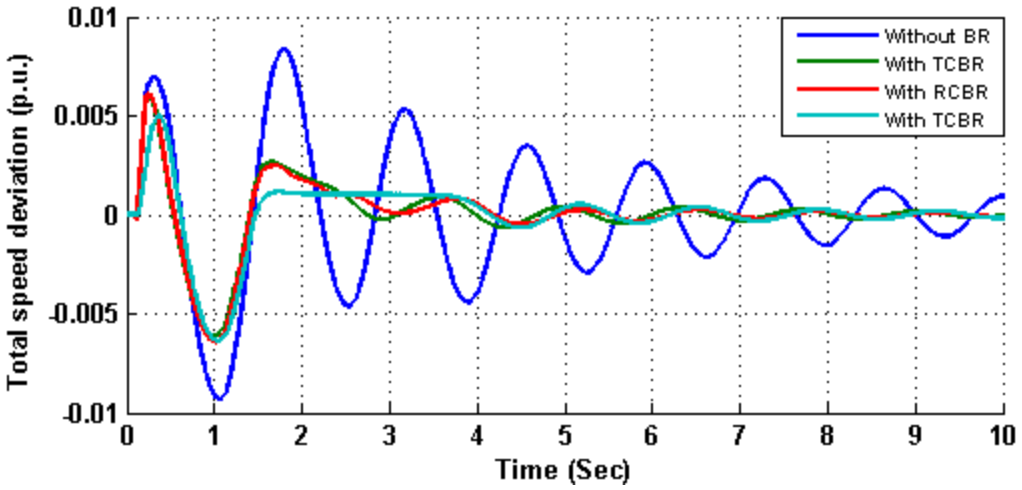


Figure 55: Total speed deviation response for 3LG temporary fault at location $F_1$

[Two speed deviation input to the controller and braking resistor inserted at location A].

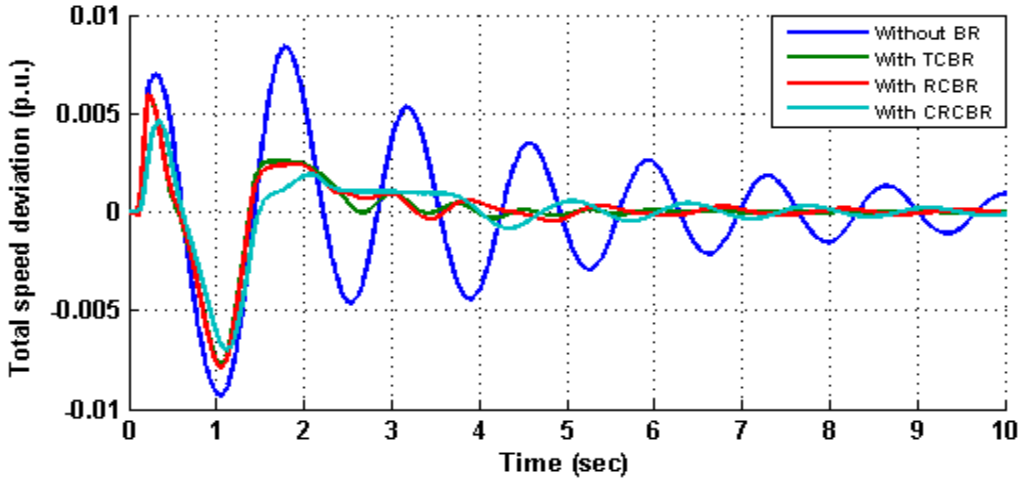


Figure 56: Total speed deviation response for 3LG temporary fault at location $F_1$

[Two speed deviations input to the controller and braking resistor inserted at location B].

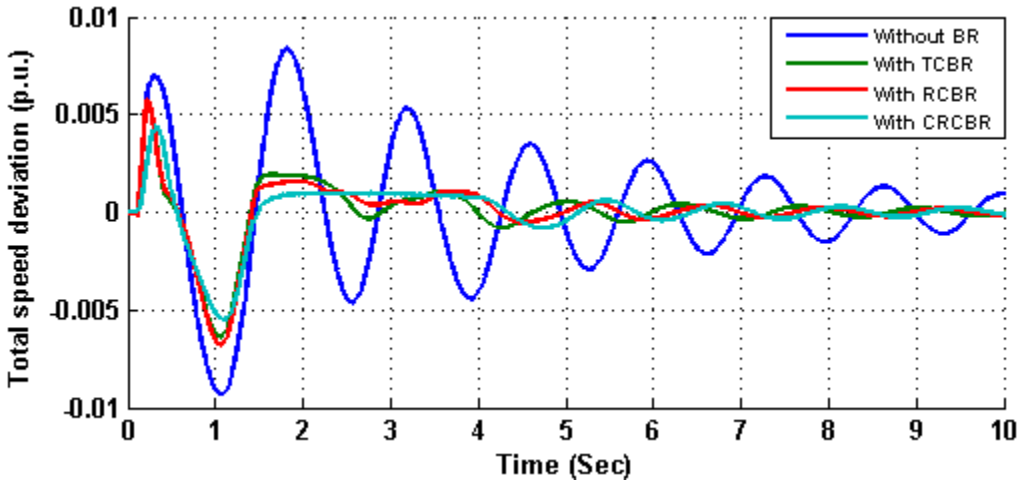


Figure 57: Total speed deviation response for 3LG temporary fault at location $F_1$ [Two speed deviations input to the controller and braking resistor inserted at location A & location B].

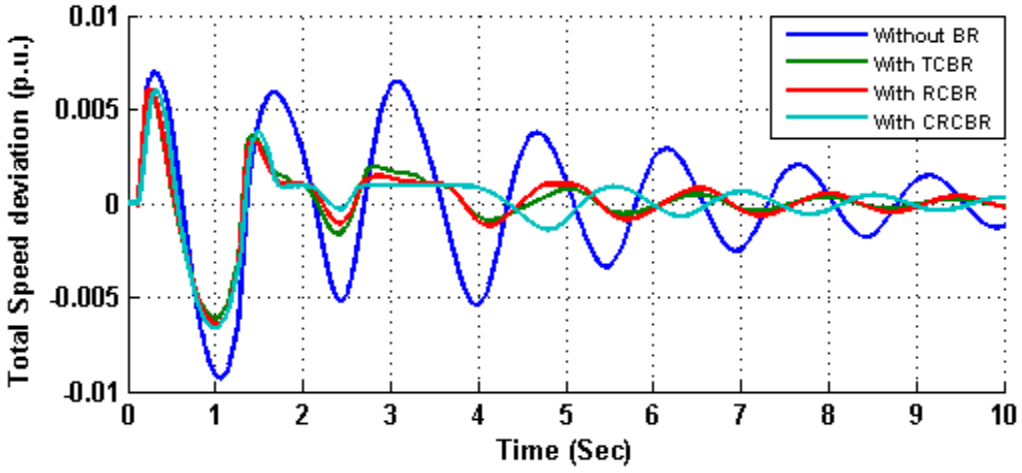


Figure 58: Total speed deviation response for 3LG temporary fault at location $F_1$ [Two speed deviation input to the controller and braking resistor inserted at location A].

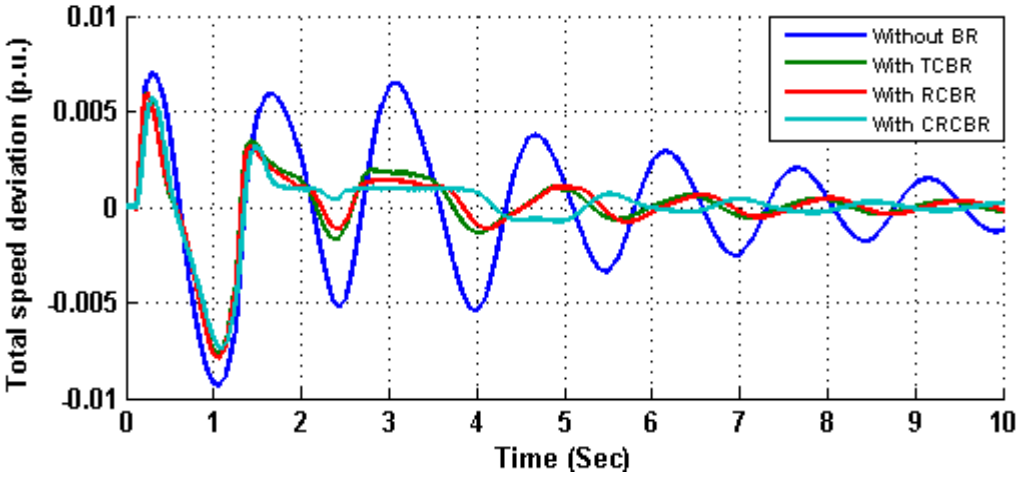


Figure 59: Total speed deviation response for 3LG temporary fault at location $F_1$ [Two speed deviations input to the controller and braking resistor inserted at location B].

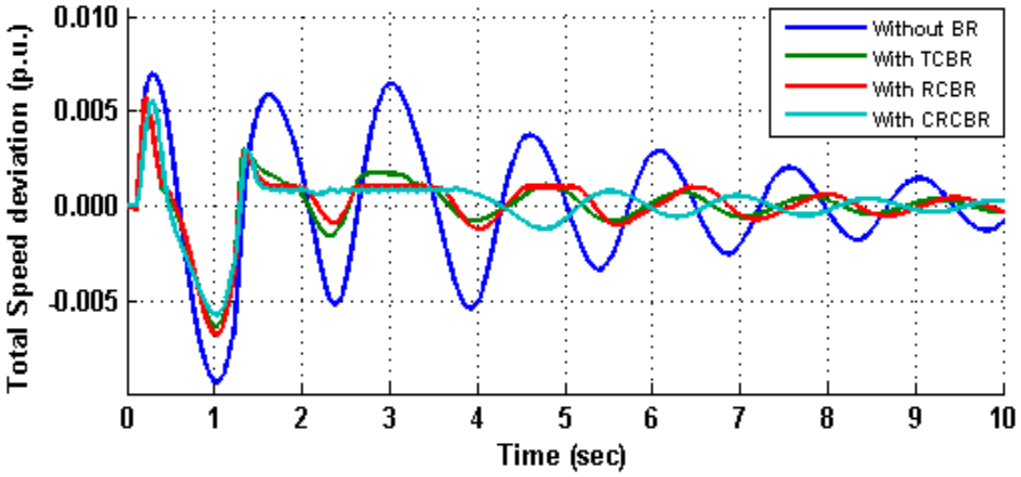


Figure 60: Total speed deviation response for 3LG temporary fault at location $F_1$ [Two speed deviations input to the controller and braking resistor inserted at location A & location B].

From Table 11, the fault location $F_2$ is a least critical point for both the temporary fault and permanent fault conditions and is closer to synchronous generator G1, as shown in Figure 29. For this fault location, insertion of the braking resistor models at any of the mentioned locations provides comparable speed index performance results for both the balanced and unbalanced temporary and permanent faults as shown in Tables 28 and 29. The tables also indicate that the speed index performance is vice-versa for all three braking resistor models when compared for temporary and permanent faults. The proposed CRCBR model's performance is better than the proposed RCBR and existing TCBR model performances for all three braking resistor insertion points as mentioned earlier. The speed index values for the existing TCBR and the proposed RCBR model are comparable for all three braking resistor insertion points. The power absorbed by the braking resistor unit by both the proposed CRCBR and RCBR models and existing TCBR models for temporary and permanent faults are shown in Tables 30 and 31.

The total speed deviation curves for the input to the controller for balanced 3LG temporary and permanent faults at location $F_2$ for braking resistor models inserted only at location A, only at location B and both at locations A and B are shown in Figures 61-66. The speed deviation curves indicate that the controller generates corresponding triggering pulses when the total speed deviation exceeds the preset limit of 3.6 rpm or 0.001 p.u., and hence the total speed deviation do not exceed the set limit.

Table 28: Speed index values (in $10^{-3}$ p.u. sec) for temporary fault at $F_2$ for two speed deviation input to the controller

| Types of Fault | Without BR | TCBR location | | | RCBR location | | | CRCBR location | | |
|---|---|---|---|---|---|---|---|---|---|---|
| | | At A | At B | At A&B | At A | At B | At A&B | At A | At B | At A&B |
| 3LG | 25.16 | 9.49 | 7.76 | 8.95 | 8.60 | 8.25 | 8.13 | 9.16 | 9.95 | 8.37 |
| 3LS | 24.89 | 9.61 | 7.70 | 8.98 | 8.55 | 8.13 | 8.07 | 9.12 | 9.41 | 8.64 |
| 2LG | 15.69 | 6.51 | 6.28 | 7.54 | 6.73 | 5.70 | 6.50 | 6.36 | 5.87 | 5.91 |
| 2LS | 11.17 | 6.31 | 5.71 | 7.70 | 6.16 | 5.24 | 6.00 | 4.01 | 4.23 | 3.54 |
| 1LG | 6.995 | 4.74 | 4.91 | 6.16 | 4.41 | 4.40 | 4.55 | 2.57 | 2.75 | 2.30 |

Table 29: Speed index values (in $10^{-3}$ p.u. sec) for permanent fault at $F_2$ for two speed deviation input to the controller

| Types of Fault | Without BR | TCBR location | | | RCBR location | | | CRCBR location | | |
|---|---|---|---|---|---|---|---|---|---|---|
| | | At A | At B | At A&B | At A | At B | At A&B | At A | At B | At A&B |
| 3LG | 28.69 | 12.1 | 9.87 | 10.8 | 11.8 | 10.8 | 10.4 | 11.9 | 10.9 | 9.83 |
| 3LS | 28.39 | 11.5 | 9.80 | 11.1 | 11.8 | 10.7 | 10.3 | 11.6 | 10.4 | 9.54 |
| 2LG | 20.34 | 10.4 | 8.31 | 9.39 | 9.32 | 8.54 | 8.84 | 7.57 | 7.31 | 6.79 |
| 2LS | 14.44 | 8.41 | 7.21 | 11.00 | 7.94 | 7.41 | 7.87 | 5.26 | 4.75 | 4.25 |
| 1LG | 10.45 | 7.67 | 7.46 | 9.44 | 6.60 | 6.65 | 6.74 | 4.18 | 4.01 | 5.86 |

Table 30: Total power consumed (in MW) for temporary fault at $F_2$ for two speed deviation input to the controller

| Types of Fault | TCBR location | | | RCBR location | | | CRCBR location | | |
|---|---|---|---|---|---|---|---|---|---|
| | At A | At B | At A&B | At A | At B | At A&B | At A | At B | At A&B |
| 3LG | 53.8 | 53.8 | 71.5 | 72.2 | 69.7 | 93.1 | 134 | 162 | 146 |
| 3LS | 52.9 | 53.1 | 70.9 | 71.2 | 68.7 | 92.3 | 131 | 161 | 142 |
| 2LG | 28.9 | 30.5 | 44.7 | 37.2 | 44.5 | 62.7 | 46.2 | 61.9 | 52.8 |
| 2LS | 22.7 | 21.4 | 41.2 | 30.4 | 35.0 | 49.7 | 25.3 | 27.9 | 29.6 |
| 1LG | 12.4 | 12.1 | 24.8 | 19.9 | 19.6 | 22.6 | 11.3 | 10.3 | 10.8 |

Table 31: Total power consumed (in MW) for permanent fault at for two speed deviation input to the controller

| Types of Fault | TCBR location | | | RCBR location | | | CRCBR location | | |
|---|---|---|---|---|---|---|---|---|---|
| | At A | At B | At A&B | At A | At B | At A&B | At A | At B | At A&B |
| 3LG | 68.1 | 64.8 | 91.9 | 83.7 | 84.5 | 118 | 83.6 | 85.5 | 98.0 |
| 3LS | 66.3 | 64.3 | 92.8 | 82.6 | 83.9 | 118 | 80.5 | 83.6 | 96.2 |
| 2LG | 49.5 | 46.9 | 72.6 | 60.0 | 63.4 | 90.3 | 54.9 | 53.2 | 62.2 |
| 2LS | 33.1 | 29.7 | 64.8 | 44.9 | 45.0 | 57.2 | 33.1 | 31.0 | 34.5 |
| 1LG | 25.9 | 23.6 | 53.1 | 34.1 | 32.2 | 38.7 | 19.2 | 20.1 | 22.7 |

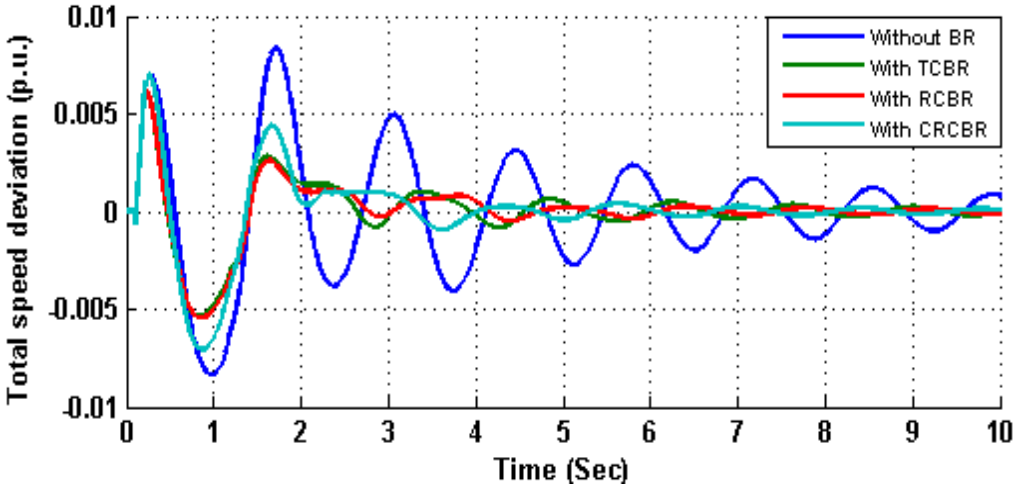


Figure 61: Total speed deviation response for 3LG temporary fault at location $F_2$

[Two speed deviations input to the controller and braking resistor inserted at location A].

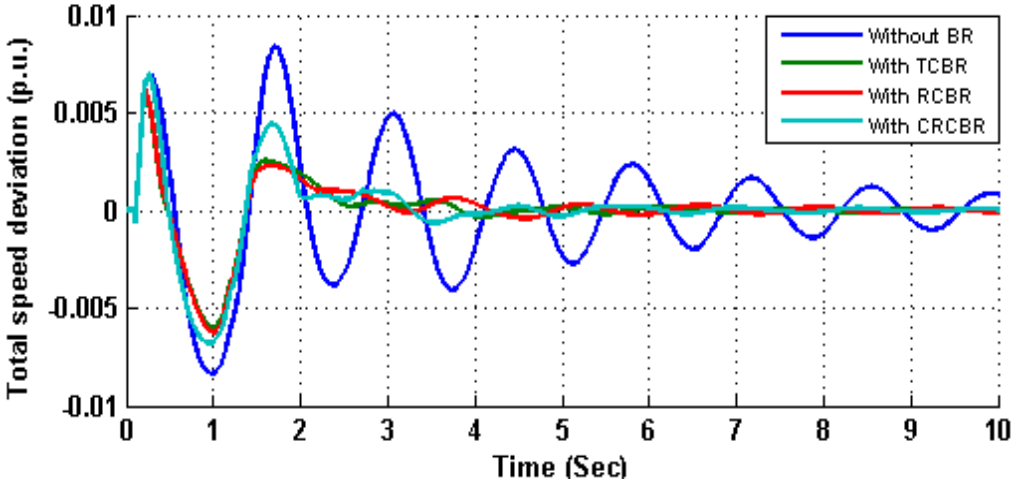


Figure 62: Total speed deviation response for 3LG temporary fault at location $F_2$

[Two speed deviations input to the controller and braking resistor inserted at location B].

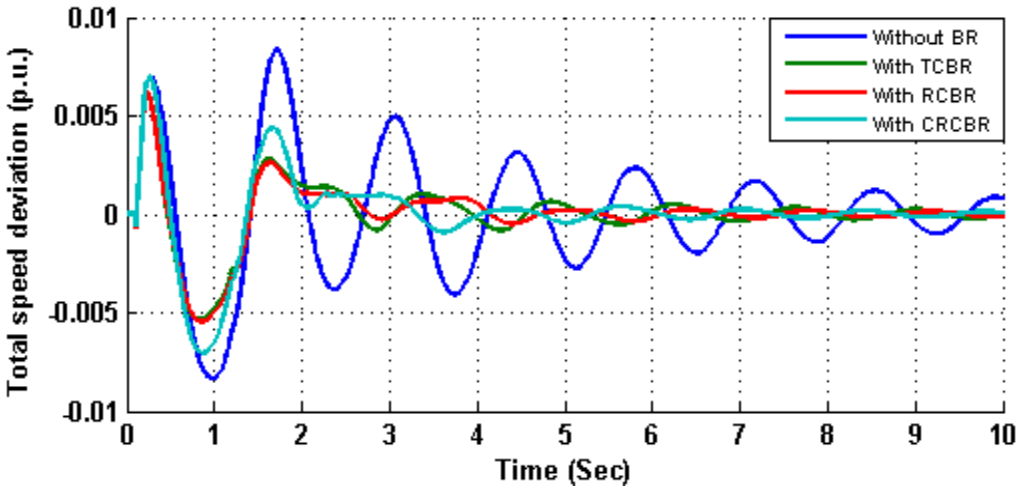


Figure 63: Total speed deviation response for 3LG temporary fault at location $F_2$ [Two speed deviations input to the controller and braking resistor inserted at location A & location B].

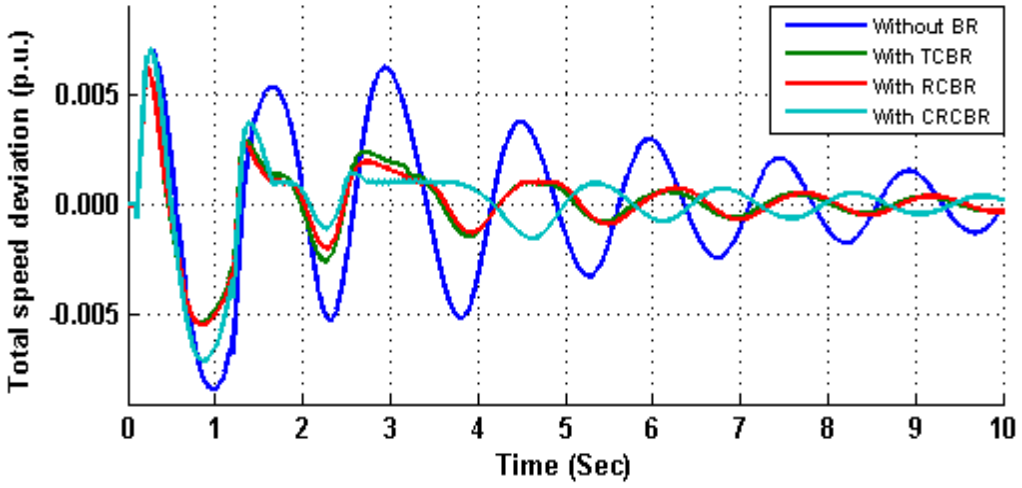


Figure 64: Total speed deviation response for 3LG permanent fault at location $F_2$ [Two speed deviations input to the controller and braking resistor inserted at location A].

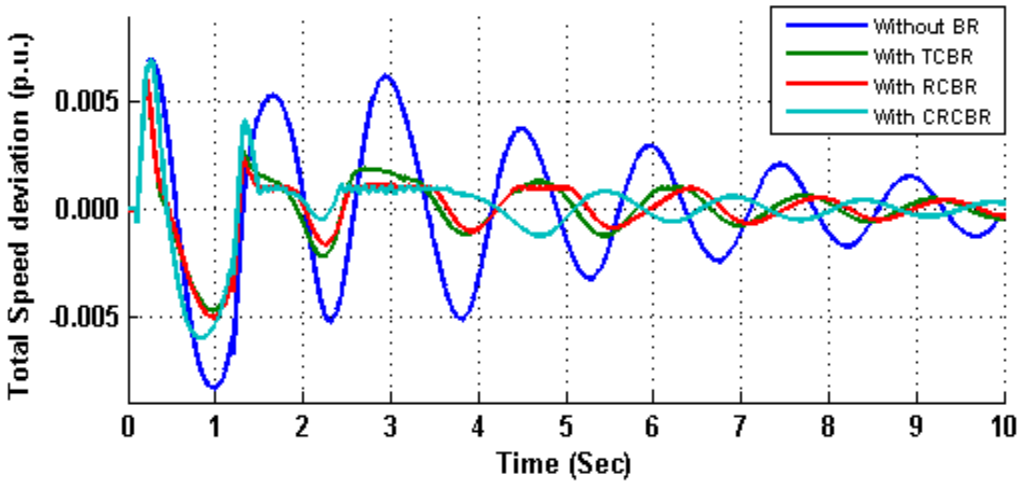


Figure 65: Total speed deviation response for 3LG permanent fault at location $F_2$ [Two speed deviations input to the controller and braking resistor inserted at location B].

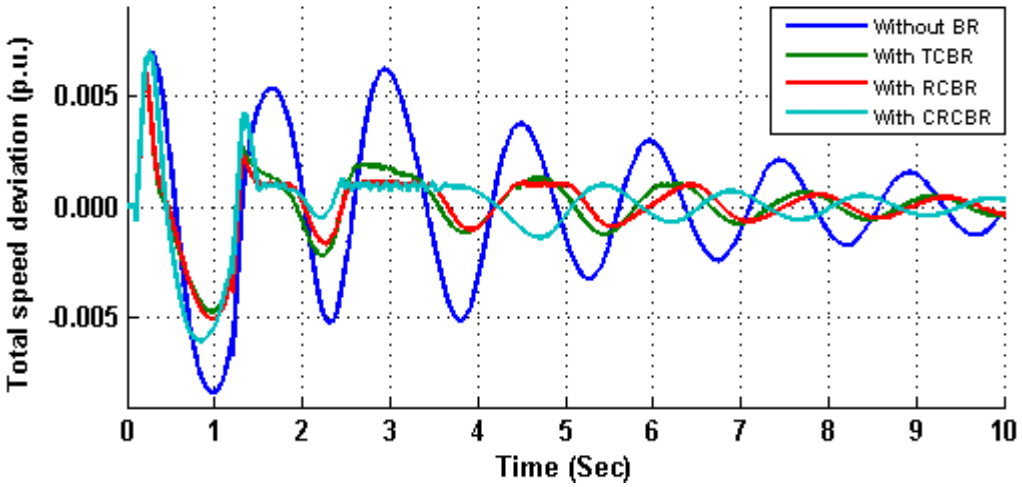


Figure 66: Total speed deviation response for 3LG permanent fault at location $F_2$ [Two speed deviations input to the controller and braking resistor inserted at location A & location B].

From Table 11, the fault location $F_3$ is a critical point for both the temporary fault and permanent fault conditions and is in-between synchronous generator G1 and G2, as shown in Figure 29. For this fault location, insertion of the braking resistor models at any of the mentioned locations provides comparable speed index performance results for both the balanced and unbalanced temporary and permanent faults as shown in Tables 32 and 33. The tables also indicate that the speed index performance is vice-versa for all three braking resistor models when compared for temporary and permanent faults. The proposed RCBR model's performance is better than the proposed CRCBR and existing TCBR model performances for temporary fault conditions, whereas the proposed CRCBR model's performance is better than the proposed RCBR and existing TCBR model performances for permanent fault conditions. The power absorbed by the braking resistor unit by both the proposed CRCBR and RCBR models and existing TCBR models for temporary and permanent faults are shown in Tables 34 and 35.

The total speed deviation curves for the input to the controller for balanced 3LG temporary and permanent faults at location $F_3$ for braking resistor models inserted only at location A, only at location B and both at locations A and B are shown in Figures 67-72. The speed deviation curves indicate that the controller generates corresponding triggering pulses when the total speed deviation exceeds the preset limit of 3.6 rpm or 0.001 p.u., and hence the total speed deviation do not exceed the set limit.

Table 32: Speed index values (in $10^{-3}$ p.u. sec) for temporary fault at $F_3$ for two speed deviation input to the controller

| Types of Fault | Without BR | TCBR location | | | RCBR location | | | CRCBR location | | |
|---|---|---|---|---|---|---|---|---|---|---|
| | | At A | At B | At A&B | At A | At B | At A&B | At A | At B | At A&B |
| 3LG | 33.55 | 11.3 | 12.2 | 12.0 | 11.2 | 11.9 | 10.5 | 13.0 | 13.4 | 11.9 |
| 3LS | 33.25 | 11.2 | 12.1 | 11.9 | 11.0 | 11.8 | 10.3 | 13.0 | 13.2 | 12.1 |
| 2LG | 28.36 | 9.26 | 9.54 | 10.1 | 8.73 | 9.55 | 9.07 | 10.3 | 11.3 | 10.3 |
| 2LS | 19.71 | 6.76 | 7.16 | 7.40 | 6.56 | 6.59 | 6.85 | 7.78 | 9.01 | 7.76 |
| 1LG | 15.53 | 6.47 | 6.68 | 7.96 | 5.81 | 5.71 | 6.30 | 6.20 | 6.09 | 6.75 |

Table 33: Speed index values (in $10^{-3}$ p.u. sec) for permanent fault at $F_3$ for two speed deviation input to the controller

| Types of Fault | Without BR | TCBR location | | | RCBR location | | | CRCBR location | | |
|---|---|---|---|---|---|---|---|---|---|---|
| | | At A | At B | At A&B | At A | At B | At A&B | At A | At B | At A&B |
| 3LG | 35.79 | 19.4 | 15.1 | 16.3 | 16.8 | 15.7 | 13.6 | 17.1 | 16.2 | 13.3 |
| 3LS | 35.57 | 19.3 | 15.0 | 16.1 | 16.7 | 15.5 | 13.4 | 17.0 | 16.1 | 13.7 |
| 2LG | 34.00 | 16.2 | 12.8 | 12.9 | 14.1 | 13.0 | 11.5 | 13.9 | 13.5 | 11.9 |
| 2LS | 26.03 | 11.8 | 10.4 | 11.2 | 10.5 | 10.5 | 9.40 | 14.6 | 12.5 | 8.45 |
| 1LG | 21.82 | 9.71 | 9.67 | 10.8 | 8.68 | 8.59 | 8.56 | 6.95 | 8.44 | 7.08 |

Table 34: Total power consumed (in MW) for temporary fault at $F_3$ for two speed deviation input to the controller

| Types of Fault | TCBR location | | | RCBR location | | | CRCBR location | | |
|---|---|---|---|---|---|---|---|---|---|
| | At A | At B | At A&B | At A | At B | At A&B | At A | At B | At A&B |
| 3LG | 86.9 | 95.7 | 138 | 108 | 113 | 164 | 152 | 115 | 375 |
| 3LS | 86.1 | 95.4 | 137 | 108 | 113 | 162 | 152 | 116 | 369 |
| 2LG | 68.1 | 78.1 | 99.5 | 84.3 | 91.1 | 123 | 153 | 116 | 281 |
| 2LS | 40.4 | 49.2 | 63.4 | 51.8 | 59.6 | 81.8 | 114 | 126 | 146 |
| 1LG | 33.5 | 37.8 | 53.7 | 43.0 | 48.9 | 7.13 | 67.6 | 82.2 | 90.9 |

Table 35: Total power consumed (in MW) for permanent fault at $F_3$ for two speed deviation input to the controller

| Types of Fault | TCBR location | | | RCBR location | | | CRCBR location | | |
|---|---|---|---|---|---|---|---|---|---|
| | At A | At B | At A&B | At A | At B | At A&B | At A | At B | At A&B |
| 3LG | 102 | 107 | 149 | 109 | 121 | 167 | 149 | 146 | 259 |
| 3LS | 102 | 106 | 148 | 108 | 120 | 166 | 149 | 146 | 253 |
| 2LG | 87.3 | 94.0 | 123 | 97.0 | 105 | 143 | 153 | 147 | 206 |
| 2LS | 61.8 | 70.2 | 98.7 | 71.2 | 82.8 | 115 | 94.8 | 120 | 116 |
| 1LG | 51.9 | 56.8 | 87.4 | 60.2 | 73.4 | 103 | 67.2 | 84.0 | 81.6 |

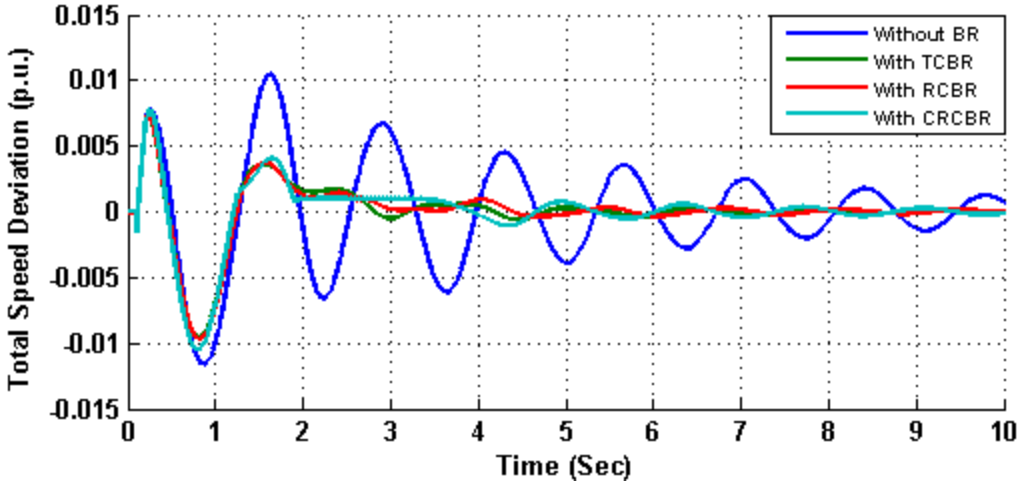


Figure 67: Total speed deviation response for 3LG temporary fault at location $F_3$

[Two speed deviations input to the controller and braking resistor inserted at location A].

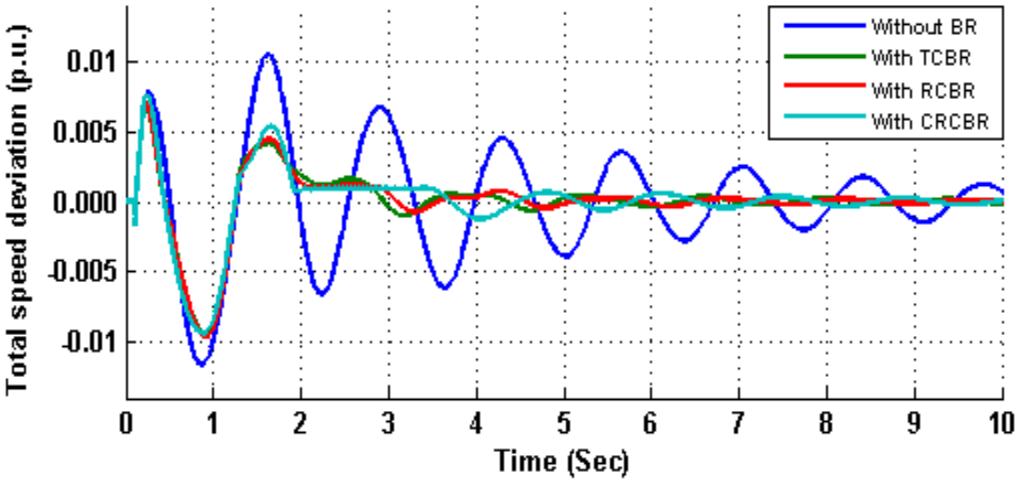


Figure 68: Total speed deviation response for 3LG temporary fault at location $F_3$

[Two speed deviations input to the controller and braking resistor inserted at location B].

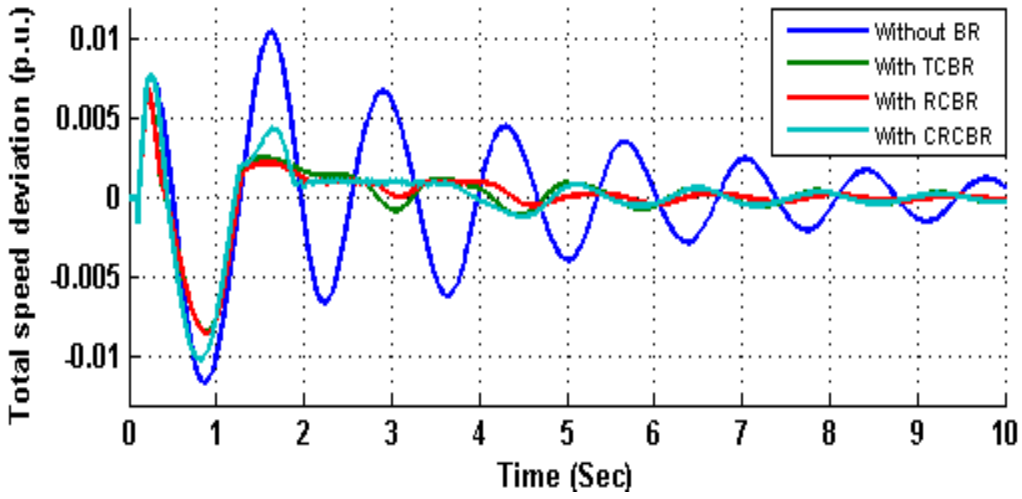


Figure 69: Total speed deviation response for 3LG temporary fault at location $F_3$ [Two speed deviations input to the controller and braking resistor inserted at location A & location B].

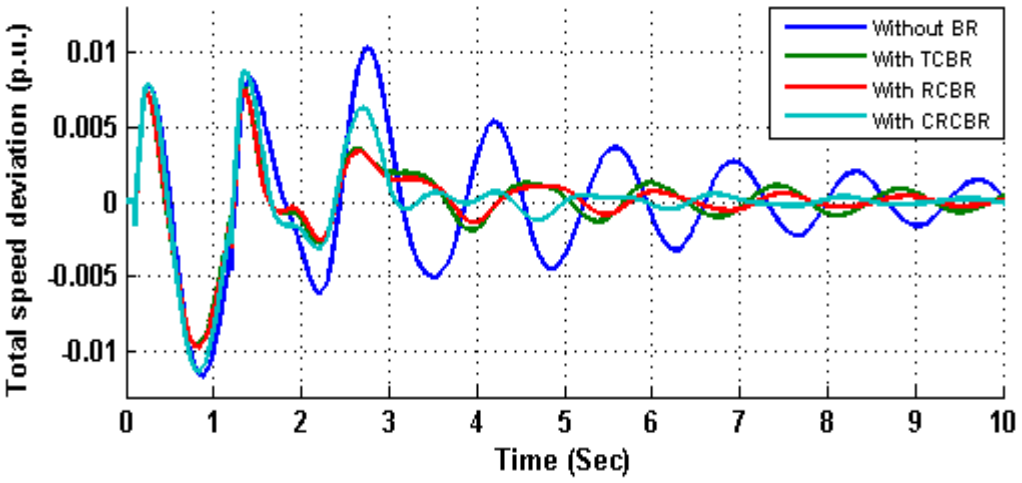


Figure 70: Total speed deviation response for 3LG permanent fault at location $F_3$ [Two speed deviations input to the controller and braking resistor inserted at location A].

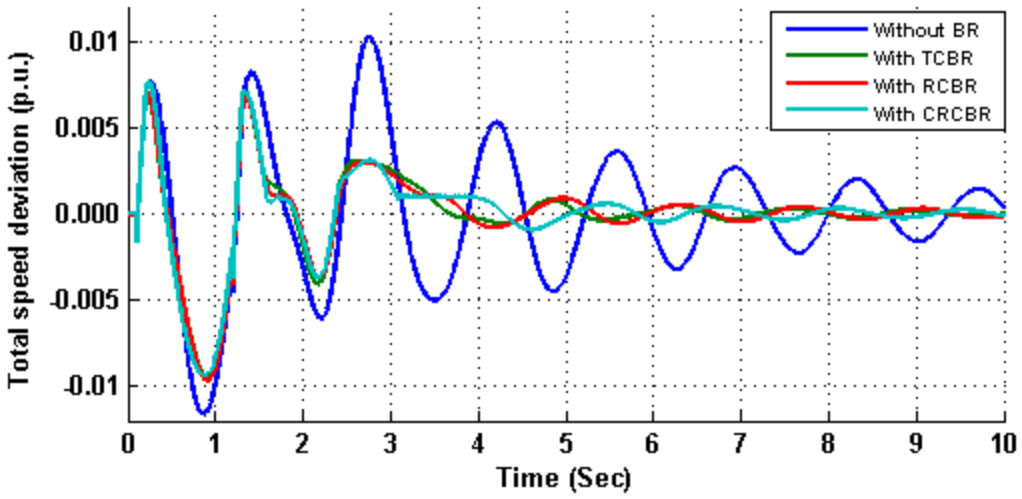


Figure 71: Total speed deviation response for 3LG permanent fault at location $F_3$ [Two speed deviations input to the controller and braking resistor inserted at location B].

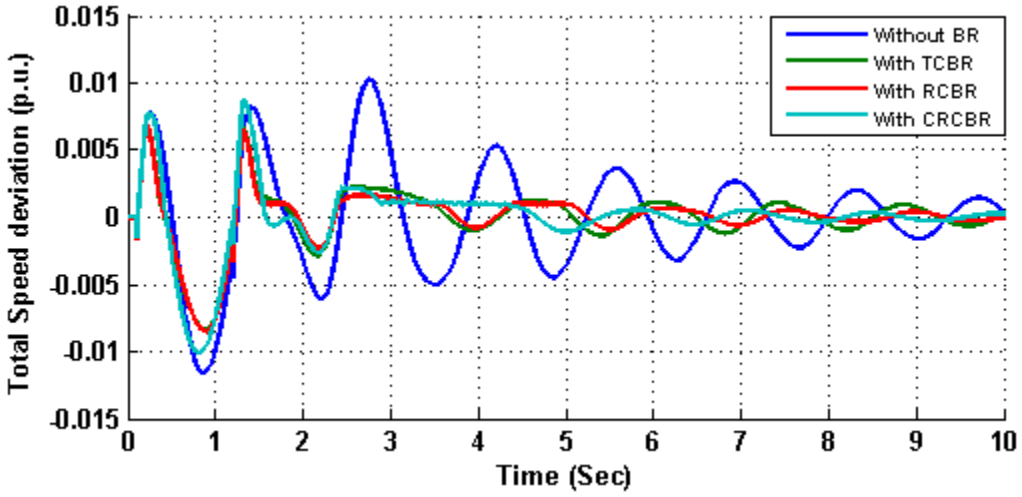


Figure 72: Total speed deviation response for 3LG permanent fault at location $F_3$ [Two speed deviations input to the controller and braking resistor inserted at location A and location B].

# VI. DISCUSSIONS

The proposed CRCBR and RCBR models and the existing TCBR model switches are compared and analyzed on the basis of cost and heat and harmonics factors. They are briefly discussed in the following sections.

## *A. COST ANALYSIS*

The important feature of the proposed models is the reduction of the number of BR units to one from three for a three-phase system because of the switch designs of the proposed models. All components used in the switch design of the existing and proposed models are compared and shown in Table 36. It can be seen that the number of braking resistor unit is reduced to one for the proposed models as compared to three braking resistor units used in proposed models. However, few components, such as the capacitance bank and diodes, are not used in the TCBR model's switch, while they are used for designing the other two model's switches. The braking resistor unit values for the proposed models and existing models for SMIB and IEEE-9 bus power system test models are discussed in the earlier sections. The braking resistor value for the proposed models is approximately twice that of a single unit of the existing TCBR braking resistor. It might be possible that with the controller switch, the overall size of the braking resistor model will be reduced and the proposed models provide a simultaneous control on three phases with single switch. The number of elements as well as their ratings used to design the existing and proposed models is nearly the same. The best feature would be the reduction of the cost of BR units with the reduced number of BR units installed.

Table 36: Components used for designing switches of proposed and existing braking resistor models discussed in this work

| Components | TCBR | RCBR | CRCBR |
|---|---|---|---|
| Thyristors | 6 | 6 | 0 |
| Diodes | 0 | 0 | 6 |
| IGBT | 0 | 0 | 1 |
| Capacitance | 0 | 0 | 1 |
| BR Units | 3 | 1 | 1 |

### *B. HEAT LOSS AND HARMONICS ANALYSIS*

The proposed models' braking resistor units absorbs DC voltage and current whereas the existing TCBR model braking resistor unit absorbs AC voltage and power. The DC voltage and current have their own advantages over AC current and voltages, such as earlier reduces harmonic current and ripples and decrease heating of BR units. Also, with the reduction of the number of BR units, the heat losses occurring due to heating of BR unit for the proposed models reduced to approximately one-third as compared to that in the existing TCBR model. The total power consumed by the CRCBR model is more as compared to that by other two models. So, the heat loss for the CRCBR model would be more. It is described in [77], [80] that the CRCBR models are more efficient as compared to the RCBR models, as they generate a load current with reduced ripple and generate less current harmonics.

The disconnection of the heavy load from the power grid system decreases the electrical load connected to the synchronous generator. The governor system takes few seconds for sensing the increase in speed of the synchronous generator and for closing the input valve of the steam turbine generator. During this period, the synchronous generator gets accelerated. The acceleration of the synchronous generator will lead to the change in the frequency of the power grid system and hence affect the loads connected to the power grid system. The instant insertion of braking resistor will absorb the accelerating power of the synchronous generator and make the system stabilize.

# VII. CONCLUSION AND FUTURE WORK

The proposed RCBR and CRCBR models can be used as an alternate solution to the existing TCBR model for the enhancement of power system transient stability. Also, each of the proposed BR model has an advantage of reduced number of BR units with few trade-off conditions, such as speed index, cost, heat loss and harmonics.

## *A. CONTRIBUTION OF THE THESIS*

The transient stability enhancement is related to achieving the stabilized and synchronized power grid system following a severe load transition due to any fault occurrence in the system or due to failure of the system. The insertion of the braking resistor into the power grid system helps in enhancing the power system stability as well as the bulk power transmission without affecting the existing power grid system. The effectiveness of the two new braking resistor models, designed in this work, and the existing braking resistor model are compared on the basis of the performance indices, heat and harmonic, and cost. The transient stability analysis is performed for both kinds of temporary and permanent faults.

This thesis proposes the RCBR and CRCBR models with an advantage of reduced number of BR units which may lead to reduced overall size and cost of the BR model. The speed curves and speed indices calculated for both balanced and unbalanced fault conditions imply that the proposed models are alternate solutions to the existing BR model considering few trade-off conditions, such as speed index, cost, heat loss and harmonics. Also, the CRCBR model is better than the other models, whereas heat losses by the CRCBR model would be higher due to higher power dissipation in BR.

## B. *FUTURE WORK*

As an extension to this work, the following points can be considered in the future.

a) In future, by getting the exact market price for all the components used to design the proposed models and the existing models, the analysis can be made for the economical, small-sized, and efficient braking resistor models.

b) For this work, the required triggering pulses for the switching operation of the braking resistor models are generated by the designed PID controller. The designed PID controller takes change in speed of synchronous generator as an input and generates the required pulses. It is also reported in literature that the transient stability of the power grid system can be enhanced by controlling the other steady state parameters of the synchronous generator, such as the change in steady-state voltage, change in steady state load angle, change in kinetic energy of the synchronous generators, etc. Hence, in the future, a PID based controller can be designed for different inputs from synchronous generators to generate the required triggering pulses for the proposed models and results can be compared.

c) There is also a scope of designing a non-linear controller except the existing fuzzy logic and neural network controllers and can be compared with the existing controller performances.

d) These models are needed to be tested on a multi-machine system to see the effectiveness for a large system. The optimal insertion point for the insertion of braking resistor models can be analyzed.

e) The braking resistor unit value of 1 p.u. is used for this work. There is no work reported regarding the use of an optimal value of braking resistor unit. So, an

analysis is required to determine the resistor optimal value that can improve the transient stability.

# REFERENCES


[1] K. K. Y. Poon, Z. Lan and Y. X. Ni, "An Overview on Transient Stability Control in Modern Power Systems," in 7th IET International Conference on Advances on Power System Control, Operation and Management (APSCOM 2006), 2006.

[2] W. H. Croft and R. H. Hartley, "Improving Transient Stability by use of Dynamic Braking," AIEE Trans. on Power Apparatus and Systems, Part III, vol. 81, no. 3, pp. 17-24, 1962.

[3] R. H. Park, "The Design and Use of Braking Resistors," in Proceedings: IEEE resources (electrical and electronics engineering resources) roundup; a record of technical papers presented at the Region 6 conference,, Del Webb's TownHouse, Phoenix, Arizona, April 16, 17, 18, 1969.

[4] D. Y. Trofimenko, "The Stability of a Hydro-Electric The Stability of a Hydro-Electric Generator with Electric Braking," Electric Technology U.S.S.R., vol. 1, pp. 70-78, August 1962.

[5] V. M. Gornshtein and Y. N. Luginskii, "The Use of Repeated Electrical Braking and Unloading to Improve the Stability of Power Systems," Electric Technology, vol. 2, pp. 292-302, 1962.

[6] J. F. Conroy and R. Watson, "Low-Voltage Ride-Through of a Full Converter Wind Turbine with Permanent Magnet Generator," IET Renewable Power Generation, Vol. 1, No. 3, pp. 182-189, September 2007.

[7] A. H. M. A. Rahim, "A Minimum-Time Based Fuzzy Logic Dynamic Braking Resistor Control for Sub-Synchronous Resonance," Electrical Power and Energy Systems, vol. 26, pp. 191-198, 2004.

[8] H. M. Ellis, J. E. Hardy, A. L. Blythe and J. W. Skooglund, "Dynamic Stability of Peace River Transmission System," IEEE Trans. on Power Apparatus and Systems, vol. PAS-85, no. 6, pp. 586-600, June 1966.

[9] K. Yoshida, M. Fukunishi and A. J., "Development of System-Damping Resistors for Stabilizing Bulk Power Transmission," Electrical Engineering in Japan, vol. 91, no. 3, pp. 79-90, May 1971, pp. 79-90, May 1971.

[10] M. L. Shelton, P. F. Winkelman, W. A. Mittelstadt and W. J. Bellerby, "Bonneville Power Administration 1400-MW Braking Resistor," IEEE Trans. on Power

Apparatus and Systems, vol. PAS-94, p. 1975, 602-611.

[11] C. Rao and T. Nag Sarkar, "Digital Simulation of Thyristor Controlled Braking Device," in Fifth National Systems Conference, N. S. C. – 78, Punjab Agricultural University, vol. 2, India, 1978.

[12] C. Rao and T. Nag Sarkar, "Transient Stability Improvement with Thyristor Controlled Braking Device," IEEE Winter Power Meeting, pp. 1-6, 1980.

[13] C. Rao and T. Nag Sarkar, "Some Aspects of Transient Stability Improvement with Thyristor Controlled Dynamic Brake," IEEE Winter Power Meeting, pp. 1-6, 1980.

[14] C. Rao and T. Nag Sarkar, "Halfwave Thyristor Controlled Dynamic Brake to Improve Transient Stability," in IEEE Summer Power Meeting Conference, paper no.83 SM 386-0, July 1983.

[15] C. Rao and T. Nag Sarkar, "Half Wave Thyristor Controlled Dynamic Brake to Improve Transient Stability," IEEE Trans. on Power Apparatus and Systems, vol. PAS-103, no. 5, pp. 1077-1083, May 1984.

[16] S. Chatterji, C. Rao and T. Nag Sarkar, "Fuzzy Logic Based Half Wave Thyristor Controlled Dynamic Brake," in Fifth International Conference on Power Electronics and Drive Systems, PEDS – 2003, November, 2003.

[17] M. H. Ali, T. Murata and J. Tamura, "Influence of Communication Delay on the Performance of Fuzzy Logic-Controlled Braking Resistor Against Transient Stability," IEEE Trans. on Control Systems Technology, vol. 16, no. 6, pp. 1232-1241, November 2008.

[18] M. H. Ali, M. Park and I. Yu, "Minimization of Shaft Torsional Oscillations by Fuzzy Controlled Braking Resistor Considering Communication Delay," WSEAS Trans. on Power Systems, vol. 3, no. 3, pp. 82-89, March 2008.

[19] M. H. Ali, M. Park, I.-K. Yu, T. Murata and J. Tamura, "Coordination of Fuzzy Controlled Braking Resistor and Optimal Reclosing for Damping Shaft-Torsional Oscillations of Synchronous Generator," in ICEMS International Conference Electrical Machines and Systems, 8-11 Oct. 2007.

[20] M. H. Ali, T. Murata and J. Tamura, "Effect of Fuzzy Controlled Braking Resistor on Damping Turbine Generator Shaft Torsional Oscillations During Unsuccessful Reclosing," International Review of Electrical Engineering (IREE), vol. 1, no. 5, pp.

711-718, December 2006.

[21] M. H. Ali, T. Murata and J. Tamura, "Effect of Coordination of Optimal Reclosing and Fuzzy Controlled Braking Resistor on Transient Stability During Unsuccessful Reclosing," IEEE Trans. on Power Systems, vol. 21, no. 3, pp. 1321- 1330, August 2006.

[22] M. H. Ali, T. Murata, S. Y. and J. Tamura, "Transient Stability Improvement By Fuzzy Logic Controlled Braking Resistor," International Journal of Power and Energy Systems, vol. 25, no. 3, pp. 143-150, October 2005.

[23] M. H. Ali, Murata and J. T. and Tamura, "The Effect Of Temperature Rise of the Fuzzy Logic Controlled Braking Resistors on Transient Stability," IEEE Trans. on Power Systems, vol. 19, no. 2, pp. 1085-1095, May 2004.

[24] M. H. Ali, T. Murata and J. Tamura, "Transient Stability Augmentation by Fuzzy Logic Controlled Braking Resistor in Multi-Machine Power System," in Proceedings of IEEE/PES Transmission And Distribution Conference and Exhibition 2002: Asia Pacific, vol. 2, Yokohama, Japan, October 2002.

[25] M. H. Ali, T. Murata and J. Tamura, "Augmentation of Transient Stability by Fuzzy-Logic Controlled Braking Resistor in Multi-Machine Power System," in Proceedings of the IEEE Powertech 2005 Conference, St. Petersburg, Russia, June 2005.

[26] M. H. Ali, T. Murata, S. Y. and J. Tamura, "A Fuzzy Logic Controlled Braking Resistor Scheme for Stabilization of Synchronous Generator," in Proceedings of IEMDC (IEEE International Electric Machines and Drives Conference) 2001, MIT, USA, June 2001.

[27] A. H. M. A. Rahim, A. M. Al-Shehri and A. I. J. Al-Sammak, "Optimum Control Strategies for Transient as well as Oscillatory Instability of Power Systems," IEEE Trans. on Power System, vol. 8, no. 2, pp. 491-496, 1993.

[28] A. M. Mehdi, M. S. M. Al-Hafid and A. K. Al-Sulaifanie, "Improvement of Transient Stability Limit Using Microprocessor Controlled Dynamic Braking System," Electrotechnical Conference, Proceedings, 6th Mediterranean, vol. 2, p. 1314 – 1317, 1991.

[29] B. Das, A. Ghosh and P. Sachchidanand, "Control Of Dynamic Brake Through Heuristic Rule," Electric Machines and Power Systems, vol. 28, no. 11, pp. 1091-

1105, 2000.

[30] K. Nakamura and S. Muto, "Improvement of Power System Transient Stability by Optimum Bang-Bang Control of Series and Parallel Resistors," Electrical Engineering in Japan, vol. 96, no. 2, pp. 47-54, 1976.

[31] D. F. Peelo, D. W. Hein and F. Peretti, "Application of a 138 KV 200 MW Braking Resistor," Power Engineering Journal, Vol. 8, No. 4, pp. 188 -192, August 1994.

[32] S. S. Joshi and D. G. Tamaskar, "Augmentation of Transient Stability Limit of a Power System by Automatic Multiple Application of Dynamic Braking," IEEE Trans. on Power Apparatus and Systems, vol. PAS-104, no. 11, pp. 3004-3012, November 1985.

[33] M. K. Donnelly, J. R. Smith, R. M. Johnson, J. F. Hauer and R. W. a. A. R. Brush, "Control of a Dynamic Brake to Reduce Turbine Generator Shaft Transient Torques," IEEE Trans. on Power Systems, vol. PWRS-8, pp. 67 -73, 1993.

[34] Y. Wang, W. Mittelstadt and D. J. Maratukulam, "Variable Structure Braking Resistor Control in a Multimachine Power System," IEEE Trans. on Power Systems, vol. 9, no. 3, pp. 1557-1562, 1994.

[35] A. Sen and J. Meisel, "Transient Stability Augmentation with a Braking Resistor Using Optimal Aiming Strategies," Proc. IEE, vol. 125, no. 11, pp. 1249-1255, November 1978.

[36] J. Meisel, A. Sen and M. L. Gilles, "Alleviation of a Transient Stability Crisis Using Shunt Braking Resistors and Series Capacitors," International Journal of Electrical Power and Energy Systems, vol. 3, no. 1, pp. 25-37, 1981.

[37] K. M. K. S. Bandara, A. Arulampalam and S. G. Abeyratne, "Dynamic Breaking Resistor Based Control Of Generator For Improved Dynamics," in International Conference on Industrial and Information Systems (ICIIS), December, 2009.

[38] F. Ishiguro, S. Tanaka, M. Shimomura, T. Maeda, K. Matsushita and H. Sugimoto, "Coordinated Stabilizing Control of Exciter, Turbine and Breaking Resistor," IEEE Trans. on Power Systems, vol. 1, no. 3, pp. 74 -80, 1986.

[39] T. Hiyama, M. Mishiro, H. Kihara and T. H. Ortmeyer, "Fuzzy Logic Switching Of Thyristor Controlled Braking Resistor Considering Coordination With SVC," IEEE

Trans. on Power Delivery, Vol. 10, No. 4, pp. 2020-2026, October 1995.

[40] R. Patel, T. Bhatti and D. Kothari, "Improvement Of Power System Transient Stability By Coordinated Operation Of Fast Valving And Braking Resistor," IEE Proceedings –Generation, Transmission, and Distribution, vol. 150, no. 3, May 2003.

[41] M. Yagami and J. Tamura, "Power System Stabilization by Fault Current Limiter and Thyristor Controlled Braking Resistor," in IEEE Energy Conversion Congress and Exposition, (ECCE 2009), 2009.

[42] M. Yagami and J. Tamura, "Enhancement of Transient Stability Using Fault Current Limiter and Thyristor Controlled Braking Resistor," in Power Tech, IEEE, Lausanne, 2007.

[43] B. S. Surjan and G. Singh, "Modeling of Power System Embedded With Thyristor Controlled Resistive Brake and Static Reactive Power Compensator for Small Signal Stability Investigation," in Power System Technology And IEEE Power India Conference, (POWERCON) 2008, Joint International Conference on, India, 2008.

[44] Y. Mikuni, G. Shirai, R. Yokoyama and G. Fujita, "A Method of Enhancement of Transmission Capability Limit Using System Damping Resistor and Series — Shunt Capacitors," Power & Energy Society General Meeting, (PES '09) IEEE, pp. 1-9, 2009.

[45] K. Ichiyanagi, Y. Goto, K. Yukita, T. Kato and H. Yamada, "Study of Power Transient Stability Using Facts and SDR," in International Conference on Power System Technology, Proceedings, (Powercon – 2000), vol. 1, 2000.

[46] D. L. Lubkeman and G. T. Heydt, "The Application of Dynamic Programming in a Discrete Supplementary Control for Transient Stability Enhancement of Multimachine Power Systems," IEEE Trans. on Power Apparatus and Systems, vol. PAS-104, no. 9, pp. 2342 - 2348, September 1985.

[47] A. H. M. A. Rahim and D. A. H. Alamgir, "A Closed Loop Quasi Optimal Dynamic Braking Resistor and Shunt Reactor Control Strategy for Transient Stability," IEEE Trans. on Power Systems, vol. 3, no.3, pp. 879-886, August 1988.

[48] Y. Wang, W. Mittelstadt, R. R. Mohler and R. Spee, "Variable Structure Facts Controllers for Power System Transient Stability," IEEE Trans. on Power Systems,

vol. 7, no. 1, pp. 307-313, 1992.

[49] J. Machowski, A. Smolarczyk and J. Bialek, "Damping Of Power Swings By Control Of Braking Resistors," International Journal of Electrical Power & Energy Systems, vol. 23, no. 7, p. 2001, 539-548.

[50] C. Yuning and M. E. El-Harway, "An EAC Based Braking Resistor Approach for Transient Stability Improvement," IEEE International Symposium in Industrial Electronics, vol. 3, p. 1869 – 1874, 9-13 July 2006.

[51] A. Rubaai, "Design and Analysis of Nonlinear Hierarchical Controllers for Electric Utility Industry," in IEEE 37th Industry Applications Society, IEEE-IAS Annul Meeting, Conference Record, 2002.

[52] A. Rubaai and A. R. Ofoli, "Design and Analysis of Nonlinear Digital Controllers-Based Two Level Hierarchy for Electric Utility Industry," IEEE Trans. on Industry Applications, vol. 39, no. 2, pp. 395-407, March/April 2003.

[53] A. Rubaai and D. Cobbinah, "Optimal Control Switching of Thyristor Controlled Braking Resistor for Stability Augmentation," in IEEE Industry Applications Conference, vol. IAS-2004, 2004.

[54] A. Rubaai and A. R. Ofoli, "Multilayer Fuzzy Controller For Control Of Power Networks," IEEE Trans. on Industry Applications, vol. 40, no. 6, p. 1521, 2004.

[55] A. Rubaai, A. R. Ofoli, D. Cobbinah and M. D. Kankam, "Two-Layer Supervisory Controller – Based Thyristor – Controlled Braking Resistor For Transient Stability Crisis," IEEE Trans. on Industry Applications, vol. 41, no. 6, p. 1539 – 1547, December 2005.

[56] M. Glavic, D. Ernst and L. Wehenkel, "A Reinforcement Learning Based Discrete Supplementary Control for Power System Transient Stability Enhancement," Engineering Intelligent Systems for Electrical Engineering and Communications, vol. 13, pp. 81-88, 2003.

[57] M. Glavic, "Design Of A Resistive Brake Controller For Power System Stability Enhancement Using Reinforcement Learning," IEEE Trans. on Control Systems Technology, vol. 13, no. 5, pp. 743 -751, September 2005.

[58] V. R. Sherkat, J. S. Thorp and R. J. Thomas, "Impact Of Dynamic Braking On Shaft Torques," IEEE Trans. on Power Apparatus and Systems, vol. PAS-99, no. 6, pp.

2253-2264, November 1980.

[59] O. Wasynczuk, "Damping Shaft Torsional Oscillations Using a Dynamically Controlled Resistor Bank," IEEE Trans. on Power Apparatus and Systems, vol. PAS-100, no. 7, pp. 3340-3349, 1981.

[60] L. Wang and C.-H. Lee, "Application of Dynamic Resistance Braking on Stabillizing Torsional Oscillations," in Proceeding of the 1993 IEEE Region 10 Conference on Computer, Communication, Control and Power Engineering, Beijing, 1993.

[61] R. M. Hamouda, Z. R. Alzaid and M. A. Mostafa, "Coordinated Design Of Thyristors Controlled Braking Resistors And Power System Stabilizer For Damping Electro-Mechanical Oscillations," in Power Engineering Conference, AUPEC, Australian Universities, 27 -30 September 2009.

[62] R. M. Hamouda, Z. R. Alzaid and M. A. Mostafa, "Damping Torsional Oscillations in Large Turbo-Generators Using Thyristor Controlled Braking Resistors," in Power Engineering Conference, AUPEC,, Australian Universities, 14 – 17 December 2008.

[63] S. Helmy and A. S. El-Wakeel, "Mitigating Sub-synchronous Resonance Torques using Dynamic Braking Resistor," in Proceedings of the 14th International Middle East Power Systems Conference (MEPCON'10), 2010.

[64] A. H. M. A. Rahim and H. M. Al-Maghraby, "Dynamic Braking Resistor for Control of Subsynchronous Resonant Modes," Power Engineering Society Summer Meeting, 2000. IEEE, vol. 3, pp. 1930-1935, 2000.

[65] A. H. M. A. Rahim and S. A. Al-Baiyat, "Dynamic Brake Switching Strategies for Stabilization of Power Systems Using Artificial Neural Networks," Expert Systems with Applications, vol. 18, pp. 101-109, 2000.

[66] E. Huseinbasic, I. Kuzle and T. Tomisa, "Inter-Area Oscillations Damping Using Dynamic Braking And Phasor Measurements," in IEEE/PES Power Systems Conference and Exposition, (PSCE'09), 2009.

[67] B. Das, A. Ghosh and P. Sachchidanand, "A Novel Control Strategy For A Braking Resistor," International Journal of Electrical Power and Energy Systems, vol. 20, no. 6, pp. 391-403, 1998.

[68] H. Jiang, J. Dorsey, T. Habetler and K. V. Eckroth, "A Cost Effective Generator Brake for Improved Generator Transient Response," IEEE Trans. on Power Systems, vol. 9, no. 4, pp. 1840-1846, November 1994.

[69] W. Freitas, A. Morelato and W. Xu, "Improvement Of Induction Generator Stability Using Braking Resistors," IEEE Trans. on Power System, vol. 19, no. 2, pp. 1247 - 1249, 2004.

[70] X. Wu, A. Arulampalam, C. Zhan and N. Jenkins, "Application Of A Static Reactive Power Compensator (STATCOM) And A Dynamic Braking Resistor (DBR) for the Stability Enhancement of a Large Wind Farm," Wind Engineering, vol. 27, no. 2, pp. 93-106, 2003.

[71] A. Causebrook, D. J. Atkinson and A. G. Jack, "Fault Ride-Through Of Large Wind Farms Using Series Braking Resistors (March 2007)," IEEE Trans. on Power Systems, vol. 22, no. 3, pp. 966-975, August 2007.

[72] R. M. Tumilty, C. G. Bright, G. M. Burt, O. Anaya-Lara and J. R. Mcdonald, "Applying Series Braking Resistors To Improve The Transient Stability Of Low Inertia Synchronous Distributed Generators," in 19th International Conference On Electricity Distribution, Vienna, 21-24 May 2007.

[73] P. Kundur, J. Paserba, V. Ajjarapu, G. Andersson, A. Bose, C. Canizares, N. Hatziargyriou, D. Hill, A. Stankovic, C. Taylor, T. V. Cutsem and V. Vittal, "Definition and Classification of Power System Stability," IEEE Trans. Power Systems, vol. 19, no. 2, pp. 1387-1401, May 2004.

[74] P. Kundur, Power System Stability and Control, Tata McGraw-Hill, 1994.

[75] P. Raschio, W. Mittelstadt, R. Spee and J. H. R. Enslin, "Selection Of Input Locations For Power System Control," in IEEE Technical Applications Conference and Workshops Northcon95, 1995.

[76] N. Mohan, T. M. Undeland and W. P. Robbins, Power Electronics, Converters, Applications and Design, John Wiley & Sons, Inc., 1994.

[77] V. Scaini and B. M. Urban, "High Current DC Chopper and Their Operational Benefits," Petroleum and Chemical Industry conference, 1998. Industry Applications Society 45th Annual, pp. 173-180, 1998.

[78] M. H. Rashid, Power Electronics Circuits, Devices And Applications, Third Edition, UpperSaddle River,NJ: Pearson Prentice Hall, 2004.

[79] A. R. Bergen and V. Vittal, Power Systems Analysis, Prentice-Hall Series: Tom Robbins, 2000.

[80] J. Beak, P. Buddingh and V. Scaini, "Re-using and Re-rating Older Rectifiers with New DC/DC Choppers," IEEE Trans. on Industry Applications, vol. 37, no. 4, pp. 1160-1166, July/August 2001.